DIETARY EARLY GLYCATION PRODUCTS MODULATE HOST IMMUNITY AND DIFFERENTIALLY AFFECT TYPE 1 DIABETES AND PROSTATE CANCER

by

YINGJIA CHEN

(Under the Direction of Tai L. Guo)

ABSTRACT

Advanced glycation end-products (AGEs) are studied extensively for their detrimental effects on health. This is largely due to their pro-inflammatory and oxidative characteristics. AGEs can generate a non-specific pro-inflammatory stress on various organs including the immune system, and lead to diseases associated with diet. Surprisingly, little is known about their homologous product, the early glycation products (EGPs). Existing literature show that EGPs exhibit desirable physiochemical properties, which might improve food quality. Thus, understanding the physiologic effects of EGPs could impact their use in food. In this study, the immunoregulatory effects of EGPs were investigated. A food model system was established to produce dietary EGPs and AGEs, and they were studied with the non-reacted mixture employed as control. EGPs at 10 mg/ml *in vitro* did not inhibit cell viability of human macrophages. Interestingly, EGPs activated macrophages denoted by a general increase in cytokine/chemokine levels with IL-10 and CCL4 being the most up-regulated, suggesting that EGPs have an anti-inflammatory effect. In contrast, AGEs exposure under the same conditions largely decreased the cell viability.

To further explore the immunomodulatory effects of EGPs during disease, prostate cancer (PCa) and type 1 diabetes (T1D) animal models were employed. C57BL/6 male mice were subcutaneously transplanted with TRAMP-C2 cells, and EGP gavage (600 mg/kg body weight/day) enhanced PCa cell growth more than AGEs, with the tumor-associated macrophages displaying an M2 polarized phenotype. Further, this effect was enhanced by co-injecting macrophages with the TRAMP-C2 cells. This EGP-driven M2 pre-dominant phenotype was reproduced in a human macrophage-PCa cell (LNCaP) co-culture system. In T1D studies, EGPs decreased the T1D incidence, non-fasting blood glucose levels, insulin resistance, pancreatic immune infiltration, and increased glucose metabolism in NOD mice. These protective effects were accompanied by decreased $CD8^+$ T cells and serum insulin autoantibody levels, and increased splenic $CD4^+CD25^+$ T cells, macrophage M2/M1 ratio and serum IL-10 level. This would suggest that EGPs might be beneficial for individuals with T1D or insulitis, but detrimental to PCa patients at advanced stages. Sub-chronic intake of EGPs could have various impacts on human health, and the effect might depend on individual's health and disease status.

INDEX WORDS: early glycation products, anti-inflammation, prostate cancer, type 1 diabetes, advanced glycation end-products

DIETARY EARLY GLYCATION PRODUCTS MODULATE HOST IMMUNITY AND DIFFERENTIALLY AFFECT TYPE 1 DIABETES AND PROSTATE CANCER

by

YINGJIA Chen

B. Sc. (Agr.), Jiangnan University, China, 2010

M. Eng., Jiangnan University, China, 2013

A Dissertation Submitted to the Graduate Faculty of The University of Georgia in Partial Fulfillment of the Requirements for the Degree

DOCTOR OF PHILOSOPHY

ATHENS, GEORGIA

2019

DIETARY EARLY GLYCATION PRODUCTS MODULATE HOST IMMUNITY AND DIFFERENTIALLY AFFECT TYPE 1 DIABETES AND PROSTATE CANCER

by

YINGJIA CHEN

Major Professor:	Tai L. Guo
Committee:	Robert M. Gogal Jr
	Nikolay M. Filipov
	Fanbin Kong

Electronic Version Approved:

Suzanne Barbour
Dean of the Graduate School
The University of Georgia
August 2019

ACKNOWLEDGEMENTS

During my PhD studies, I met many great people, especially my advisor Dr. Tai Guo and advisory committee members: Drs. Fanbin Kong, Nikolay M. Filipov, and Robert Gogal. They provided valuable suggestions for this project, and supported my research and learning. I would also thank Mr. James Barber, Dr. Tamas Nagy, and Dr. Carla Jarrett for helping with flow cytometric data analysis, pathological analysis, and Western blots. Last but not least, I want to thank Ms. Joanne Mauro for taking care of the administrative works.

TABLE OF CONTENTS

Page

LIST OF ABBREVIATIONS

AGEs, advanced glycation end-products; **AP,** anterior prostate; **APCs,** antigen presenting cells; **BCRs,** B cell receptors; **BGL,** blood glucose level; **BW,** body weight; **CCL4,** chemokine (C-C motif) ligand 4; **CEL,** carboxyethyl lysine; **CM,** conditioned medium; **CML,** carboxymethyl lysine; **CTLA-4,** cytotoxic T lymphocyte associated protein 4; **DC,** dendritic cells; **DSP,** degree of substitution per protein; **EAE,** experimental autoimmune encephalomyelitis; **EGPs,** early glycation products; **ER,** endoplasmic reticulum; **FL,** fructoselysine; **FMO,** fluorescence minus one; **GI,** gastrointestinal; **GO,** glyoxal; **GTT,** glucose tolerance test; **IAA,** insulin autoantibodies; **H&E,** hematoxylin and eosin; **iNOS,** inducible nitric oxide synthase, **ITT,** insulin tolerance test; **KIR,** killer cell immunoglobulin-like receptor; **LIRs,** leukocyte immunoglobulin like receptors; **MAPK,** mitogen-activated protein kinase; **MGO,** methylglyoxal; **MHC,** major histocompatibility complex; **MLD,** multiple low dose; **MQ**, 2-methyl-quinoxaline; **Mφ,** macrophage; **NCR,** natural cytotoxicity receptors; **NF-κB,** nuclear factor kappa-light-chain-enhancer of activated B cells; **NK,** natural killer; **NKG2D**, NK receptor member D of the lectin-like receptor; **NOD,** non-obese diabetic; **NR,** non-reacted samples; **OPA,** o-phthalaldehyde assay**;** **OPD,** o-phenylenediamine; **PCa,** prostate cancer; **PCA,** principle component analysis; **PD-1,** programmed cell death protein 1; **PD-L1,** programmed death ligand 1; **PMA,** phorbol 12-myristate 13-acetate; **PSA,** prostate specific antigen; **Q**, quinoxaline; **RAGE,** receptor for AGEs; **RH,** relative humidity; **ROS,** reactive oxygen species; **STZ,** streptozotocin; **SV,** seminal vesicle;

T1D, type 1 diabetes; **TAM,** tumor-associated macrophage; **TCR,** T cell receptors; **TLR,** toll-like receptor; **TME,** tumor microenvironment; **Treg,** regulatory T cell; **WBC,** white blood cell; **WPI,** whey protein isolate.

LIST OF FIGURES

Page

CHAPTER 1

INTRODUCTION AND LITERATURE REVIEW

1.1 Overview of the chemistry of glycation/Maillard reaction

Maillard reaction or glycation refers to a series of spontaneous and complex reactions between reducing sugars and proteins/peptides/amino acids. Hodge (1953) first mapped the whole process, and Namiki & Hayashi (Namiki and Hayashi, 1983) added an additional pathway to it. According to Hodge, the whole reaction can be divided into three stages: initial, intermediate and final. In the initial stage, the reducing ends of the sugars react to the amino groups of amino acids/peptides/proteins to form a Schiff base, which is reversible. The irreversible rearrangements take place afterward, leading to the formation of Amadori compounds for aldoses or Heyns compounds for ketoses (Hodge, 1953). The reactions at this stage are well characterized, and the products generated are named as early glycation products (EGPs) (Beisswenger, 2012), and their structures are well described (Poulsen et al., 2013). An example of glucose-derived Amadori compound is shown in Fig 1.1.

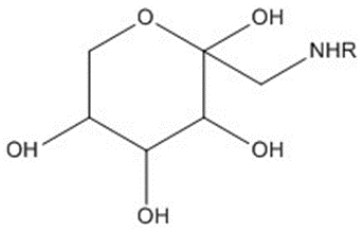

Fig 1.1 Structure of glucose-derived Amadori compounds.

The intermediate stage starts with the degradation of Amadori or Heyns compounds, which include amino acid degradation, sugar dehydration and fragmentation. Highly unsaturated

compounds are produced at this stage. They undergo polymerization and form fluorescent and/or colored polymers in the final stage (Hodge, 1953). Among the various products, dicarbonyls are important intermediates and precursors for advanced glycation end-products (AGEs), as well as a proportion of aromatic products and pigments. They can be formed from Amadori products or Schiff bases via the Namiki pathway (Namiki and Hayashi, 1983), sugar degradation or protein cross-linking (e.g., lysine dimers, arginine-lysine cross-linking). The frequently mentioned dicarbonyls include glyoxal (GO), methylglyoxal (MG) and 3-deoxyglucosone (3-DG) (Poulsen et al., 2013), but their derivatives can be diverse. For example, maltose and lysine incubation can result in the synthesis of 19 α-dicarbonyls (Smuda and Glomb, 2011). Dicarbonyls are highly reactive, and they are quickly converted to AGEs. The structures of AGEs are more heterogeneous when compared to EGPs. The well-known AGEs, such as N-carboxymethyl-lysine (CML), pyrraline and pentosidine, are referring to the key structures (Poulsen et al., 2013). Cross-linking, degradation and fragmentation make each one highly diverse. It is worth of mentioning that there are alternative pathways for AGE synthesis besides glycation/Maillard reaction, which include polyol pathway (Huebschmann et al., 2006, Ott et al., 2014, Singh et al., 2001), carbonyl stress (Huebschmann et al., 2006) and lipid peroxidation (Ott et al., 2014, Singh et al., 2001).

1.2 Dietary EGPs

The dietary content of AGEs has been revealed by quantitating the level of CML (a marker for AGEs) in over 500 different foods using ELISA (Goldberg et al., 2004, Uribarri et al., 2010). Compared to AGEs, the EGP level in food is not as well characterized. The most well-studied

EGP containing food is bovine milk and milk powders. They are particularly prone to glycation because their concentrations of protein and sugar have been adjusted according to human milk, and temperature-dependent processes such as sterilization or spray drying have been applied for the purpose of microbiological safety (Pischetsrieder and Henle, 2012). Birlouez-Aragon et al. assessed the protein glycation markers in infant formulas, which included 19 UHT milk, 5 in-bottle sterilized milk, and 17 powdered infant formulas (Birlouez-Aragon et al., 2004). The results showed that commercial samples had a loss of 16.9-30.4% lysine depending on the processing procedures, and the content of furosine (a derived early glycation marker) was a thousand times higher than CML (an AGE marker) (Birlouez-Aragon et al., 2004). Another study profiled the glycation products in the early stage (fructoselysine (FL)) and advanced stage (i.e., CML, pyrraline) in commercially available dairy products, and the results showed that the amount of FL considerably outweighed CML and pyrraline in raw and processed cow milk (i.e., pasteurized milk, skimmed milk, UHT milk, condensed milk, half cream milk) (Hegele et al., 2008). Collectively, these data indicate that glycation in the dairy products is limited to the early stage, resulting in the abundant presence of EGPs. In addition to bovine milk proteins, glycation is also identified in other dietary proteins, such as soy proteins (Platteau et al., 2011).

The content of dietary EGPs is determined by the glycation process in the food matrix. A condensation between reducing sugars and proteins/peptides/amino acids can increase EGPs, and further reaction decreases the amounts of EGPs while increasing that of AGEs. The reaction process can be affected by food storage time and temperature. For example, there was no detectable lactosylation for κ-caseins in untreated milk protein concentrate (MPC85), whereas a 7-day storage of MPC85 at 50 °C added up to 2 lactose moieties to α_{S1}-, α_{S1}-, β- and κ-caseins

with the modification rate at about 50% for β- and κ-caseins and over 60% for α-caseins (Anema et al., 2006).

Besides temperature, the glycation reaction is highly dependent on reactants and reaction conditions. The glycation reactivity varies among different milk proteins. In standard experimental conditions, caseins are less glycated than whey proteins (Cardoso et al., 2018). For saccharides, the increase in molecular size decreases the glycation reactivity (Chen et al., 2013, Ter Haar et al., 2011). A comparison of the condensation reactivity of 15 monosaccharides shows that aldose is more reactive than ketose (Bunn and Higgins, 1981). The negative charge of the sugars can reduce the glycation speed and extent (Chen et al., 2013, Ter Haar et al., 2011). Water activity or relative humidity (RH) affects the reaction as well: 50%RH generates the highest glycation speed after equilibration, followed by 67% and 75%RH; the fluorescence intensity and absorbance at 420 nm (formation of AGEs and brown pigments) of samples at 50%RH are less than half of those generated at 67% and 75%RH (Pan and Melton, 2007). From the perspective of reaction controlling, time and space saving, the dry condition is more desirable for industrial production of EGPs than the solution condition (Oliver et al., 2006).

Bovine milk protein can cause food allergy because it contains some protein components that are absent in human milk (e.g., β-lactoglobulin). Protein modification, including glycation, is considered a method to reduce the allergenicity of the bovine milk. One *in vitro* study that focused on glycated β-lactoglobulin showed that when compared to native β-lactoglobulin, the uptake by bone marrow-derived dendritic cells (BMDC) was increased, the degradation inside BMDC was faster, the cytokine stimulation on β-lactoglobulin-specific $CD4^+$ T cells was

decreased, and the degranulation of β-lactoglobulin-specific IgE sensitized basophil cells was less efficient (Perusko et al., 2018). When the lactose glycated β-lactoglobulin (EGPs) was incubated with β-lactoglobulin-specific IgE from patients who were allergic to cow's milk, the binding capacity was dramatically decreased when compared to the ribose glycated β-lactoglobulin (AGEs), and instead, it was comparable to the heat-denatured β-lactoglobulin (Taheri-Kafrani et al., 2009). Comparatively, AGE-ovalbumin (AGE-OVA) increased internalization by immature dendritic cells (DC) (Hilmenyuk et al., 2010) and bone marrow-derived murine myeloid DC (Ilchmann et al., 2010), activated the expression of RAGE and NF-κB in immature DC, enhanced the Th2 response in mature DC (Hilmenyuk et al., 2010), and enhanced the activation of OVA-specific $CD4^+$ T cells (Ilchmann et al., 2010). Taking together, EGPs may be less allergic than the original proteins, and this is opposite to AGEs. However, most studies are conducted *in vitro*, and the IgE or IgG-binding capacity is used as endpoint, which does not accurately predict the allergenicity of glycated proteins. Further *in vivo* and systematic works are required in this perspective.

The other aspects of immunity have rarely been studied following dietary EGPs exposure, while dietary AGEs have been reported to induce inflammatory responses and mediate pathological progression in multiple organs or tissues (Kellow and Coughlan, 2015). We hypothesized that EGPs behave differently from AGEs in regulating the immune responses. Therefore, the immunoregulatory effects of dietary EGPs were investigated in the present work. After exposing to EGPs *in vitro*, human macrophages were activated to upregulate almost all the cytokines/chemokines measured, and the functional analysis based on cytokine/chemokine data suggested that EGPs might be anti-inflammatory. Then, two disease models - prostate cancer

(PCa) and type 1 diabetes (T1D) - were used to further explore the effects of EGPs on disease progression through immunomodulation.

1.3 Dietary AGEs

1.3.1 AGEs in food and factors that affect dietary AGE formation

A dietary AGE database containing over 500 foods has been established based on CML quantitation by ELISA (Goldberg et al., 2004, Uribarri et al., 2010). Generally speaking, foods with high AGE content include nuts (e.g. almonds, chestnuts, pine nuts), cheese, oil, cooked meat and fish/seafood, pancake, waffle, cookies/pies, and a combination of other foods (e.g. Big Mac from McDonald's, pizza, sandwich). Foods with low AGE content include fruits, vegetables, milk, juice, coffee, tea and Coke/Pepsi; the AGE levels of raw meat and fish/seafood are in between (Uribarri et al., 2010). For the raw food materials, the AGEs levels vary over 20,000-fold. Fat (butter and oil) is the most AGE-rich foods in the uncooked form. These AGEs may come from the extraction and purification procedures in which heating and high pressure are involved, as well as lipid peroxidation during storage. Cheese is another AGE-rich food: parmesan, American, Swiss, feta and cheddar are abundant in AGEs, while cottage and mozzarella have a lower amount, which seems to be related to the original fat content and aging time (Uribarri et al., 2010). Nuts are naturally abundant in AGEs, and followed by meat, fish/seafood, vegetable and fruits. It is no surprise that food with mainly carbohydrates are lower in AGEs than fat and meat due to the higher water content and antioxidants, which may also be effective in inhibiting new AGE formation.

The AGE levels can be dramatically increased by cooking. For example, 4 minutes on the grill increases the AGE content in the raw beef more than 10 folds (Uribarri et al., 2010). Theoretically, the Maillard reaction rate can be increased 4-8 fold/10 °C (Kannane and Labuza, 1989). Cooking method also matters. Broiling and frying increase the AGE level most, which is due to the heating time, temperature and humidity. Higher temperature, longer time and a_W of 0.5-0.8 are favorable conditions for Maillard reaction (Kannane and Labuza, 1989). Sun et al. showed that the levels of CML and carboxyethyllysine (CEL) in ground beef steadily increased with heating time and heating temperature (Sun et al., 2015). Of note, cooking fat used also significantly affects the AGE production. For instance, scrambled eggs cooked with oil or cooking spray have 27-65% less AGEs than cooked with butter (Uribarri et al., 2010).

Other food components and ingredients, such as water, also affect the AGE formation during food processing. High a_W is a natural prevention for the Maillard reaction, and the liquid base dilutes the reactants. This probably explains all the liquid foods (juice, milk etc.) are low in AGEs. Dietary polyphenols are inhibitors for AGE formation, and they are phenolic acids, flavonoids (flavonols, flavones, isoflavones, flavanones, anthocyanidins and flavanols), stilbenes, and lignans (Manach, Scalbert, Morand, Remesy, & Jimenez, 2004). Zhang et al. quantitated the amount of various AGE intermediates in the co-heated casein-glucose solution with different types of dietary polyphenols. The authors suggested that the AGE-preventing effect of polyphenols occurred in multiple steps of the Maillard reaction, which included the sugar attachment, rearrangement, α-dicarbonyl formation and AGE formation. The role of polyphenols in the intermediate and final stages of the Maillard reaction is related to their antioxidant effect,

yet their role in early glycation needs further investigation (Zhang et al., 2014). Other additives such as antioxidants and vitamins also can to some degree diminish the AGE formation (Uribarri et al., 2010).

1.3.2 Dietary AGE exposure and absorption, distribution, metabolism, and excretion

Exposure to dietary AGEs is highly dependent on eating habit and age. Based on the AGE content in different foods, Western diet (high in processed and red meats, high-fat dairy, refined grains, sweets and desserts) contains much higher AGEs than a prudent diet (high in vegetable, fruits, fish, legumes, and whole grains) (Lopez-Garcia et al., 2004, Yang et al., 2015). A 70-kg adult fed on a Western diet is estimated to have a daily intake of 1 mg CML/kg body weight (BW) through food, while a 6-kg infant can ingests over 2.5 mg CML/kg BW/day through the consumption of 1 L of infant formulas (Delgado-Andrade et al., 2007, Hull et al., 2012, van Rooijen et al., 2014).

After oral digestion, about 10% of dietary AGEs can be absorbed in the gastrointestinal (GI) tract (Koschinsky et al., 1997). Due to the low absorption rate, the physiological and pathological effects of dietary AGEs have long been neglected. Admittedly, there is a threshold for dietary AGEs to exert an effect on the circulating levels of AGEs in our bodies. Koschinsky et al. showed that the dietary AGE consumption below 0.5×10^6 unit from a breakfast substitute would not result in the serum AGE increase. Once the threshold had been reached, a significant correlation ($r = 0.8$, $p < 0.05$) was observed between the AGE amount ingested per person (diabetic and renal failure patients) and the resulting elevation in serum AGE kinetics

(Koschinsky et al., 1997). In a cohort with 450 participants, an increased uptake of dietary AGEs resulted in the elevation of free CML, CEL and N^{δ}-(5-hydro-5-methyl-4-imidazolon-2-yl)-ornithine (MG-H1) levels in plasma and urine, but not the protein-bound ones (Scheijen et al., 2018). In another study involving 90 healthy people showed that the reduction of dietary AGEs intake was associated with an average 30-40% decrease in serum AGE levels (Uribarri et al., 2005). Interestingly, the serum AGE plateau had also been observed in a mouse study, and the serum CML level remained stable when the food CML intake increased from 24.4×10^4 to 30×10^4 U/day (Cai et al., 2012).

The fate of intestinal absorbed dietary AGEs is currently under investigation. A human study showed that 1/3 of the absorbed AGEs secreted through urine within 48 h (Koschinsky et al., 1997), and another study revealed that the urinary secretion of CML was related to the form and complexity of CML, i.e., high molecular weight and insoluble fractions extracted from bread crust decreased the urinary secretion rate when compared to the whole bread crust extraction, and this was likely due to the anti-digestive properties of insoluble protein-bound CML (Roncero-Ramos et al., 2013). Fecal excretion is another major route for AGE excretion, which eliminates about 1/3 dietary AGEs based on CML quantitation (Roncero-Ramos et al., 2013). This quantity can be underestimated, because part of the dietary AGEs is possibly degraded by colonic microflora into low molecular weight compounds (Tuohy et al., 2006).

Approximately half of dietary AGEs consumed is not accounted for based on the urinary and fecal elimination data. The remaining dietary AGEs may be deposited in animal organs and tissues, including kidney (Kita, 2011, Li et al., 2015), liver (Li et al., 2015, Kita, 2011), lung (Li

et al., 2015), cardiac tissue (Li et al., 2015, Roncero-Ramos et al., 2013, van Rooijen et al., 2014), and tendons (van Rooijen et al., 2014, Roncero-Ramos et al., 2013).

1.3.3 Effect of AGEs on immune system

The immune system is composed of physical & chemical barriers (e.g. intestinal mucosal and lysozymes), immune cells, lymphoid organs (e.g. thymus and Peyer's patches), and cytokines/chemokines. These components play like an orchestrated symphony to maintain the homeostasis. Any imbalance, either enhancement or suppression, can affect the host defense and promote a broad range of immune related diseases, including inflammatory diseases, autoimmune diseases and cancer. AGEs are reported as one of the immunotoxins, in spite of their overall and nonspecific toxicities (Kellow and Coughlan, 2015). The main mechanism for

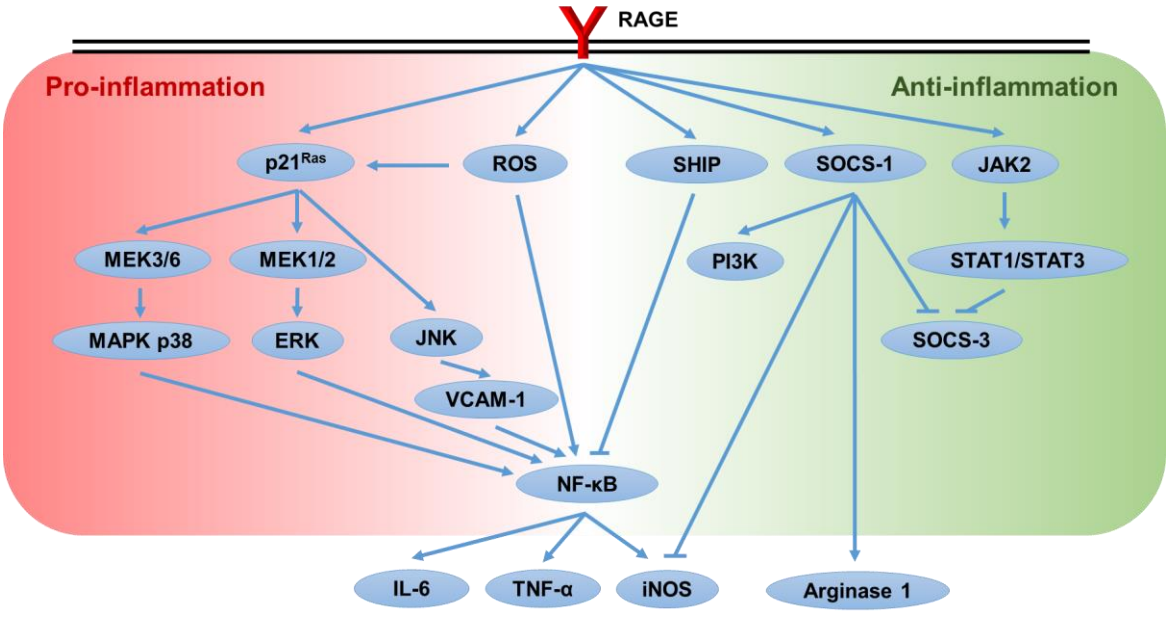

Fig 1.2 Schematic representation of the paradox control of pro-inflammation and anti-inflammation by RAGE activation.

AGEs on immunity is to induce pro-inflammatory responses. The major receptor that AGEs bind to induce pro-inflammation is the receptor for AGEs (RAGE), which is expressed on a range of cell types, including immune cells (e.g., macrophages, lymphocytes, dendritic cells (DC)) (Ott et al., 2014). Up-regulation of RAGE expression in different organs and tissues was observed when rodents were on AGE/methylglyoxal (MG) containing diets/drinking water (Cai et al., 2012, Sena et al., 2012). Activation of RAGE results in intracellular ROS production (Coughlan et al., 2009) and the activation of p21(ras)-dependent mitogen-activated protein kinase (MAPK) pathway (Lander et al., 1997), which eventually leads to the upregulation of NF-κB and inflammation (Fig 1.2).

Interestingly, Kitts's group reported that the mixed and purified AGEs containing Maillard reaction products were anti-oxidative and anti-inflammatory when applied to Caco-2 cell line (Chen and Kitts, 2011, Kitts et al., 2012). Qin et al. (2018) showed that the ribose-tryptophan Maillard reaction products (RRT-MRPs) had anti-inflammatory effects in the LPS-treated murine macrophage cell line, Raw 264.7, and the structure of a 532.24 Da RRT-MRP was identified as 3-((1H-indol-3-yl)methyl)-8-(5-((1H-indol-3-yl)methyl)-6-oxomorpholin-2-yl)-9-hydroxy-1,7,4-dioxazecan-2-one. Huang et al. reported that AGEs attenuated the effect of nitric oxide on human renal tubular cells. Moreover, they demonstrated it was through RAGE-JAK2-STAT1/STAT3 activation and thus SOCS-3 suppression (Huang et al., 2015). These apparently contradictory findings to the majority of literature may reflect the fact that the binding of RAGE ligands could not only lead to pro-inflammation, but also anti-inflammation (Fig 1.2). For example, THP-1 cells were polarized toward M2 after being treated by HMGB1 at 1 μg/mL, and

this was through RAGE-SHIP/SOCS1 (Rojas et al., 2016). The dual role of RAGE in inflammatory balance seems to be dose/concentration related, but it needs further studies.

In addition to direct up-regulation of RAGE, decreases in the degradation of receptors for AGE (e.g., AGER1, SR-A (Ott et al., 2014)) can be another reason for AGE-induced pro-inflammation. For example, AGE receptor 1 (AGER1), which is reported for endocytic uptake and degradation of AGEs, suppress the RAGE expression and negatively regulate the oxidative stress and inflammation induced by AGEs (Ott et al., 2014, Lu et al., 2004). Cai et al. showed that dietary AGE consumption could deplete AGER1 in adipocytes, resulting in pro-inflammation, oxidative stress and insulin resistance (Cai et al., 2012).

More and more evidence show that AGEs can induce gut dysbiosis probably because they are resistant to enzymatic digestion. A high-AGE diet decreased the species richness and α diversity of the gut microbiota when the Sprague-Dawley rats and C57BL/6 mice were exposed for up to 18 weeks. Additionally, *Ruminococcaceae*, *Lachnospiraceae*, *Alloprevotella* and *Butyrivibrio* were dramatically decreased, whereas *Desulfovibrio* and *Bacteroides* were increased, which led to more production of ammonia and branched-chain fatty acids, but decreased short-chain fatty acids (Qu et al., 2017). Similar regulations were found in C57BL/6 male mice after 8-month exposure (Qu et al., 2018). Sulfate-reducing bacteria (Loubinoux et al., 2002) and *Bacteroides fragilis* (Wang et al., 2007) were frequently found of high abundance in patients with inflammatory bowel diseases. Additionally, the prevalence of *Bacteroides spp.* was associated with early-onset of autoimmune diseases and impaired endotoxin tolerance which led to higher immunological stimulation (Blander et al., 2017). However, the health effect of dietary AGEs on

gut microbiota, and the influence of gut microbes and their metabolites on health are still under debate. For example, the butyrate (a short-chain fatty acid) fermented from soluble fiber was reported to initiate cholestasis, hepatocyte death, and neutrophilic inflammation in the liver, and eventually lead to hepatocellular carcinoma in T5KO mice (Singh et al., 2018). In a human study with 20 end-stage renal disease patients, the group consuming high AGE diet had increased *Pevotella copri* and *Bifidobecterium*, and reduced *Alistipes indistinctus*, *Clostridium citroniae*, *Clostridium hathewayi* and *Ruminococcus gauvreauii* when compared to the dietary AGE restricted group (Yacoub et al., 2017). Of note, the regulated bacteria in the human study showed little similarity when compared to those in rodent models. This discrepancy might be related to the health conditions, and also the differences in intestinal structures and gut microbiota compositions between humans and mice (Nguyen et al., 2015).

1.4 Cancer immunology: from immunosurveillance to immune escape

Cancer is a hyperproliferative disorder with mutations in oncogenes or tumor-suppressor genes that allow the normal cells to acquire the malignant phenotype. Its initiation (normal cells become malignant), promotion (malignant cells continue to grow), and progression (growing tumor becomes aggressive) involve the participation of immune system. On the one hand, the immune components detect and eliminate the emerging tumor cells; on the other hand, tumor cells evade or even alter the immune system. The whole process is termed as “cancer immunoediting” (Dunn et al., 2004), emphasizing the dual immunosurveillance versus tumor-driven immune sculpting.

1.4.1 Immunosurveillance

The role of the immune system in combating tumor initiation and growth can be demonstrated through cancer research with immunodeficient mice. Examples include spontaneous tumor development in SCID mice (immunodeficiency: T, B, natural killer (NK) cells) (Huang et al., 2011) and NOD mice (immunodeficiency: defective NK, functionally differentiated DC and Mφ, and reduced complement activity) (Leiter, 1993), and rapid tumor growth in nude mice (immunodeficiency: T cells) (Engel et al., 1996) and RAG-$2^{-/-}$ mice (Immunodeficiency: T and B cells) (Shankaran et al., 2001) comparing to wild-type mice.

NK cells play a key role in recognizing tumor cells, and thus lead to effector anti-tumor responses. Two general mechanisms have been described regarding how NK cells specifically recognize tumor cells. One is the "missing self" recognition – that is to bind and attack via inhibitory receptors of the major histocompatibility complex (MHC) class I-deficient cells (Ljunggren and Karre, 1990, Berraondo et al., 2016). NCK^{KD} mice, low LY49 receptor expression, exhibited uncontrolled subcutaneously transplanted tumor growth (i.e., RMA, RMA-S, B16F10.LacZ, B16F10.H-2Kb H-2Db, or B lymphoma cells) and metastases (B16F10.LacZ cells), and restoring NK cell education with a transgene for LY49I receptor in this strain suppressed cancer growth (Tu et al., 2014). Mechanistically, in the absence of MHC I ligand, the inhibitory receptors (e.g., killer cell immunoglobulin-like receptor (KIR in human, LY49 receptor in mouse), leukocyte immunoglobulin-like receptor (LIR), CD94–NKG2 receptor) (Martinet and Smyth, 2015, Campbell and Hasegawa, 2013) are left unbound and the inhibition does not exist, leading to the NK cell activation via natural cytotoxicity receptors (NCRs) and

NK receptor member D of the lectin-like receptor (NKG2D) (Campbell and Hasegawa, 2013). The other is antibody-dependent recognition, in which the Fc receptor (CD16) recognizes the Fc portion of antibodies binding to tumor antigen. After activation, NK cells directly kill tumor cells with cytolytic granules (e.g., perforin), death ligands (e.g., Fas ligands) and cytokines (e.g., IFN-γ), and/or indirectly mediate anti-tumor immunity through cytokines, chemokines and growth factors (Martinez-Lostao et al., 2015).

Tumor-associated Mφ (TAM) plays a dual role during tumor development. M1 polarized Mφs are involved in anti-tumor response. Clinical findings showed that M1 Mφ density in tumor positively predicted survival time in lung cancer patients (Ma et al., 2010) and experimental data further supported it by showing a decreased colon cancer cell metastasis was accompanied by a skewed Mφ polarization toward M1 (Ryan et al., 2015). M1 Mφs nonspecifically eliminate cancer cells by releasing pro-inflammatory cytokines, and cytotoxic reactive oxygen and nitrogen species. Besides the activated macrophages (M1 and M2), another subset of macrophages, $CD169^+$ macrophages, was reported to be associated with favorable prognosis in patients with endometrial carcinoma (Ohnishi et al., 2016) and colorectal carcinoma (Ohnishi et al., 2013). Their expansion into the lymph nodes was positively correlated with increasing infiltration of T and NK cells within the tumor tissues (Ohnishi et al., 2013, Ohnishi et al., 2016), suggesting the potential role of Mφs as APCs for cellular anti-tumor immunity.

The adaptive immunosurveillance involves T cells and B cells, with the former mediating the cellular anti-tumor response and the latter participating in the humoral anti-tumor response. The $CD4^+$ and $CD8^+$ αβ T cells recognize tumor cells through binding the antigens to T cell receptors

(TCRs). Two distinct antigen processing and presentation pathways have been described: 1) tumor cells directly present endogenous antigens in the context of MHC class I molecules; 2) professional APCs present antigens bound to both MHC class I and II molecules (Kaufman et al., 2007). The tumor antigens are summarized into five categories (Dunn et al., 2004): 1) differentiation antigens; 2) mutational antigens; 3) overexpressed/amplified antigens; 4) cancer-testis antigens; 5) viral antigens. In addition to tumor antigens presented on MHC molecules, tumor cells can up-regulate other molecules that function as recognition targets for T cells. For example, NKG2D ligands overexpressing on tumor cell can bind to NKG2D receptor on T cells (Bauer et al., 1999).

B cells have dual roles in tumor development. Its anti-tumor function is indicated by the clinical facts that B cell infiltrates were positively correlated with good outcomes for melanoma (Erdag et al., 2012) and lung cancer (Al-Shibli et al., 2008). Their anti-tumor role is realized by producing antibodies for tumor clearance. When severe combined immunodeficiency (SCID) mice were transplanted with xenograft human lung tumors, an elevated B cell-derived IgG was detected in the mouse serum (Mizukami et al., 2006). B cell-derived antibodies can bind to mouse tumors (Li et al., 2005), and the binding of antibodies to tumor cells directly kill the tumor. Antibodies mediate other immune processes for tumor clearance, including complement-mediated killing of tumor cells, Fc-mediated phagocytosis by Mφ, and antibody-dependent cell-mediated cytotoxicity (ADCC) by NK cells (Berraondo et al., 2016). B cells can also act as APCs that promote anti-tumor immunity. Tumor antigens are processed and presented by B cell receptors (BCRs). Targeting CD40 on B cells abolished the antitumor response from T cells (Li et al., 2005). In addition, B cells can secrete inflammatory molecules that regulate other immune

cells. The lymphotoxin generated by B cells reduced PCa relapse in mice, which activated IKK-α and STAT3 in PCa cells to increase the survival (Ammirante et al., 2010). In pancreatic islets, B cell infiltration was accompanied by T cell and DC infiltrations in a lymphotoxin-dependent manner (Luther et al., 2000).

1.4.2 Immunosuppression

While attacking the tumor cells, the immunity continuously sculpts the tumor cells as well, leading to the immune selection of tumor cells with reduced immunogenicity. The surviving cells are generally characterized with altered cell surface protein expression and secretions, which directly avoid the immune attack or induce immune dysfunction. Highly invasive and metastasis tumor cells usually possess decreased or altered tumor-specific antigen – MHC molecules (Algarra et al., 2004). It is considered as a mechanism of escaping the T cell recognition, but the outcome is opposite for the NK cell-mediated killing, which has been reviewed in *1.4.1*.

Tumor cells may lack the expression of costimulatory proteins, such as B7-1 and B7-2. The progressive outgrowth of tumors was regressed after transduction of the B7 gene, and the immunogenicity alteration was realized through binding to CD28 on $CD8^+$ T cells (Chen et al., 1994). Further studies showed that both B7-1 and B7-2 showed low affinity to CD28 and high affinity to CTLA-4 (Linsley et al., 1994). The interaction of costimulatory molecules on tumor cells with cytotoxic T lymphocyte associated protein 4 (CTLA-4) can inhibit T cell function by blocking TCR-CD3-mediated signal (Fallarino et al., 1998). One of these homologues, programmed death ligand 1 (PD-L1, also known as B7-H1 or CD274), was later extensively

studied as inhibitory molecules overexpressed on tumor cells. PD-L1 interacts with programmed cell death protein 1 (PD-1) expressed on T cells, leading to the inhibition of antigen cross-presentation, T cell proliferation, TCR activation, and cytokine production (Tamura et al., 2003; Efremova et al., 2018).

Tumor cells can not only change their own cell surface proteins, but also the proteins on immune cells. Numerous studies have shown that tumor-infiltrating T lymphocytes in renal, hepatic colorectal, head and neck squamous cell carcinomas have decreased CD3γ chain when comparing to healthy controls (Finke et al., 1993, Nakagomi et al., 1993, Maccalli et al., 1999). The peripheral blood lymphocytes of PCa patients were shown to regain normal CD3γ levels after 48 h culture in the serum-free medium (Healy et al., 1998). Therefore, tumor growth may affect the TCR-CD3 signal transduction, which is possibly induced by tumor-associated chronic inflammation (e.g. IFN-γ-dependent lysosomal degradation) (Bronstein-Sitton et al., 2003).

In addition to cell surface protein modification, an impressive wide variety of tumor promoting immunosuppressive cytokines and factors has been reported. Tumor cells secret GM-CSF and VEGF to disrupt the cytokine balance for the maturation of fully functional APCs (Wang et al., 2014) and effector lymphocyte differentiation (Huang et al., 2011b). TGF-β was the first discovered immunosuppressive cytokine, and its pro-tumoral roles include directly promoting tumorigenesis and converting naïve $CD4^+$ to $Foxp3^+$ iTreg (Roychoudhuri et al., 2015). IL-10 is another important immune dysregulatory cytokine secreted by tumor cells, which is shown to inhibit T cell proliferation, pro-inflammatory cytokine production, antigen presentation, and lymphokine-activated killer cell cytotoxicity (Pawelec et al., 1999), and induce anergy in tumor

antigen-specific T cells (Steinbrink et al., 2002). Tumor metastasis is positively correlated with IL-10 and CCL22, and negatively associated with IL-12, IL-6 produced by Mφs (Rossowska et al., 2015). Increased IL-10 and decreased IL-12 and IL-6 are associated with maintaining the immunosuppressive tumor microenvironment. Increased CCL22 acts as a chemoattractant for Treg cells (Ishida et al., 2006). Intracellular adhesion molecule (ICAM/CD54), lymphocyte function-associated antigen-3 (LFA-3/CD58), and other soluble forms of T cell interaction molecules promote tumor progression through inhibiting cellular aggregation and cytotoxic lysis (Teunissen et al., 1994). Soluble Fas ligand, Annexin II, MUC-1 and MUC-2 molecules from tumor may delete or suppress T cells through suppressing CD3ζ chain expression (Taylor et al., 2003) or tumor counterattack (Martinez-Lorenzo et al., 2004). Tumor cells produce oxygen and nitrogen radicals and angiogenic factors that promote tumor growth and metastasis. Mφs, granulocytes and NK cells presenting in the tumor-draining lymph nodes also show increased reactive oxygen metabolites and reactive nitrogen intermediates that induce CD3ζ chain down-regulation.

1.4.3 Dietary AGEs and Cancer

AGEs are a cluster of known cancer promoters. In cancer patients, the levels of AGEs were elevated in sera and tumors in a cancer stage-dependent manner (Foster et al., 2014). RAGE ablation in TAMs was able to abolish angiogenesis in glioma (Chen et al., 2014). Besides immune cells, RAGE is expressed in a variety of human tumors, including but not limited to colorectal, prostate, pancreatic, breast and ovarian cancers (Logsdon et al., 2007). The AGE treatment of various tumor cells, including cancer cell lines originated from prostate, colon, lung,

liver, pancreas, breast, oral cavity, kidney and skin, increased cancer cell proliferation, invasion, migration and angiogenesis (Lin et al., 2016). Animal experiment with AGEs showed that RAGE upregulation in pancreatic tissue could enhance autophagy, and then activate IL-6-STAT3 and regulate cell proliferation, resulting in pancreatic neoplasia (Kang et al., 2012).

1.5 Immune mechanisms in type 1 diabetes (T1D)

Diabetes is a group of diseases characterized by high blood glucose level (BGL), which include type 1, type 2, gestational, and prediabetes. Among them, T1D is an autoimmune disease characterized as the immune destruction of the insulin-producing pancreatic β-cells. The aetiology and pathogenesis of T1D are still unclear.

1.5.1 Cause of T1D

Both genetic background and environmental factors contribute to T1D initiation and development. HLA class II genes at 6p21, the major T1D susceptibility locus, accounts for up to 30%–50% genetic risk of T1D (Steck and Rewers, 2011). Other non-HLA loci include the insulin gene (*INS*)[3], cytotoxic T-lymphocyte-associated protein 4 (*CTLA-4*) gene, the protein tyrosine phosphatase, non-receptor type 22 (lymphoid) (*PTPN22*) gene, the interleukin 2 receptor alpha (*IL2RA*), interferon induced with helicase C domain 1 (*IFIH1*) genes and others (Steck and Rewers, 2011). The T1D risk is 20% for an individual with HLA-risk gene with a family history of T1D, but rapidly drops to 5% if without a family history (Steck and Rewers, 2011). This strongly implies that a genetic background is a prerequisite for developing T1D.

It has been suggested that infection is an important trigger for T1D. This sounds paradox to the hygiene hypothesis that exposure to pathogens could increase the self-tolerance. Experimental murine model NOD shows that dirty environment decreased the T1D incidence (Singh and Rabinovitch, 1993). However, things may go wrong when the immune cells attempt to eliminate the invading virus or parasites. For example, JunB expression was associated with decreased inducible nitric oxide synthase (iNOS) and endoplasmic reticulum (ER) stress in rat primary pancreatic β-cells and insulin-producing cell line (INS-1E), protecting β-cells from apoptosis (Gurzov et al., 2008). Controversially, $Cd4^{Cre}Junb^{fl/fl}$ mice were resistant to myelin oligodendrocyte glycoprotein (MOG)35–55 peptide immunization, while the control mice, which express JunB in T cells, developed severe experimental autoimmune encephalomyelitis (EAE) (Hasan et al., 2017). This inferred an important role of JunB expression in T cells for disease development in the experimental autoimmune model. The mechanistic study showed that JunB facilitated DNA binding of BATF in T cells, and thus activated the expression of RORγt and IL-23 receptor in IL-23-dependent Th17, which was essential for the pathogenic progress (Hasan et al., 2017).

In addition to infection, increased awareness was given to nutrition in terms of T1D development. T1D patients have profound metabolic changes, including increased energy expenditure and whole-body protein breakdown, leading to net protein loss (Hebert and Nair, 2010). However, cow milk may increase T1D risk (Virtanen and Knip, 2003). In contrast, breastfeeding, zinc, vitamins C and D are reported as protective nutrients for T1D (Virtanen and Knip, 2003).

Mechanistically, the role of ten-eleven translocation (TET) in hyperglycemia and diabetes gives a fundamental support for the protective role of vitamin C against T1D (Ding and Huang, 2014).

1.5.2 Immune mechanisms for β-cell death

The mechanisms for β-cell death in autoimmune T1D are not exactly clear, which involve the initiation and effector immune response against β-cells. One study showed that over 50% of the identified genes associated with T1D were expressed in human pancreas, and many of them could be upregulated by pro-inflammatory stimuli (Eizirik et al., 2012), indicating pro-inflammation as a trigger. On the one hand, the stimuli increased the expression of MHC class I on β-cells and pro-inflammatory cytokines (von Herrath, 2009). On the other hand, the exogenous ligands (e.g., viral dsRNA) activated the innate immune cells through binding to pattern-recognition receptors (e.g., toll-like receptors (TLRs)) (Eizirik et al., 2009).

A study with patients with newly developed T1D found that $CD4^+$ T cells, $CD8^+$ T cells, $CD20^+$ B cells and $CD68^+$ Mφ were all present in the β-islets (Willcox et al., 2009), confirming that many cell subsets were involved in the T1D pathogenesis. For β-cells destruction, a well-acknowledged mechanism considers $CD8^+$ T cells the core attackers, either through cell-cell contact or recognition of the β-cell antigens presented by APCs (Mathis et al., 2001). $CD8^+$ T cells from T1D patients recognized pre-proinsulin signal peptides (Skowera et al., 2008) and were able to kill human β-cells *in vitro* (Knight et al., 2013). Even though $CD8^+$ T cells are predominantly for killing β-cells, their activation and propagation highly rely on $CD4^+$ T cells. In T1D, the $CD4^+$ T cells are Th1 differentiated, evident by the facts that a Th1 biased phenotype is

identified in neonatal NOD mice which developed T1D later (Katz et al., 1995), and IFN-γ is positively correlated with the progression T1D in the same strain (Rabinovitch, 1994). B cell depletion by anti-CD20 monoclonal antibody in NOD mice was able to prevent the incidence of T1D (Hu et al., 2007). However, the transfer of autoantibody-containing serum to B cell-deficient NOD mice was unable to restore the normal disease level (Serreze et al., 1998). These observations probably suggest that B cells participate in the T1D pathogenesis through both antibody production and antigen presentation. The role of Mφ in T1D onset and development is not clear, which might be relevant to the inflammatory status. TNF-producing Mφ was found in the islets of newly developed T1D (Uno et al., 2007); however, injection of M2 macrophages to the prediabetic NOD recipients protected >80% of treated mice against T1D for at least 3 months (Parsa et al., 2012).

1.5.3 Non-obese diabetic (NOD) mouse

NOD is a strain of mouse that spontaneously develop T1D sharing many similarities with human T1D. Therefore, it is widely used in T1D studies for dissecting and understanding tolerance pathways for disease progression. Genetically, NOD mice harbor a unique MHC haplotype, H-2^{g7}, which express I-A^{g7} but not I-E or H-2$K^{d}D^{b}$, of which the I-A^{g7} is the highest contributor for T1D susceptibility (Wicker et al., 1995, Tisch and McDevitt, 1996, Pearson et al., 2016). Innate immune cells (e.g., dendritic cells, macrophages, neutrophils) infiltrate the pancreas as early as 3 weeks of age, and then attract $CD4^{+}$ and $CD8^{+}$ T cells into the pancreas at 4-6 weeks of age (Pearson et al., 2016). According to the literature, T1D onset can occur as early as 9-10 weeks of age and the incidence is 60-80% in females. Males have delayed onset and incidence lower than

40%. Studies with NOD strain demonstrated that the penetrance of diabetic genotype was strongly modified by both microbiota and diet (Leiter, 1993).

1.5.4 Dietary AGEs and diabetes.

Universally, serum or plasma AGE levels are elevated in diabetic patients due to the increased BGL and dietary AGE consumption was related to the rapid development of diabetic complications. Direct evidence linking AGEs to T1D was found in the research in which parental NOD8.3 male and NOD/ShiLt female mice were exposed to diets with low or high AGE content throughout pregnancy and lactation, the NOD8.3^{+} female offspring from the high dietary AGE litters had elevated circulating AGEs, pancreatic AGEs, RAGE expression and glucagon secretion in islets, increased insulitis, lower expression of Ins2 in islets, and decreased islet insulin secretion *ex vivo*. Collectively, these data indicated that perinatal exposure to AGE exacerbated insulitis and T1D in mice prone to developing T1D (Borg et al., 2018).

Taken together, AGEs are tumor and T1D promotors through direct effect or immunoregulation. However, the physiological effect of EGPs remains unclear. Thus, this dissertation focused on the immunoregulatory effect of EGPs using two unique disease models: PCa and T1D.

References

AL-SHIBLI, K. I., DONNEM, T., AL-SAAD, S., PERSSON, M., BREMNES, R. M. & BUSUND, L. T. 2008. Prognostic effect of epithelial and stromal lymphocyte infiltration in non-small cell lung cancer. Clin Cancer Res, 14, 5220-7.

ALGARRA, I., GARCIA-LORA, A., CABRERA, T., RUIZ-CABELLO, F. & GARRIDO, F. 2004. The selection of tumor variants with altered expression of classical and nonclassical MHC class I molecules: implications for tumor immune escape. Cancer Immunol Immunother, 53, 904-10.

AMMIRANTE, M., LUO, J. L., GRIVENNIKOV, S., NEDOSPASOV, S. & KARIN, M. 2010. B-cell-derived lymphotoxin promotes castration-resistant prostate cancer. Nature, 464, 302-5.

ANEMA, S. G., PINDER, D. N., HUNTER, R. J. & HEMAR, Y. 2006. Effects of storage temperature on the solubility of milk protein concentrate (MPC85). Food Hydrocolloids, 20, 386-393.

BAUER, S., GROH, V., WU, J., STEINLE, A., PHILLIPS, J. H., LANIER, L. L. & SPIES, T. 1999. Activation of NK cells and T cells by NKG2D, a receptor for stress-inducible MICA. Science, 285, 727-9.

BEISSWENGER, P. J. 2012. Glycation and biomarkers of vascular complications of diabetes. Amino Acids, 42, 1171-83.

BERRAONDO, P., MINUTE, L., AJONA, D., CORRALES, L., MELERO, I. & PIO, R. 2016. Innate immune mediators in cancer: between defense and resistance. Immunol Rev, 274, 290-306.

BIRLOUEZ-ARAGON, I., PISCHETSRIEDER, M., LECLERE, J., MORALES, F. J., HASENKOPH, K., KIENTSCH-ENGEL, R., DUCAUZE, C. J. & RUTLEDGE, D. 2004. Assessment of protein glycation markers in infant formulas. Food Chem, 87, 7.

BLANDER, J. M., LONGMAN, R. S., ILIEV, I. D., SONNENBERG, G. F. & ARTIS, D. 2017. Regulation of inflammation by microbiota interactions with the host. Nat Immunol, 18, 851-860.

BORG, D. J., YAP, F. Y. T., KESHVARI, S., SIMMONS, D. G., GALLO, L. A., FOTHERINGHAM, A. K., ZHUANG, A., SLATTERY, R. M., HASNAIN, S. Z., COUGHLAN, M. T., KANTHARIDIS, P. & FORBES, J. M. 2018. Perinatal exposure to high dietary advanced glycation end products in transgenic NOD8.3 mice leads to pancreatic beta cell dysfunction. Islets, 10, 10-24.

BRONSTEIN-SITTON, N., COHEN-DANIEL, L., VAKNIN, I., EZERNITCHI, A. V., LESHEM, B., HALABI, A., HOURI-HADAD, Y., GREENBAUM, E., ZAKAY-RONES, Z., SHAPIRA, L. & BANIYASH, M. 2003. Sustained exposure to bacterial antigen induces interferon-gamma-dependent T cell receptor zeta down-regulation and impaired T cell function. Nat Immunol, 4, 957-64.

BUNN, H. F. & HIGGINS, P. J. 1981. Reaction of Monosaccharides with Proteins - Possible Evolutionary Significance. Science, 213, 222-224.

CAI, W., RAMDAS, M., ZHU, L., CHEN, X., STRIKER, G. E. & VLASSARA, H. 2012. Oral advanced glycation endproducts (AGEs) promote insulin resistance and diabetes by depleting the antioxidant defenses AGE receptor-1 and sirtuin 1. Proc Natl Acad Sci U S A, 109, 15888-93.

CAMPBELL, K. S. & HASEGAWA, J. 2013. Natural killer cell biology: an update and future directions. J Allergy Clin Immunol, 132, 536-544.

CARDOSO, H. B., WIERENGA, P. A., GRUPPEN, H. & SCHOLS, H. A. 2018. Maillard induced glycation behaviour of individual milk proteins. Food Chem, 252, 311-317.

CHEN, L., MCGOWAN, P., ASHE, S., JOHNSTON, J., LI, Y., HELLSTROM, I. & HELLSTROM, K. E. 1994. Tumor immunogenicity determines the effect of B7 costimulation on T cell-mediated tumor immunity. J Exp Med, 179, 523-32.

CHEN, X., ZHANG, L., ZHANG, I. Y., LIANG, J., WANG, H., OUYANG, M., WU, S., DA FONSECA, A. C. C., WENG, L., YAMAMOTO, Y., YAMAMOTO, H., NATARAJAN, R. & BADIE, B. 2014. RAGE expression in tumor-associated macrophages promotes angiogenesis in glioma. Cancer Res, 74, 7285-7297.

CHEN, X. M. & KITTS, D. D. 2011. Antioxidant and anti-inflammatory activities of Maillard reaction products isolated from sugar-amino acid model systems. J Agric Food Chem, 59, 11294-303.

CHEN, Y. J., LIU, X. M., LABUZA, T. P. & ZHOU, P. 2013. Effect of molecular size and charge state of reducing sugars on nonenzymatic glycation of beta-lactoglobulin. Food Research International, 54, 1560-1568.

COUGHLAN, M. T., THORBURN, D. R., PENFOLD, S. A., LASKOWSKI, A., HARCOURT, B. E., SOURRIS, K. C., TAN, A. L., FUKAMI, K., THALLAS-BONKE, V., NAWROTH, P. P., BROWNLEE, M., BIERHAUS, A., COOPER, M. E. & FORBES, J. M. 2009. RAGE-induced cytosolic ROS promote mitochondrial superoxide generation in diabetes. J Am Soc Nephrol, 20, 742-52.

DELGADO-ANDRADE, C., SEIQUER, I., NAVARRO, M. P. & MORALES, F. J. 2007. Maillard reaction indicators in diets usually consumed by adolescent population. Mol Nutr Food Res, 51, 341-51.

DING, G. L. & HUANG, H. F. 2014. Role for tet in hyperglycemia-induced demethylation: a novel mechanism of diabetic metabolic memory. Diabetes, 63, 2906-8.

DUNN, G. P., OLD, L. J. & SCHREIBER, R. D. 2004. The immunobiology of cancer immunosurveillance and immunoediting. Immunity, 21, 137-48.

EFREMOVA, M., RIEDER, D., KLEPSCH, V., CHAROENTONG, P., FINOTELLO, F., HACKL, H., HERMANN-KLEITER, N., LOWER, M., BAIER, G., KROGSDAM, A. &

TRAJANOSKI, Z. 2018. Targeting immune checkpoints potentiates immunoediting and changes the dynamics of tumor evolution. Nat Commun, 9, 32.

EIZIRIK, D. L., COLLI, M. L. & ORTIS, F. 2009. The role of inflammation in insulitis and beta-cell loss in type 1 diabetes. Nat Rev Endocrinol, 5, 219-26.

EIZIRIK, D. L., SAMMETH, M., BOUCKENOOGHE, T., BOTTU, G., SISINO, G., IGOILLO-ESTEVE, M., ORTIS, F., SANTIN, I., COLLI, M. L., BARTHSON, J., BOUWENS, L., HUGHES, L., GREGORY, L., LUNTER, G., MARSELLI, L., MARCHETTI, P., MCCARTHY, M. I. & CNOP, M. 2012. The human pancreatic islet transcriptome: expression of candidate genes for type 1 diabetes and the impact of pro-inflammatory cytokines. PLoS Genet, 8, e1002552.

ENGEL, A. M., SVANE, I. M., MOURITSEN, S., RYGAARD, J., CLAUSEN, J. & WERDELIN, O. 1996. Methylcholanthrene-induced sarcomas in nude mice have short induction times and relatively low levels of surface MHC class I expression. APMIS, 104, 629-39.

ERDAG, G., SCHAEFER, J. T., SMOLKIN, M. E., DEACON, D. H., SHEA, S. M., DENGEL, L. T., PATTERSON, J. W. & SLINGLUFF, C. L., JR. 2012. Immunotype and immunohistologic characteristics of tumor-infiltrating immune cells are associated with clinical outcome in metastatic melanoma. Cancer Res, 72, 1070-80.

FALLARINO, F., FIELDS, P. E. & GAJEWSKI, T. F. 1998. B7-1 engagement of cytotoxic T lymphocyte antigen 4 inhibits T cell activation in the absence of CD28. J Exp Med, 188, 205-10.

FINKE, J. H., ZEA, A. H., STANLEY, J., LONGO, D. L., MIZOGUCHI, H., TUBBS, R. R., WILTROUT, R. H., O'SHEA, J. J., KUDOH, S., KLEIN, E. & ET AL. 1993. Loss of T-cell receptor zeta chain and p56lck in T-cells infiltrating human renal cell carcinoma. Cancer Res, 53, 5613-6.

FOSTER, D., SPRUILL, L., WALTER, K. R., NOGUEIRA, L. M., FEDAROVICH, H., TURNER, R. Y., AHMED, M., SALLEY, J. D., FORD, M. E., FINDLAY, V. J. & TURNER, D. P. 2014. AGE metabolites: a biomarker linked to cancer disparity? Cancer Epidemiol Biomarkers Prev, 23, 2186-91.

GOLDBERG, T., CAI, W., PEPPA, M., DARDAINE, V., BALIGA, B. S., URIBARRI, J. & VLASSARA, H. 2004. Advanced glycoxidation end products in commonly consumed foods. J Am Diet Assoc, 104, 1287-91.

GURZOV, E. N., ORTIS, F., BAKIRI, L., WAGNER, E. F. & EIZIRIK, D. L. 2008. JunB Inhibits ER Stress and Apoptosis in Pancreatic Beta Cells. PLoS One, 3, e3030.

HASAN, Z., KOIZUMI, S. I., SASAKI, D., YAMADA, H., ARAKAKI, N., FUJIHARA, Y., OKITSU, S., SHIRAHATA, H. & ISHIKAWA, H. 2017. JunB is essential for IL-23-dependent pathogenicity of Th17 cells. Nat Commun, 8, 15628.

HEALY, C. G., SIMONS, J. W., CARDUCCI, M. A., DEWEESE, T. L., BARTKOWSKI, M., TONG, K. P. & BOLTON, W. E. 1998. Impaired expression and function of signal-transducing zeta chains in peripheral T cells and natural killer cells in patients with prostate cancer. Cytometry, 32, 109-19.

HEBERT, S. L. & NAIR, K. S. 2010. Protein and energy metabolism in type 1 diabetes. Clin Nutr, 29, 13-7.

HEGELE, J., BUETLER, T. & DELATOUR, T. 2008. Comparative LC-MS/MS profiling of free and protein-bound early and advanced glycation-induced lysine modifications in dairy products. Anal Chim Acta, 617, 85-96.

HILMENYUK, T., BELLINGHAUSEN, I., HEYDENREICH, B., ILCHMANN, A., TODA, M., GRABBE, S. & SALOGA, J. 2010. Effects of glycation of the model food allergen ovalbumin on antigen uptake and presentation by human dendritic cells. Immunology, 129, 437-45.

HODGE, J. E. 1953. Dehydrated Foods - Chemistry of Browning Reactions in Model Systems. Journal of Agricultural and Food Chemistry, 1, 928-943.

HU, C. Y., RODRIGUEZ-PINTO, D., DU, W., AHUJA, A., HENEGARIU, O., WONG, F. S., SHLOMCHIK, M. J. & WEN, L. 2007. Treatment with CD20-specific antibody prevents and reverses autoimmune diabetes in mice. J Clin Invest, 117, 3857-67.

HUANG, J. S., LEE, Y. H., CHUANG, L. Y., GUH, J. Y. & HWANG, J. Y. 2015. Cinnamaldehyde and nitric oxide attenuate advanced glycation end products-induced the Jak/STAT signaling in human renal tubular cells. J Cell Biochem, 116, 1028-38.

HUANG, P., WESTMORELAND, S. V., JAIN, R. K. & FUKUMURA, D. 2011a. Spontaneous nonthymic tumors in SCID mice. Comp Med, 61, 227-34.

HUANG, Y., LIN, L., SHANKER, A., MALHOTRA, A., YANG, L., DIKOV, M. M. & CARBONE, D. P. 2011b. Resuscitating cancer immunosurveillance: selective stimulation of DLL1-Notch signaling in T cells rescues T-cell function and inhibits tumor growth. Cancer Res, 71, 6122-31.

HUEBSCHMANN, A. G., REGENSTEINER, J. G., VLASSARA, H. & REUSCH, J. E. 2006. Diabetes and advanced glycoxidation end products. Diabetes Care, 29, 1420-32.

HULL, G. L. J., WOODSIDE, J. V., AMES, J. M. & CUSKELLY, G. J. 2012. N-epsilon-(carboxymethyl)lysine content of foods commonly consumed in a Western style diet. Food Chemistry, 131, 170-174.

ILCHMANN, A., BURGDORF, S., SCHEURER, S., WAIBLER, Z., NAGAI, R., WELLNER, A., YAMAMOTO, Y., YAMAMOTO, H., HENLE, T., KURTS, C., KALINKE, U., VIETHS, S. & TODA, M. 2010. Glycation of a food allergen by the Maillard reaction enhances its T-cell immunogenicity: role of macrophage scavenger receptor class A type I and II. J Allergy Clin Immunol, 125, 175-83 e1-11.

ISHIDA, T., ISHII, T., INAGAKI, A., YANO, H., KOMATSU, H., IIDA, S., INAGAKI, H. & UEDA, R. 2006. Specific recruitment of CC chemokine receptor 4-positive regulatory T cells in Hodgkin lymphoma fosters immune privilege. Cancer Res, 66, 5716-22.

KANG, R., LOUX, T., TANG, D., SCHAPIRO, N. E., VERNON, P., LIVESEY, K. M., KRASINSKAS, A., LOTZE, M. T. & ZEH, H. J., 3RD 2012. The expression of the receptor for advanced glycation endproducts (RAGE) is permissive for early pancreatic neoplasia. Proc Natl Acad Sci U S A, 109, 7031-6.

KANNANE, A. & LABUZA, T. P. 1989. The Maillard reaction in foods. Prog Clin Biol Res, 304, 301-327.

KATZ, J. D., BENOIST, C. & MATHIS, D. 1995. T helper cell subsets in insulin-dependent diabetes. Science, 268, 1185-8.

KAUFMAN, H. L., WOLCHOK, J. D. & SPRINGERLINK (ONLINE SERVICE) 2007. General Principles of Tumor Immunotherapy Basic and Clinical Applications of Tumor Immunology. Dordrecht: Springer,.

KELLOW, N. J. & COUGHLAN, M. T. 2015. Effect of diet-derived advanced glycation end products on inflammation. Nutr Rev, 73, 737-59.

KITA, K. 2011. Tissue distribution of albumin-glucose advanced glycation end products administrated to chickens. Anim Sci J, 82, 291-5.

KITTS, D. D., CHEN, X. M. & JING, H. 2012. Demonstration of antioxidant and anti-inflammatory bioactivities from sugar-amino acid maillard reaction products. J Agric Food Chem, 60, 6718-27.

KNIGHT, R. R., KRONENBERG, D., ZHAO, M., HUANG, G. C., EICHMANN, M., BULEK, A., WOOLDRIDGE, L., COLE, D. K., SEWELL, A. K., PEAKMAN, M. & SKOWERA, A. 2013. Human beta-cell killing by autoreactive preproinsulin-specific CD8 T cells is predominantly granule-mediated with the potency dependent upon T-cell receptor avidity. Diabetes, 62, 205-13.

KOSCHINSKY, T., HE, C. J., MITSUHASHI, T., BUCALA, R., LIU, C., BUENTING, C., HEITMANN, K. & VLASSARA, H. 1997. Orally absorbed reactive glycation products (glycotoxins): an environmental risk factor in diabetic nephropathy. Proc Natl Acad Sci U S A, 94, 6474-9.

LANDER, H. M., TAURAS, J. M., OGISTE, J. S., HORI, O., MOSS, R. A. & SCHMIDT, A. M. 1997. Activation of the receptor for advanced glycation end products triggers a p21(ras)-dependent mitogen-activated protein kinase pathway regulated by oxidant stress. J Biol Chem, 272, 17810-4.

LEITER, E. H. 1993. The NOD mouse: a model for analyzing the interplay between heredity and environment in development of autoimmune disease. Model of Type 1 Diabetes-Part One.

LI, M., ZENG, M., HE, Z., ZHENG, Z., QIN, F., TAO, G., ZHANG, S. & CHEN, J. 2015. Increased accumulation of protein-bound N(epsilon)-(carboxymethyl)lysine in tissues of healthy rats after chronic oral N(epsilon)-(carboxymethyl)lysine. J Agric Food Chem, 63, 1658-63.

LI, Q., GROVER, A. C., DONALD, E. J., CARR, A., YU, J., WHITFIELD, J., NELSON, M., TAKESHITA, N. & CHANG, A. E. 2005. Simultaneous targeting of CD3 on T cells and CD40 on B or dendritic cells augments the antitumor reactivity of tumor-primed lymph node cells. J Immunol, 175, 1424-32.

LIN, J. A., WU, C. H., LU, C. C., HSIA, S. M. & YEN, G. C. 2016. Glycative stress from advanced glycation end products (AGEs) and dicarbonyls: An emerging biological factor in cancer onset and progression. Mol Nutr Food Res, 60, 1850-64.

LINSLEY, P. S., GREENE, J. L., BRADY, W., BAJORATH, J., LEDBETTER, J. A. & PEACH, R. 1994. Human B7-1 (CD80) and B7-2 (CD86) bind with similar avidities but distinct kinetics to CD28 and CTLA-4 receptors. Immunity, 1, 793-801.

LJUNGGREN, H. G. & KARRE, K. 1990. In search of the 'missing self': MHC molecules and NK cell recognition. Immunol Today, 11, 237-44.

LOGSDON, C. D., FUENTES, M. K., HUANG, E. H. & ARUMUGAM, T. 2007. RAGE and RAGE ligands in cancer. Curr Mol Med, 7, 777-89.

LOPEZ-GARCIA, E., SCHULZE, M. B., FUNG, T. T., MEIGS, J. B., RIFAI, N., MANSON, J. E. & HU, F. B. 2004. Major dietary patterns are related to plasma concentrations of markers of inflammation and endothelial dysfunction. Am J Clin Nutr, 80, 1029-35.

LOUBINOUX, J., BRONOWICKI, J. P., PEREIRA, I. A., MOUGENEL, J. L. & FAOU, A. E. 2002. Sulfate-reducing bacteria in human feces and their association with inflammatory bowel diseases. FEMS Microbiol Ecol, 40, 107-12.

LU, C., HE, J. C., CAI, W., LIU, H., ZHU, L. & VLASSARA, H. 2004. Advanced glycation endproduct (AGE) receptor 1 is a negative regulator of the inflammatory response to AGE in mesangial cells. Proc Natl Acad Sci U S A, 101, 11767-72.

LUTHER, S. A., LOPEZ, T., BAI, W., HANAHAN, D. & CYSTER, J. G. 2000. BLC expression in pancreatic islets causes B cell recruitment and lymphotoxin-dependent lymphoid neogenesis. Immunity, 12, 471-81.

MA, J., LIU, L., CHE, G., YU, N., DAI, F. & YOU, Z. 2010. The M1 form of tumor-associated macrophages in non-small cell lung cancer is positively associated with survival time. BMC Cancer, 10, 112.

MACCALLI, C., PISARRA, P., VEGETTI, C., SENSI, M., PARMIANI, G. & ANICHINI, A. 1999. Differential loss of T cell signaling molecules in metastatic melanoma patients' T lymphocyte subsets expressing distinct TCR variable regions. J Immunol, 163, 6912-23.

MARTINET, L. & SMYTH, M. J. 2015. Balancing natural killer cell activation through paired receptors. Nat Rev Immunol, 15, 243-54.

MARTINEZ-LORENZO, M. J., ANEL, A., ALAVA, M. A., PINEIRO, A., NAVAL, J., LASIERRA, P. & LARRAD, L. 2004. The human melanoma cell line MelJuSo secretes bioactive FasL and APO2L/TRAIL on the surface of microvesicles. Possible contribution to tumor counterattack. Exp Cell Res, 295, 315-29.

MARTINEZ-LOSTAO, L., ANEL, A. & PARDO, J. 2015. How Do Cytotoxic Lymphocytes Kill Cancer Cells? Clin Cancer Res, 21, 5047-56.

MATHIS, D., VENCE, L. & BENOIST, C. 2001. beta-Cell death during progression to diabetes. Nature, 414, 792-8.

MIZUKAMI, M., HANAGIRI, T., SHIGEMATSU, Y., BABA, T., FUKUYAMA, T., NAGATA, Y., SO, T., ICHIKI, Y., SUGAYA, M., YASUDA, M., SO, T., TAKENOYAMA, M., SUGIO, K. & YASUMOTO, K. 2006. Effect of IgG produced by tumor-infiltrating B lymphocytes on lung tumor growth. Anticancer Res, 26, 1827-31.

NAKAGOMI, H., PETERSSON, M., MAGNUSSON, I., JUHLIN, C., MATSUDA, M., MELLSTEDT, H., TAUPIN, J. L., VIVIER, E., ANDERSON, P. & KIESSLING, R. 1993. Decreased expression of the signal-transducing zeta chains in tumor-infiltrating T-cells and NK cells of patients with colorectal carcinoma. Cancer Res, 53, 5610-2.

NAMIKI, M. & HAYASHI, T. 1983. A New Mechanism of the Maillard-Reaction Involving Sugar Fragmentation and Free-Radical Formation. Acs Symposium Series, 215, 21-46.

NGUYEN, T. L., VIEIRA-SILVA, S., LISTON, A. & RAES, J. 2015. How informative is the mouse for human gut microbiota research? Dis Model Mech, 8, 1-16.

OHNISHI, K., KOMOHARA, Y., SAITO, Y., MIYAMOTO, Y., WATANABE, M., BABA, H. & TAKEYA, M. 2013. CD169-positive macrophages in regional lymph nodes are associated with a favorable prognosis in patients with colorectal carcinoma. Cancer Sci, 104, 1237-44.

OHNISHI, K., YAMAGUCHI, M., ERDENEBAATAR, C., SAITO, F., TASHIRO, H., KATABUCHI, H., TAKEYA, M. & KOMOHARA, Y. 2016. Prognostic significance of CD169-positive lymph node sinus macrophages in patients with endometrial carcinoma. Cancer Sci, 107, 846-52.

OLIVER, C. M., MELTON, L. D. & STANLEY, R. A. 2006. Creating proteins with novel functionality via the Maillard reaction: A review. Critical Reviews in Food Science and Nutrition, 46, 337-350.

OTT, C., JACOBS, K., HAUCKE, E., NAVARRETE SANTOS, A., GRUNE, T. & SIMM, A. 2014. Role of advanced glycation end products in cellular signaling. Redox Biol, 2, 411-29.

PAN, G. G. & MELTON, L. D. 2007. Nonenzymatic browning of lactose and caseinate during dry heating at different relative humidities. J Agric Food Chem, 55, 10036-42.

PARSA, R., ANDRESEN, P., GILLETT, A., MIA, S., ZHANG, X. M., MAYANS, S., HOLMBERG, D. & HARRIS, R. A. 2012. Adoptive transfer of immunomodulatory M2 macrophages prevents type 1 diabetes in NOD mice. Diabetes, 61, 2881-92.

PAWELEC, G., SCHLOTZ, E. & REHBEIN, A. 1999. IFN-alpha regulates IL 10 production by CML cells in vitro. Cancer Immunol Immunother, 48, 430-4.

PEARSON, J. A., WONG, F. S. & WEN, L. 2016. The importance of the Non Obese Diabetic (NOD) mouse model in autoimmune diabetes. J Autoimmun, 66, 76-88.

PERUSKO, M., VAN ROEST, M., STANIC-VUCINIC, D., SIMONS, P. J., PIETERS, R. H. H., CIRKOVIC VELICKOVIC, T. & SMIT, J. J. 2018. Glycation of the Major Milk Allergen beta-Lactoglobulin Changes Its Allergenicity by Alterations in Cellular Uptake and Degradation. Mol Nutr Food Res, 62, e1800341.

PISCHETSRIEDER, M. & HENLE, T. 2012. Glycation products in infant formulas: chemical, analytical and physiological aspects. Amino Acids, 42, 1111-8.

PLATTEAU, C., CUCU, T., DE MEULENAER, B., DEVREESE, B., DE LOOSE, M. & TAVERNIERS, I. 2011. Effect of protein glycation in the presence or absence of wheat proteins on detection of soybean proteins by commercial ELISA. Food Addit Contam Part A Chem Anal Control Expo Risk Assess, 28, 127-35.

POULSEN, M. W., HEDEGAARD, R. V., ANDERSEN, J. M., DE COURTEN, B., BUGEL, S., NIELSEN, J., SKIBSTED, L. H. & DRAGSTED, L. O. 2013. Advanced glycation endproducts in food and their effects on health. Food Chem Toxicol, 60, 10-37.

QIN, D., LI, L., LI, J., LI, J., ZHAO, D., LI, Y., LI, B. & ZHANG, X. 2018. A New Compound Isolated from the Reduced Ribose-Tryptophan Maillard Reaction Products Exhibits Distinct Anti-inflammatory Activity. J Agric Food Chem, 66, 6752-6761.

QU, W., NIE, C., ZHAO, J., OU, X., ZHANG, Y., YANG, S., BAI, X., WANG, Y., WANG, J. & LI, J. 2018. Microbiome-Metabolomics Analysis of the Impacts of Long-Term Dietary Advanced-Glycation-End-Product Consumption on C57BL/6 Mouse Fecal Microbiota and Metabolites. J Agric Food Chem, 66, 8864-8875.

QU, W., YUAN, X., ZHAO, J., ZHANG, Y., HU, J., WANG, J. & LI, J. 2017. Dietary advanced glycation end products modify gut microbial composition and partially increase colon permeability in rats. Mol Nutr Food Res, 61.

RABINOVITCH, A. 1994. Immunoregulatory and cytokine imbalances in the pathogenesis of IDDM. Therapeutic intervention by immunostimulation? Diabetes, 43, 613-21.

ROJAS, A., DELGADO-LOPEZ, F., PEREZ-CASTRO, R., GONZALEZ, I., ROMERO, J., ROJAS, I., ARAYA, P., ANAZCO, C., MORALES, E. & LLANOS, J. 2016. HMGB1 enhances the protumoral activities of M2 macrophages by a RAGE-dependent mechanism. Tumour Biol, 37, 3321-9.

RONCERO-RAMOS, I., DELGADO-ANDRADE, C., TESSIER, F. J., NIQUET-LERIDON, C., STRAUCH, C., MONNIER, V. M. & NAVARRO, M. P. 2013. Metabolic transit of N(epsilon)-carboxymethyl-lysine after consumption of AGEs from bread crust. Food Funct, 4, 1032-9.

ROSSOWSKA, J., ANGER, N., KICIELINSKA, J., PAJTASZ-PIASECKA, E., BIELAWSKA-POHL, A., WOJAS-TUREK, J. & DUS, D. 2015. Temporary elimination of IL-10 enhanced the effectiveness of cyclophosphamide and BMDC-based therapy by decrease of the suppressor activity of MDSCs and activation of antitumour immune response. Immunobiology, 220, 389-98.

ROYCHOUDHURI, R., EIL, R. L. & RESTIFO, N. P. 2015. The interplay of effector and regulatory T cells in cancer. Curr Opin Immunol, 33, 101-11.

RYAN, A. E., COLLERAN, A., O'GORMAN, A., O'FLYNN, L., PINDJACOVA, J., LOHAN, P., O'MALLEY, G., NOSOV, M., MUREAU, C. & EGAN, L. J. 2015. Targeting colon cancer cell NF-kappaB promotes an anti-tumour M1-like macrophage phenotype and inhibits peritoneal metastasis. Oncogene, 34, 1563-74.

SCHEIJEN, J., HANSSEN, N. M. J., VAN GREEVENBROEK, M. M., VAN DER KALLEN, C. J., FESKENS, E. J. M., STEHOUWER, C. D. A. & SCHALKWIJK, C. G. 2018. Dietary intake of advanced glycation endproducts is associated with higher levels of advanced glycation endproducts in plasma and urine: The CODAM study. Clin Nutr, 37, 919-925.

SENA, C. M., MATAFOME, P., CRISOSTOMO, J., RODRIGUES, L., FERNANDES, R., PEREIRA, P. & SEICA, R. M. 2012. Methylglyoxal promotes oxidative stress and endothelial dysfunction. Pharmacol Res, 65, 497-506.

SERREZE, D. V., FLEMING, S. A., CHAPMAN, H. D., RICHARD, S. D., LEITER, E. H. & TISCH, R. M. 1998. B lymphocytes are critical antigen-presenting cells for the initiation of T cell-mediated autoimmune diabetes in nonobese diabetic mice. J Immunol, 161, 3912-8.

SHANKARAN, V., IKEDA, H., BRUCE, A. T., WHITE, J. M., SWANSON, P. E., OLD, L. J. & SCHREIBER, R. D. 2001. IFNgamma and lymphocytes prevent primary tumour development and shape tumour immunogenicity. Nature, 410, 1107-11.

SINGH, B. & RABINOVITCH, A. 1993. Influence of microbial agents on the development and prevention of autoimmune diabetes. Autoimmunity, 15, 209-13.

SINGH, R., BARDEN, A., MORI, T. & BEILIN, L. 2001. Advanced glycation end-products: a review. Diabetologia, 44, 129-46.

SINGH, V., YEOH, B. S., CHASSAING, B., XIAO, X., SAHA, P., AGUILERA OLVERA, R., LAPEK, J. D., JR., ZHANG, L., WANG, W. B., HAO, S., FLYTHE, M. D., GONZALEZ, D. J., CANI, P. D., CONEJO-GARCIA, J. R., XIONG, N., KENNETT, M. J., JOE, B., PATTERSON, A. D., GEWIRTZ, A. T. & VIJAY-KUMAR, M. 2018. Dysregulated Microbial Fermentation of Soluble Fiber Induces Cholestatic Liver Cancer. Cell, 175, 679-694 e22.

SKOWERA, A., ELLIS, R. J., VARELA-CALVINO, R., ARIF, S., HUANG, G. C., VAN-KRINKS, C., ZAREMBA, A., RACKHAM, C., ALLEN, J. S., TREE, T. I., ZHAO, M., DAYAN, C. M., SEWELL, A. K., UNGER, W. W., DRIJFHOUT, J. W., OSSENDORP, F., ROEP, B. O. & PEAKMAN, M. 2008. CTLs are targeted to kill beta cells in patients with type 1 diabetes through recognition of a glucose-regulated preproinsulin epitope. J Clin Invest, 118, 3390-402.

SMUDA, M. & GLOMB, M. A. 2011. Novel Insights into the Maillard Catalyzed Degradation of Maltose. Journal of Agricultural and Food Chemistry, 59, 13254-13264.

STECK, A. K. & REWERS, M. J. 2011. Genetics of type 1 diabetes. Clin Chem, 57, 176-85.

STEINBRINK, K., GRAULICH, E., KUBSCH, S., KNOP, J. & ENK, A. H. 2002. CD4(+) and CD8(+) anergic T cells induced by interleukin-10-treated human dendritic cells display antigen-specific suppressor activity. Blood, 99, 2468-76.

SUN, X., TANG, J., WANG, J., RASCO, B. A., LAI, K. & HUANG, Y. 2015. Formation of advanced glycation endproducts in ground beef under pasteurisation conditions. Food Chem, 172, 802-7.

TAHERI-KAFRANI, A., GAUDIN, J. C., RABESONA, H., NIOI, C., AGARWAL, D., DROUET, M., CHOBERT, J. M., BORDBAR, A. K. & HAERTLE, T. 2009. Effects of heating and glycation of beta-lactoglobulin on its recognition by IgE of sera from cow milk allergy patients. J Agric Food Chem, 57, 4974-82.

TAMURA, H., OGATA, K., DONG, H. & CHEN, L. 2003. Immunology of B7-H1 and its roles in human diseases. Int J Hematol, 78, 321-8.

TAYLOR, D. D., GERCEL-TAYLOR, C., LYONS, K. S., STANSON, J. & WHITESIDE, T. L. 2003. T-cell apoptosis and suppression of T-cell receptor/CD3-zeta by Fas ligand-containing membrane vesicles shed from ovarian tumors. Clin Cancer Res, 9, 5113-9.

TER HAAR, R., SCHOLS, H. A. & GRUPPEN, H. 2011. Effect of saccharide structure and size on the degree of substitution and product dispersity of alpha-lactalbumin glycated via the Maillard reaction. J Agric Food Chem, 59, 9378-85.

TEUNISSEN, M. B., RONGEN, H. A. & BOS, J. D. 1994. Function of adhesion molecules lymphocyte function-associated antigen-3 and intercellular adhesion molecule-1 on human epidermal Langerhans cells in antigen-specific T cell activation. J Immunol, 152, 3400-9.

TISCH, R. & MCDEVITT, H. 1996. Insulin-dependent diabetes mellitus. Cell, 85, 291-7.

TU, M. M., MAHMOUD, A. B., WIGHT, A., MOTTASHED, A., BELANGER, S., RAHIM, M. M., ABOU-SAMRA, E. & MAKRIGIANNIS, A. P. 2014. Ly49 family receptors are required for cancer immunosurveillance mediated by natural killer cells. Cancer Res, 74, 3684-94.

TUOHY, K. M., HINTON, D. J., DAVIES, S. J., CRABBE, M. J., GIBSON, G. R. & AMES, J. M. 2006. Metabolism of Maillard reaction products by the human gut microbiota--implications for health. Mol Nutr Food Res, 50, 847-57.

UNO, S., IMAGAWA, A., OKITA, K., SAYAMA, K., MORIWAKI, M., IWAHASHI, H., YAMAGATA, K., TAMURA, S., MATSUZAWA, Y., HANAFUSA, T., MIYAGAWA, J. & SHIMOMURA, I. 2007. Macrophages and dendritic cells infiltrating islets with or without beta cells produce tumour necrosis factor-alpha in patients with recent-onset type 1 diabetes. Diabetologia, 50, 596-601.

URIBARRI, J., CAI, W., SANDU, O., PEPPA, M., GOLDBERG, T. & VLASSARA, H. 2005. Diet-derived advanced glycation end products are major contributors to the body's AGE pool and induce inflammation in healthy subjects. Ann N Y Acad Sci, 1043, 461-6.

URIBARRI, J., WOODRUFF, S., GOODMAN, S., CAI, W., CHEN, X., PYZIK, R., YONG, A., STRIKER, G. E. & VLASSARA, H. 2010. Advanced glycation end products in foods and a practical guide to their reduction in the diet. J Am Diet Assoc, 110, 911-16 e12.

VAN ROOIJEN, C., BOSCH, G., VAN DER POEL, A. F., WIERENGA, P. A., ALEXANDER, L. & HENDRIKS, W. H. 2014. Quantitation of Maillard reaction products in commercially available pet foods. J Agric Food Chem, 62, 8883-91.

VIRTANEN, S. M. & KNIP, M. 2003. Nutritional risk predictors of beta cell autoimmunity and type 1 diabetes at a young age. Am J Clin Nutr, 78, 1053-67.

VON HERRATH, M. 2009. Can we learn from viruses how to prevent type 1 diabetes?: the role of viral infections in the pathogenesis of type 1 diabetes and the development of novel combination therapies. Diabetes, 58, 2-11.

WANG, M., MOLIN, G., AHRNE, S., ADAWI, D. & JEPPSSON, B. 2007. High proportions of proinflammatory bacteria on the colonic mucosa in a young patient with ulcerative colitis as revealed by cloning and sequencing of 16S rRNA genes. Dig Dis Sci, 52, 620-7.

WANG, Y., HAN, G., WANG, K., LIU, G., WANG, R., XIAO, H., LI, X., HOU, C., SHEN, B., GUO, R., LI, Y. & CHEN, G. 2014. Tumor-derived GM-CSF promotes inflammatory colon carcinogenesis via stimulating epithelial release of VEGF. Cancer Res, 74, 716-26.

WICKER, L. S., TODD, J. A. & PETERSON, L. B. 1995. Genetic control of autoimmune diabetes in the NOD mouse. Annu Rev Immunol, 13, 179-200.

WILLCOX, A., RICHARDSON, S. J., BONE, A. J., FOULIS, A. K. & MORGAN, N. G. 2009. Analysis of islet inflammation in human type 1 diabetes. Clin Exp Immunol, 155, 173-81.

YACOUB, R., NUGENT, M., CAI, W., NADKARNI, G. N., CHAVES, L. D., ABYAD, S., HONAN, A. M., THOMAS, S. A., ZHENG, W., VALIYAPARAMBIL, S. A., BRYNIARSKI, M. A., SUN, Y., BUCK, M., GENCO, R. J., QUIGG, R. J., HE, J. C. & URIBARRI, J. 2017. Advanced glycation end products dietary restriction effects on bacterial gut microbiota in peritoneal dialysis patients; a randomized open label controlled trial. PLoS One, 12, e0184789.

YANG, M., KENFIELD, S. A., VAN BLARIGAN, E. L., BATISTA, J. L., SESSO, H. D., MA, J., STAMPFER, M. J. & CHAVARRO, J. E. 2015. Dietary patterns after prostate cancer diagnosis in relation to disease-specific and total mortality. Cancer Prev Res (Phila), 8, 545-51.

ZHANG, X., HU, S., CHEN, F. & WANG, M. 2014. Treatment of proteins with dietary polyphenols lowers the formation of AGEs and AGE-induced toxicity. Food Funct, 5, 2656-61.

CHAPTER 2

DIETARY GLYCATION PRODUCTS REGULATE IMMUNE HOMEOSTASIS: EARLY GLYCATION PRODUCTS PROMOTE PROSTATE CANCER PROLIFERATION THROUGH MODULATING MACROPHAGES

Chen, Y, Filipov, N.M., Guo, T.L. Dietary glycation products regulate immune homeostasis: early glycation products promote prostate cancer cell proliferation through modulating macrophages. *Molecular Nutrition & Food Research* **2018**, 62(3): 1700641.

2.1 Abstract

Scope: Well-controlled glycation (generally limited to the early stages) has been proposed as a strategy to improve the physiochemical properties of dietary proteins, but the functional studies of glycation products were mostly on advanced glycation end-products (AGEs) rather than early glycation products (EGPs). Since cytokines are important modulators of various biological processes, this study aimed to determine whether EGPs and AGEs affected immune homeostasis differentially and did so through modulating macrophage-derived factors.

Methods and results: Two systems (glycine-glucose and whey protein isolate (WPI)-glucose) were established to generate glycation products. They were applied to human macrophages (PMA-differentiated U937 cells), and cell viability and cytokine production were measured. Furthermore, EGPs, AGEs and their conditioned medium (CM) from macrophages were applied to human prostate cancer (PCa) cells with different etiology (LNCaP and PC-3) and murine PCa cells (TRAMP-C2) to determine their direct and indirect effects on PCa cell proliferation. EGPs enhanced the production of anti-inflammatory and immunosuppressive cytokines, and this enhancement was associated with increased PCa cell proliferation. In contrast, AGEs inhibited macrophages to secret cytokines, but increased PCa cell proliferation directly.

Conclusions: Our data suggest that EGPs promote the prostate tumor proliferation indirectly through modulating macrophages, while AGEs have a direct effect.

2.2 Introduction

Nonenzymatic glycation, or the Maillard reaction, is a series of chemical reactions that predominately occur between proteins and reducing sugars both *in vivo* and *in vitro* [1]; the resulting glycation products can be classified into two categories: early & intermediate glycation products (EGPs), and advanced glycation end-product (AGE) precursors & AGEs [2]. The EGPs generally refer to the Schiff's base and Amadori & Heyns* compounds, which are generated during the first two steps of glycation reaction – N-substitution and rearrangement [3]. As reactions progress, AGE precursors – α-dicarbonyls are formed; two well-known α-dicarbonyls are glyoxal (GO) and methylglyoxal (MGO) [3]. AGE precursors eventually become AGEs [3, 4]. However, AGE precursors are not the only source for AGEs. Another AGE generation pathway is the classic rearrangement of Amadori or Heyns* compounds [3]. AGEs are a collection of various molecular entities and include carboxymethyl lysine (CML), pentosidine, pyrraline and others, with CML being probably the best characterized and studied AGE [5]. Food is a major source for exogenous glycation products. AGEs' dietary level [5], absorption and metabolism [6], and physiological and pathological effects [7] are well described. However, those of EGPs are largely unknown except that slightly glycated proteins have shown improved physicochemical properties [8, 9], such as increased solubility and foaming, which can be applied in the food industry to enhance product quality and reduce cost.

*Page 39 and 41: "Henys" in Chen, Y, Filipov, N.M., Guo, T.L. *Molecular Nutrition & Food Research* **2018**, 62(3): 1700641.

Macrophages are the largest mononuclear phagocyte population in the lamina propria of the intestine where initial contact between the immune system and dietary glycation products takes place. As one of the important cytokine-secreting cells involving in both innate and adaptive immune responses, macrophages are associated with various immune-mediated diseases. For example, macrophages have dual roles in tumor development. Necrotic tumor cells activate macrophages to eliminate the tumor cells through phagocytosis or secreting pro-inflammatory cytokines. In contrast, macrophages in actively growing tumors help maintain an immunosuppressive tumor microenvironment (e.g., IL-10), turn on the "angiogenic switch" (e.g., vascular endothelial growth factor (VEGF)), and directly promote tumorigenesis (e.g., chemokine (C-C motif) ligand 4 (CCL4) for prostate cancer (PCa)) [10]. It is well documented that AGEs can induce macrophages to become proinflammatory [11-13], while the effect of EGPs on macrophages remained unknown.

It was hypothesized that dietary glycation products of early and advanced stages could differentially regulate immune homeostasis through modulating cytokine secretion, which would lead to an altered disease manifestation, such as cancer cell proliferation. To test this hypothesis, two glycation systems (glycine-glucose and whey protein isolate (WPI)-glucose) were established to produce glycation products at different stages, and they were used to treat human macrophages (phorbol 12-myristate 13-acetate (PMA)-differentiated U937 cells). Based on the cytokine profile, the biological functions of EGPs were characterized. Furthermore, the differential effects of EGPs and AGEs were explored in three different *in vitro* PCa models.

2.3 Materials and Methods

2.3.1 Glycation products preparation

Glycine/WPI and glucose were dissolved in distilled water to reach a molar ratio of free amino groups and reducing ends at 1:2. The amount of free amino group for WPI was determined using o-phthalaldehyde assay (OPA) [14]. The solution was freeze-dried and then incubated in a desiccator containing saturated aqueous $Mg(NO_3)_2$ solution at 45 °C for glycine and 55 °C for WPI systems, respectively. At different times during the reaction, the samples were collected and stored at -20 °C prior to use.

2.3.2 Glycation progression determination

Different methods were employed to evaluate the glycation progress. First, the interaction between glucose and the potential glycated site was determined by OPA [14], which is one of the widely used methods for quantifying the Amadori (or Heyns*) compounds [15]. The OPA reagent was prepared by mixing 2 ml 95% methanol containing 80 mg OPA (MP Biomedicals, Solon, OH), 50 ml sodium tetraborate buffer (0.1 M; pH=9.0), 5 ml SDS (20% w/v) and 0.2 ml β-mercaptoethanol. The mixture was then diluted to a final volume of 100 ml with double distilled water and used immediately. A 4-ml OPA reagent was mixed with 100 µl protein/amino acid solution. The absorbance of the mixture was measured at 340 nm (SmartSpecTM 3000, Bio-Rad, Hercules, CA) after 2 min reaction at 20 °C. A standard curve was generated using glycine standard solution (0-0.6 mg/ml), with an R^2 of 0.9992.

GO and MGO are two key intermediates of AGEs [4]. They were quantified by HPLC after sample derivatization [16]. The derivatization was conducted by mixing 40 µl sample (10.00 and 35.22 mg/ml for glycine-glucose and WPI-glucose, respectively) with 10 µl PBS (10×) and 40 µl 340 mM o-phenylenediamine (OPD, Sigma-Aldrich, St. Louis, MO), followed by incubating the solution at 70 °C in an oven for 3 h. At the end of incubation, a 10-µl of acetic acid was added to terminate the reaction. After derivatization, GO and MGO were quantified as quinoxaline (Q) and 2-methyl-quinoxaline (MQ) by HPLC. The system was Waters e2695 Separation Module equipped with a Waters Symmety C18 column (5 µm, 150 × 4.6 mm, Waters Co., MA) with the temperature setting between 25-30 °C. An aliquot of 10 µl sample was applied to the system. Solvent A was 100% methanol and solvent B was 0.5% (v/v) acetic acid in double distilled water. Elusion was performed at a flow rate of 0.8 ml/min using gradient steps: 0-2 min 20% B, 15 min 32%, 30 min 55%, 40 min 32%, 45 min 20%, and 55 min 20%. The detector was Waters 2489 UV-vis, and it was set at 315 nm.

Because of the complicated composition of AGEs, CML and fluorescent AGEs were measured as markers to estimate the total AGEs. CML was quantitated by OxiSelect CML competitive ELISA kit (Cell Biolabs, San Diego, CA) following the manufacturer's instruction. Briefly, CML conjugates were coated on the ELISA plate. A 50-µl sample was added. After incubation, the anti-CML monoclonal antibody was added, and followed by an HRP-conjugated secondary antibody. The absorbance was read at 450 nm in a Synergy 4 hybrid multi-mode microplate reader (BioTek Instruments, Inc, Winooski, VT). The standard curve (0-12.5 µg/ml) was constructed with CML-BSA. Finally, the fluorescent AGEs were measured at

excitation/emission wavelengths of 370/440 nm in a Synergy 4 hybrid multi-mode microplate reader.

2.3.3 Cell culture

U937 cells, a human monocytic cell line, were cultured in the complete RPMI 1640 medium (10% fetal bovine serum (FBS), 10 mM HEPES, and 0.1% gentamycin) at 37 °C in a 5% CO_2 atmosphere. The cells were subcultured weekly. LNCaP and PC-3 cells, two human PCa cell lines (the differences of the two cell lines were listed in Supplement 1), were cultured in the complete RPMI 1640 medium. TRAMP-C2 [17], a murine PCa cell line, was cultured in DMEM medium (supplemented with 4.5 g/L glucose, 4 nM L-glutamine, 10% FBS, 5 μg/ml bovine insulin, 1×10^{-8} dehydroisoandroterone, and 0.1% gentamycin).

2.3.4 Macrophage viability and PCa cell proliferation

U937 cells were differentiated into macrophages by treating them with PMA (10 nM) for 24 h. One hundred microliter U937 cells (5×10^5/ml) were pipetted into each well of flat-bottom 96 well plates (Corning Incorporated, Kennebunk, ME). After 24 h of differentiation, one hundred microliter of samples containing different glycation products were added. After 48 h treatment, the supernatant was collected and stored for cytokine determination or used as the conditioned medium (CM). The cells were then washed with 1× PBS (pH 7.4) and stained with Alamar blue (Bio-rad Laboratories, Inc., Raleigh, NC) for 4 h. Fluorescence was measured at excitation/emission wavelengths of 530/590 nm using the Synergy 4 hybrid multi-mode

microplate reader. To determine the biological effects of CM, 1×10^4 LNCaP cells or 5×10^3 PC-3 cells were pre-seeded for 24 h, and treated with glycated samples or CM. The CM was prepared by mixing the supernatant collected from macrophage cultures and fresh medium at a volume ratio of 1:1.

Murine peritoneal macrophages were isolated from female C57BL/6 mice by lavage without thioglycollate recruitment [18] because thioglycolate would induce inflammatory stress to macrophages. A total number of 2×10^6 peritoneal cells were cultured in DMEM medium (supplemented with 4.5 g/L glucose, 4 nM L-glutamine, 10% FBS and 0.1% gentamycin) for 4 h in a 48-well plate, and then washed with cold PBS. The attached cells were considered macrophages, and treated with glycation products for 48 h. The supernatants were collected and mixed with fresh medium at a volume ratio of 1:1 as CM. 5×10^3 TRAMP-C2 cells were pre-seeded for 24 h, and then treated with glycated samples or CM.

2.3.5 Cytokine determination and analysis

The quantities of thirty cytokines were measured using the MILLIPLEX MAP human cytokine/chemokine kit (Millipore, Billerica, MA) according to the manufacturer's instructions. Briefly, supernatants and beads were added, and the plates were incubated on a shaker at 4 °C overnight. Then detection antibody was added and followed by streptavidin-phycoerythrin addition. Plates were run on a Bio-Plex MAGPIXTM Multiplex Reader with Bio-Plex ManagerTM MP Software (Luminex, Austin, TX). Each biomarker concentration was calculated as pg/ml.

2.3.6 Functional bioinformatics and statistical analysis

The cytokine expression patterns induced by glycation products were categorized by Principle Component Analysis (PCA) on log10-transformed cytokines in SAS (SAS Institute Inc, Cary, NC). Then, the cytokines significantly induced by EGPs were used for pathway analysis, which was carried out using Gene Ontology (GO) categories and Kyoto Encyclopedia of Genes and Genomes (KEGG) in Cytoscape 3.4.0 [19, 20] with ClueGo 2.2.6 [21] and CluePedia 1.2.6 [22]. A minimum level of 3 and a maximum level of 11 were set as the GO level interval with at least 2% association for 2 or more genes or at least 4% association for 1 gene. Only functions with a p value < 0.05 were considered for functional analysis.

Data are presented as means ± SD. Statistical analysis was performed using a one-way analysis of variance (ANOVA), and mean differences were compared with Duncan's Multiple Range and/or Holm-Sidak *post hoc* tests. All the statistical analysis was conducted at α level of 0.05 using SAS 9.4 (SAS Institute Inc, Cary, NC).

2.4 Results

2.4.1 Glycation stage determination

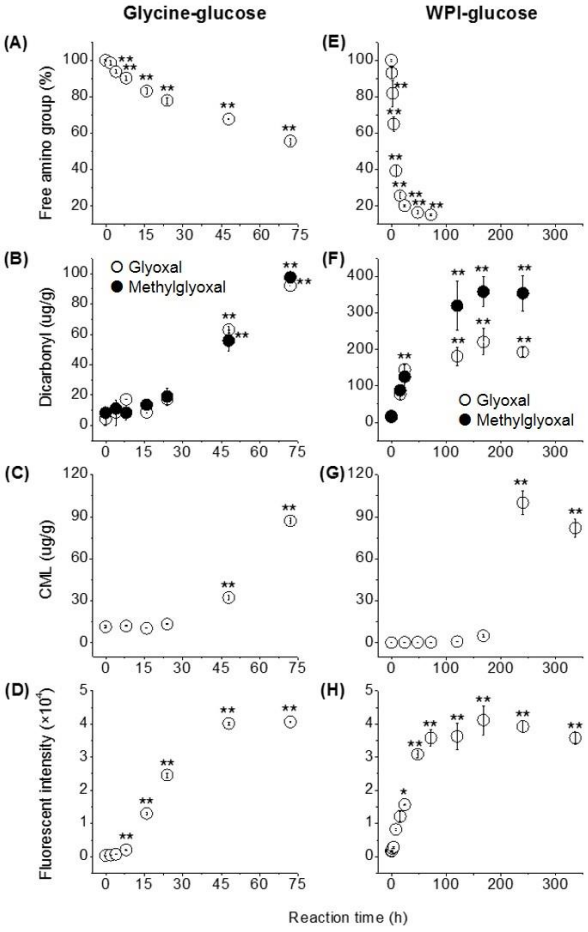

Fig 2.1 Maillard reaction progression. Free amino consumption, α-dicarbonyls (glyoxal (GO) and methylglyoxal (MGO**)**), carboxymethyl lysine (CML) and fluorescent AGEs production were measured in glycine-glucose (A, B, C, & D) and WPI-glucose systems (E, F, G, & H), respectively (mean ± SD, n = 3). *, $p < 0.05$, **, $p < 0.01$ vs. 0-h samples.

In both systems, the reactants gradually turned brown after reaction, indicating the occurrence of glycation (Supplement 2). Five markers were quantitated to determine the glycation stages (Figure 2.1). Free amino group consumption reflects the reaction between glucose and the potential glycated sites [14]; the production of α-dicarbonyls indicates the successive reactions following rearrangement; CML and fluorescent AGEs are two markers for AGEs. In the glycine-glucose system, the decrease of free amino groups was accompanied with increases of α-dicarbonyls (GO and MGO, Figure 2.1B), CML (Figure 2.1C) and fluorescent AGEs (Figure 2.1D), indicating co-occurrence of glucose attachment and formation of AGEs. After 48-h reaction, a decrease in solubility was observed, and insoluble samples appeared after 72 h, indicating that the reaction was close to completion. In comparison, the reaction in the WPI-glucose system produced better stage

separation; free amino groups decreased rapidly within 24 h (Figure 2.1E) without significant increases in AGEs and their precursors. When over 20% free amino groups were consumed, which was at 24 h, a significant increase in α-dicarbonyls (GO and MGO) was observed, and it reached its maximum at 168 h (Figure 2.1F). CML levels also increased and peaked at 240 h (Figure 2.1G), while the fluorescent AGEs showed a significant increase after 24 h, peaked at 168 h, and slightly decreased afterwards (Figure 2.1H). The minor differences between CML and fluorescent AGEs data were likely caused by pathways other than the α-dicarbonyl pathway to form fluorescent AGEs [3].

2.4.2 Modulation of cytokine production by glycation products is related to the reaction stages

To determine the cytokine modulation in macrophages, the concentrations of glycated products applied should be optimal, e.g., neither too low to generate any effects nor too high to induce overt cytotoxicity. Therefore, their optimal concentration was determined by macrophage viability assay of non-reacted samples (NR). Highly concentrated parent reactants in the systems might be toxic to the cell; therefore, different concentrations of non-reacted samples were used to treat the macrophages to determine the maximum non-toxic concentrations, which were identified as 20 and 10 mg/ml for glycine-glucose and WPI-glucose system, respectively (Supplement 3). Macrophages were more resistant to glycine-glucose than WPI-glucose, and it was likely due to the protective effect of glycine, one of the ingredients in the medium, against cell death [23]. These concentrations were selected for samples containing glycation products to treat macrophages. The 48-h and thereafter samples from glycine-glucose system (Figure 2.2A), and the 72-h and thereafter samples from WPI-glucose system (Figure 2.2B) decreased the

macrophage viability; however, the cell viability was not overt decreased except the 72-h glycine-glucose sample.

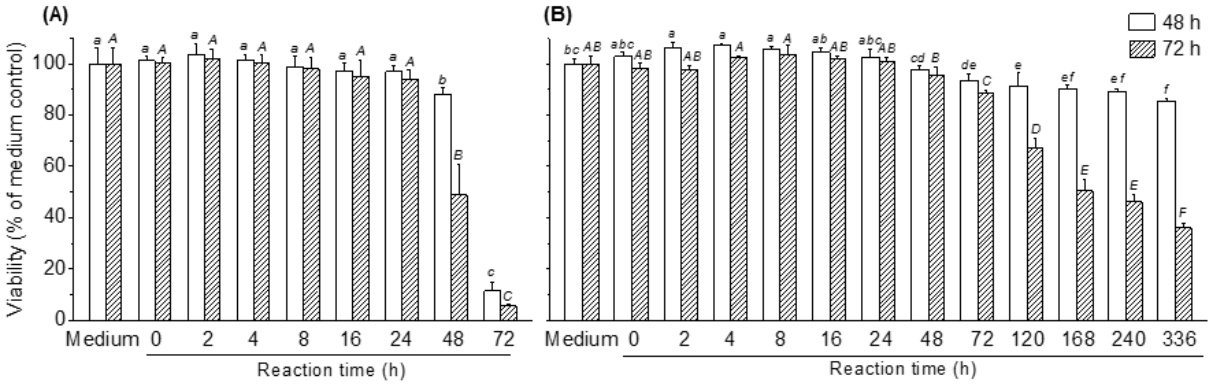

Fig 2.2 The cytotoxicity of glycation products obtained from (A) glycine-glucose (20 mg/ml) and (B) WPI-glucose (10 mg/ml) reaction systems on macrophage (PMA-differentiated U937) cell viability (mean ± SD, n = 6). Different bars indicate different treatment times. Letters in italic (lowercases for 48 h & uppercases for 72 h) above the bars indicate significant differences ($p < 0.05$).

Cytokine levels in the supernatants of human macrophages following 48 h treatment with 0-48 h glycine-glucose samples or 0-336 h WPI-glucose samples were determined. For glycine-glucose samples, the glycation products generated within 8-h incubation induced an overall increase in most of the cytokines, and those generated at 16-h incubation started to show suppression in the production of cytokines (e.g., EGF, IL-1, IL-5, TNF-α). Based on the profile of cytokine modulation, PCA indicated a clear separation between 0-8, 16 and 24-48 h samples (Figure 2.3C), in spite of the disordered glycation progression shown in Figure 2.1. In WPI-glucose system, the overall effects of the glycation products were quite similar to those generated by glycine-glucose system: those produced at 0-8 h generally increased, 16-24 h both increased and

suppressed, and 48-336 h suppressed the production of cytokines (Figure 2.3B). The PCA results confirmed the clear separation between 0-8, 16-24 and 48-336 h samples (Figure 2.3D). By combining the data for glycation progression, it can be generally concluded that EGPs increase, while AGEs suppress, the production of cytokines by human macrophages.

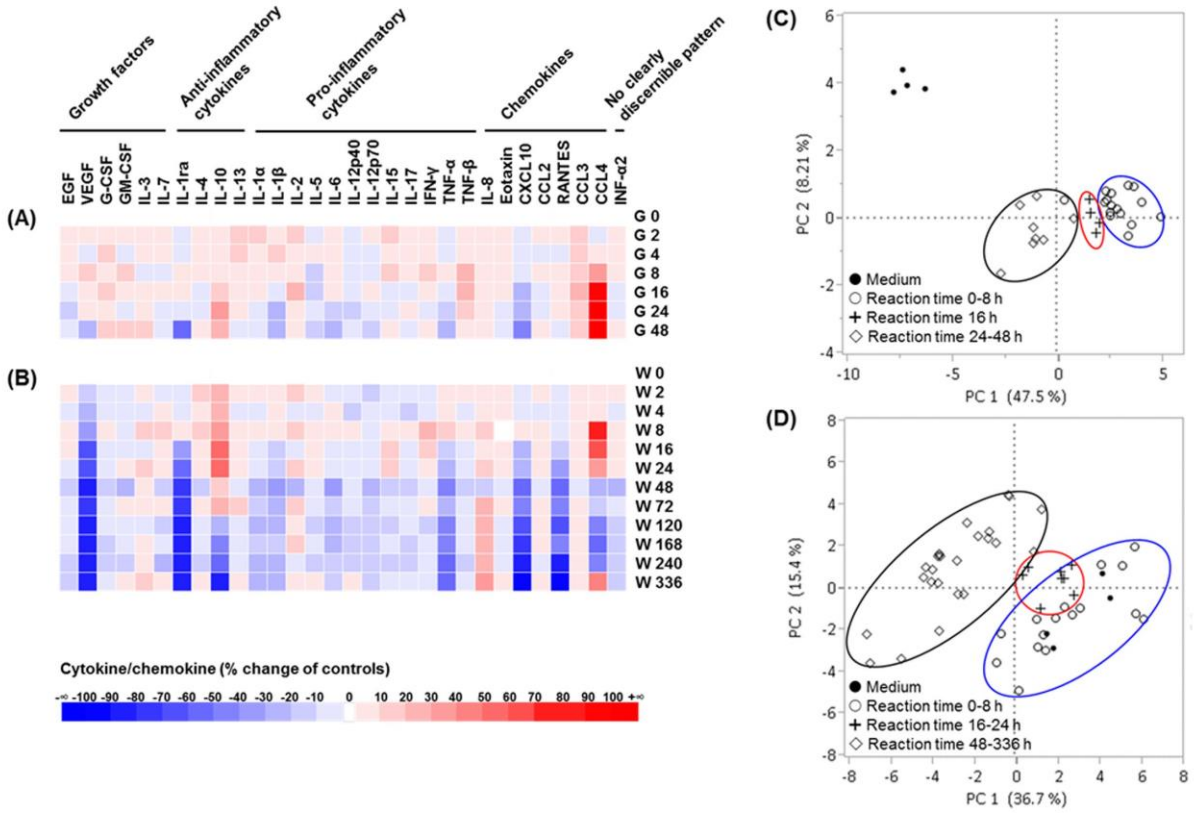

Fig 2.3 The heatmap of cytokines modulated by glycation products obtained from (A) glycine-glucose and (B) WPI-glucose systems. The %change was calculated based on the formula: $(C_x-C_0)/C_0\times100\%$, where C_x is the concentration of the cytokines/chemokines in X- h sample, and C_0 is the concentration of the cytokines/chemokines in 0-h sample. The levels of cytokines/chemokines from the 0-h sample treatment were in Supplement 4. PCA showed that the mode of cytokine/chemokine modulation was related to reaction stages in (C) glycine-glucose and (D) WPI-glucose systems.

2.4.3 Differential biological functions of EGPs and AGEs: verified by human PCa cell proliferation in vitro

Based on the results above, the 8-h samples of glycine-glucose and WPI-glucose systems were used as representative EGP samples. They significantly upregulated the productions of CCL4, IL-10, IL-4 and IL-8. These cytokines were used to map the biological functions of EGPs by functional enrichment analysis. Forty-three terms with directional alterations showing considerable enrichment ($P < 0.05$; Figure 2.4A) were grouped in functionalities of receptor interaction, signal transduction, chemotaxis, modulating innate and adaptive immunity (B and T cells), modulating cytokine secretion, host defense, as well as others such as apoptosis, anti-inflammation and anti-oxidation (Figure 2.4B). Some directionally altered terms, for example, negative regulation of IL-8 production, were likely due to the functions of the upregulated cytokines instead of direct effect of EGPs, and these terms were included in Supplement 5 together with the non-directionally altered terms.

The 48-h sample for the glycine-glucose system and 240-h sample for the WPI-glucose system were considered as AGEs. They have an overall suppressive effect on cytokine secretion, which was likely due to the cell inhibition. Therefore, it is less meaningful to perform the functional enrichment analysis using the cytokine data. Additionally, such biological functions of AGEs had been well documented [7].

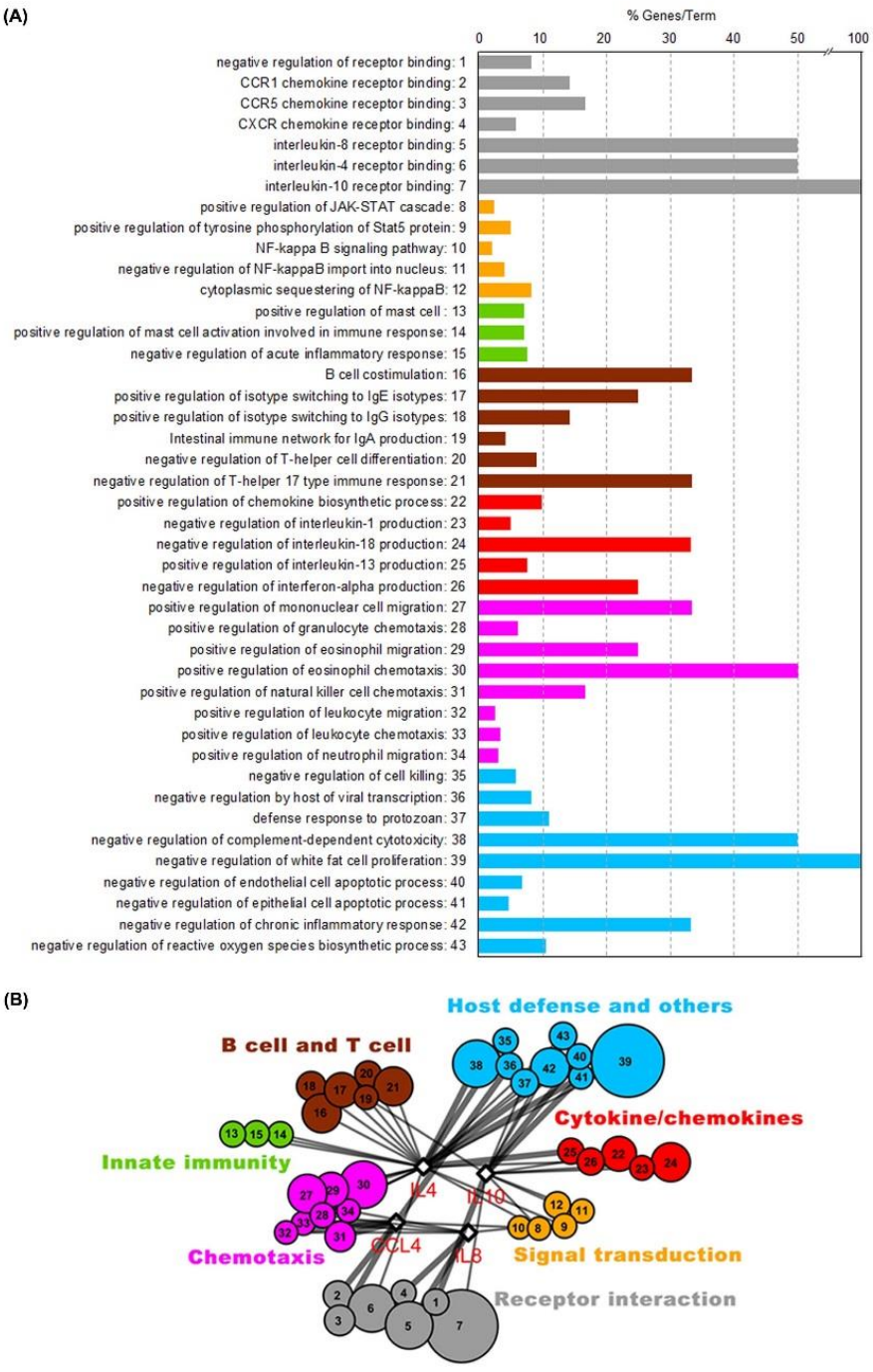

Fig 2.4 Functional enrichment analysis for EGPs based on significantly up-regulated cytokines/chemokines. (A) GO/pathway terms specific for up-regulated cytokines/chemokines. The bars represented the percentages of cytokine/chemokines associated with the term. (B) Functionally grouped network with terms were linked based on their κ score (> 0.4). The node size represented the percent association, and the numbers were corresponding to the terms numbered in (A).

To further determine the differential effects of EGPs and AGEs, WPI-glucose 0-h (NR), 8-h (EGPs), and 240-h (AGEs) samples were used to treat human PCa cell line, LNCaP. EGPs did not significantly affect the cell proliferation directly (Figure 2.5A, 5B left panel), whereas AGEs directly increased its proliferation, and the increasing effect was concentration-dependent (Figure 2.5A). However, when macrophage CM was applied to LNCaP cells, both EGPs- and AGEs-CM increased their proliferation when compared to that from NR-CM (Figure 2.5B right panel). The same experiments were conducted using a more metastatic human PCa cell line, PC-3. The PC-3 cells proliferated when EGPs or AGEs were applied to them directly (Figure 2.5C). However, EGPs-CM at the EGP non-directly proliferating concentration increased PC-3 proliferation, whereas AGEs-CM at the AGE directly proliferating concentration did not affect PC-3 cell proliferation (Figure 2.5D).

To confirm the above findings using a different system, murine peritoneal macrophages and PCa cell line TRAMP-C2 were used. AGEs but not EGPs directly increased TRAMP-C2 proliferation (Figure 2.6E, 5E, 6F 5F left panel). When compared to NR-CM, EGPs-CM but not AGEs-CM significantly increased TRAMP-C2 proliferation, although NR-CM decreased the cell proliferation relative to medium-CM (Figure 2.5F right panel). To eliminate any effects from glucose, NR, EGPs and AGEs were dialyzed to repeat the experiment in LNCaP cells. When compared to non-dialyzed samples (Figure 2.5A, 5B left panel), the direct PCa proliferative effect of AGEs disappeared (Figure 2.5G left panel), which was likely due to the fact that the small molecular AGEs were dialyzed as well. Indeed, the dialyzed AGE sample had less golden color compared to non-dialyzed sample (Figure 2.5H). However, dialyzed EGPs-CM significantly increased LNCaP cell proliferation when compared to the dialyzed NR-CM (Figure

2.5G right panel), suggesting that the tumor cell proliferative effect of EGPs-CM was due to factors secreted from macrophages.

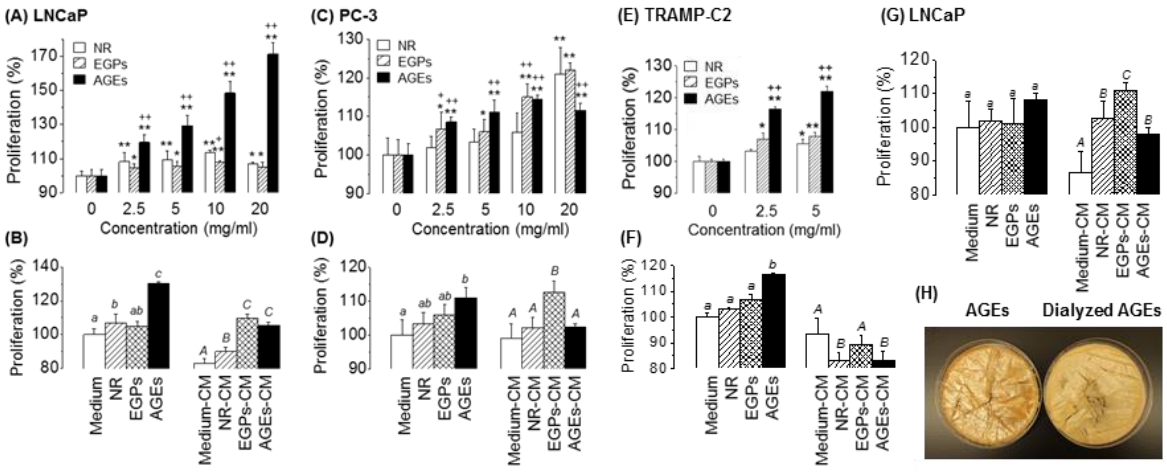

Fig 2.5 Effect of EGPs, AGEs and their conditioned media (CM) on PCa cell proliferation. (A) LNCaP cell proliferation after treatment with NR, EGPs and AGEs at different concentrations for 48 h, (C) PC-3 cell proliferation after treatment for 12 h, and (E) TRAMP-C2 cell proliferation after treatment for 24 h. *, $p < 0.05$, **, $p < 0.01$ vs. medium control; +, $p < 0.05$, ++, $p < 0.01$ vs. NR. (B) LNCaP cell proliferation after treatment with WPI-glucose samples at 5 mg/ml (left panel) or their CM (the macrophages were treated at 10 mg/ml; right panel) for 24 h, (D) PC-3 cell proliferation after treatment for 12 h, and (F) TRAMP-C2 cell proliferation after treatment with WPI-glucose samples at 2.5 mg/ml (left panel) or their CM (the macrophages were treated at 5 mg/ml; right panel) for 24 h (mean ± SD, n = 6). (G) LNCaP cell proliferation following treatment with dialyzed WPI-glucose samples. Letters in italic (lowercases for WPI-glucose samples & uppercases for CM treatment) above the bars indicate significant differences ($p < 0.05$). (H) Representative samples of AGEs and dialyzed AGEs.

2.5 Discussion

Glycation is a collection of multiple chemical reactions. The reaction species and progress are affected by various parameters, including the initial reactants. In this study, two amino sources

were studied. The glycine-glucose system has a faster glycation progress, which was probably due to the fact that the accessibility of α-NH_2 in single amino acid (glycine) is higher than the potential glycated sites in WPI. In addition, glycine-glucose reaction was chaotic [24], and it was hard to differentiate the reaction stages using the markers measured. In contrast, the WPI-glucose system showed a more organized progress: 0-8 h for the production of EGPs; 16-24 h a transition stage from early to advanced stages; and 48-336 h for the formation of AGEs.

The glycation products of early and advanced stages affected the cytokine secretion by macrophages in different directions, which suggested their potential roles in regulating immune homeostasis. EGPs exerted their effects through modulating cytokines mainly in the following four aspects: 1) activating other immune cells. Our data showed that EGPs activated the macrophages. In addition, the functional analysis expanded its effects to mast cells and B cells. 2) EGPs were immunosuppressive. The functional analysis data showed that EGPs could negatively regulate T helper cell differentiation as well as the Th17 differentiation. 3) EGPs were anti-inflammatory. The negative regulation of NF-κB signaling pathway further inhibited the pro-inflammatory cytokines. The positive regulation of JAK/STAT cascades may also be relevant to anti-inflammation. In macrophages, IL-10 activated JAK1/STAT3 to inhibit the production of pro-inflammatory cytokines through either directly modulating the transcriptional repressors and gene promoters or disturbing the components in NF-κB signaling pathway [25]. Furthermore, the expression of another inflammatory marker iNOS in PMA-differentiated U937 cells was decreased by EGPs when compared to medium and NR controls (data not shown), confirming that EGPs can induce anti-inflammation in human macrophages. 4) EGPs altered the host defense. On one hand, EGPs positively regulated the chemotaxis, but on the other hand, they

compromised the host defense by negatively regulating the IL-1 and IFN-α production, cell killing, viral transcription, and the complement system.

Although EGPs might have beneficial roles in anti-obesity and anti-oxidation through inhibition of white fat cell proliferation and reactive oxygen species (ROS) generation, its anti-apoptotic property could be one of the hallmarks to increase cancer progression. In our studies, a range of concentrations was selected in order to cover the physiological relevant dose of EGPs and AGEs. Although the physiological dose for EGPs was not known, an estimation based on previous studies [26-28] showed that the daily intake of CML is 1 mg/kg for a 70 kg adult human consuming a standard Western diet. Assuming the absorption rate was 10% [29], and the total blood volume was 5 L, the CML concentration in the blood would reach 1400 ng/ml, equivalent to 14 mg AGE-sample/ml. It should be noted that this calculation was based on average consumption of CML by an adult human and the estimated blood volume, and we did not take into consideration of tissue distribution and other body fluids. In addition, other AGEs might be absorbed at significantly different rates. This estimation, therefore, was used as a reference for the cell experiments. Instead of using a single dose, multiple concentrations ranging at 0-20 mg/ml were applied. Since EGPs and AGEs are produced in the same reaction at different stages, it is assumed that the physiological relevant concentrations of EGPs fall in the same range. At these concentrations, EGPs enhanced PCa cell proliferation in both human and murine PCa cells through modulating the macrophage to secret cytokines. Among the stimulated cytokines/chemokines in human macrophages, IL-10 and CCL4 were most upregulated: IL-10 has been associated with the tumor growth [30], and CCL4 was necessary for macrophage-mediated tumor growth [31].

AGEs directly increased the PCa cell proliferation possibly through binding to RAGE to activate P13K/Akt pathway and decrease Rb level [32]. However, LNCaP cells were more responsive to AGEs than PC-3, which might be due to the different characteristics of the two cell lines [33]. LNCaP cells retain many normal prostate cell specific properties, whereas PC-3 cells have a more aggressive phenotype. A study conducted on pancreatic cancer showed that activated RAGE was associated with the development of early pancreatic cancer precursor lesions [34]. In addition, LNCaP cells express prostate specific antigen (PSA), while PC-3 cells do not. Elangovan et al. [35] showed that silencing the RAGE on LNCaP cells inhibited the cell proliferation with a reduced PSA level. PSA transfected DU145 cells produced xenograft tumors 7-fold larger than the wild type DU145-derived tumors [36]. As for the AGEs-CM, LNCaP cells were more responsive than PC-3, possibly because LNCaP is an early stage PCa cell line and less resistant to immune attack than PC-3. Therefore, the mechanism for the proliferative effects of CM on PCa cells will be studied in future by the addition of the upregulated cytokines to exclude the additional presence of AGEs/EGPs.

In summary, glycation products regulate immune homeostasis at least in part through modulation of macrophage to secret cytokines, and do so in a glycation-stage dependent manner. EGPs increased the production of cytokines in macrophages, and enhanced the PCa cell proliferation; AGEs induced the inflammatory stress on macrophages. This study was the first to examine the biological functions of EGPs and cast doubt if glycation is an ideal way to modify the food proteins. Our *in vitro* data suggested that EGPs was possibly unsafe for PCa patients. However, based on the functions suggested by the bioinformatics analysis, EGPs are immunomodulatory

and their effect is likely disease-specific. Further mechanistic studies would provide more guidance for patients with PCa and other diseases. Our future work will focus on 1) how EGPs exacerbate PCa progression through modulating macrophages *in vivo*, and 2) if long term EGP intake will benefit the other aspects of health (e.g., prevent obesity and diabetes).

Author contributions: Y. Chen and T. L. Guo, designed the study; Y. Chen, N. M. Filipov, and T. L. Guo carried out the experiments; Y. Chen did the data analysis and bioinformatics analysis; Y. Chen wrote the manuscript, and T. L. Guo and N. M. Filipov edited it.

The authors appreciate Fonterra (USA) Inc (Rosemont, IL) for supplying WPI samples. LNCaP cell line was a gift from Dr. Lianchun Wang (Department of Biochemistry and Molecular Biology & the Complex Carbohydrate Research Center, the University of Georgia), and PC-3 cell line was a gift from Dr. Brian S. Cummings (Department of Pharmaceutical and Biomedical Sciences, the University of Georgia). This study was supported in part by NIH R21ES24487 (TL Guo) and Interdisciplinary Toxicology Program at UGA.

The authors have declared no conflict of interest.

References

1. Hodge, J.E., Dehydrated Foods - Chemistry of Browning Reactions in Model Systems. Journal of Agricultural and Food Chemistry, 1953. 1(15): p. 928-943.
2. Nagai, R., et al., Inhibition of AGEs formation by natural products. Amino Acids, 2014. 46(2): p. 261-266.

3. Singh, R., et al., Advanced glycation end-products: a review. Diabetologia, 2001. 44(2): p. 129-46.

4. Ott, C., et al., Role of advanced glycation end products in cellular signaling. Redox Biology, 2014. 2: p. 411-429.

5. Uribarri, J., et al., Advanced Glycation End Products in Foods and a Practical Guide to Their Reduction in the Diet. Journal of the American Dietetic Association, 2010. 110(6): p. 911-916.

6. Koschinsky, T., et al., Orally absorbed reactive glycation products (glycotoxins): An environmental risk factor in diabetic nephropathy. Proceedings of the National Academy of Sciences of the United States of America, 1997. 94(12): p. 6474-6479.

7. Kellow, N.J. and M.T. Coughlan, Effect of diet-derived advanced glycation end products on inflammation. Nutr Rev, 2015. 73(11): p. 737-59.

8. Oliver, C.M., L.D. Melton, and R.A. Stanley, Creating proteins with novel functionality via the Maillard reaction: A review. Critical Reviews in Food Science and Nutrition, 2006. 46(4): p. 337-350.

9. Liu, J.H., Q.M. Ru, and Y.T. Ding, Glycation a promising method for food protein modification: Physicochemical properties and structure, a review. Food Research International, 2012. 49(1): p. 170-183.

10. Noy, R. and J.W. Pollard, Tumor-Associated Macrophages: From Mechanisms to Therapy. Immunity, 2014. 41(1): p. 49-61.

11. Muscat, S., et al., Coffee and Maillard products activate NF-kappaB in macrophages via H2O2 production. Mol Nutr Food Res, 2007. 51(5): p. 525-35.

12. Wuhr, A., M. Deckert, and M. Pischetsrieder, Identification of aminoreductones as active components in Maillard reaction mixtures inducing nuclear NF-kappaB translocation in macrophages. Mol Nutr Food Res, 2010. 54(7): p. 1021-30.

13. Potzsch, S., et al., The effect of an AGE-rich dietary extract on the activation of NF-kappaB depends on the cell model used. Food Funct, 2013. 4(7): p. 1023-31.

14. Church, F.C., et al., Spectrophotometric Assay Using Ortho-Phthaldialdehyde for Determination of Proteolysis in Milk and Isolated Milk-Proteins. Journal of Dairy Science, 1983. 66(6): p. 1219-1227.

15. Fenaille, F., et al., Monitoring of beta-lactoglobulin dry-state glycation using various analytical techniques. Anal Biochem, 2003. 320(1): p. 144-8.

16. Arribas-Lorenzo, G. and F.J. Morales, Analysis, Distribution, and Dietary Exposure of Glyoxal and Methylglyoxal in Cookies and Their Relationship with Other Heat-Induced Contaminants. Journal of Agricultural and Food Chemistry, 2010. 58(5): p. 2966-2972.

17. Foster, B.A., et al., Characterization of prostatic epithelial cell lines derived from transgenic adenocarcinoma of the mouse prostate (TRAMP) model. Cancer Res, 1997. 57(16): p. 3325-30.

18. Guo, T.L., et al., Immunotoxicity of sodium bromate in female B6C3F1 mice: a 28-day drinking water study. Drug Chem Toxicol, 2001. 24(2): p. 129-49.

19. Shannon, P., et al., Cytoscape: a software environment for integrated models of biomolecular interaction networks. Genome Res, 2003. 13(11): p. 2498-504.

20. Cline, M.S., et al., Integration of biological networks and gene expression data using Cytoscape. Nat Protoc, 2007. 2(10): p. 2366-82.

21. Bindea, G., et al., ClueGO: a Cytoscape plug-in to decipher functionally grouped gene ontology and pathway annotation networks. Bioinformatics, 2009. 25(8): p. 1091-3.

22. Bindea, G., J. Galon, and B. Mlecnik, CluePedia Cytoscape plugin: pathway insights using integrated experimental and in silico data. Bioinformatics, 2013. 29(5): p. 661-3.

23. Weinberg, J.M., A. Bienholz, and M.A. Venkatachalam, The role of glycine in regulated cell death. Cellular and Molecular Life Sciences, 2016. 73(11-12): p. 2285-2308.

24. Martins, S.I.F.S. and M.A.J.S. Van Boekel, A kinetic model for the glucose/glycine Maillard reaction pathways. Food Chemistry, 2005. 90(1-2): p. 257-269.

25. Murray, P.J., The primary mechanism of the IL-10-regulated antiinflammatory response is to selectively inhibit transcription. Proc Natl Acad Sci U S A, 2005. 102(24): p. 8686-91.

26. van Rooijen, C., et al., Quantitation of Maillard Reaction Products in Commercially Available Pet Foods. Journal of Agricultural and Food Chemistry, 2014. 62(35): p. 8883-8891.

27. Hull, G.L.J., et al., N-epsilon-(carboxymethyl)lysine content of foods commonly consumed in a Western style diet. Food Chemistry, 2012. 131(1): p. 170-174.

28. Delgado-Andrade, C., et al., Maillard reaction indicators in diets usually consumed by adolescent population. Molecular Nutrition & Food Research, 2007. 51(3): p. 341-351.

29. Koschinsky, T., et al., Orally absorbed reactive glycation products (glycotoxins): an environmental risk factor in diabetic nephropathy. Proc Natl Acad Sci U S A, 1997. 94(12): p. 6474-9.

30. Zhao, S., et al., Serum IL-10 Predicts Worse Outcome in Cancer Patients: A Meta-Analysis. PLoS One, 2015. 10(10): p. e0139598.

31. Fang, L.Y., et al., Infiltrating macrophages promote prostate tumorigenesis via modulating androgen receptor-mediated CCL4-STAT3 signaling. Cancer Res, 2013. 73(18): p. 5633-46.

32. Bao, J.M., et al., AGE/RAGE/Akt pathway contributes to prostate cancer cell proliferation by promoting Rb phosphorylation and degradation. Am J Cancer Res, 2015. 5(5): p. 1741-50.

33. Russell, P.J. and E.A. Kingsley, Human prostate cancer cell lines. Methods Mol Med, 2003. 81: p. 21-39.

34. Kang, R., et al., The expression of the receptor for advanced glycation endproducts (RAGE) is permissive for early pancreatic neoplasia. Proc Natl Acad Sci U S A, 2012. 109(18): p. 7031-6.

35. Elangovan, I., et al., Targeting receptor for advanced glycation end products (RAGE) expression induces apoptosis and inhibits prostate tumor growth. Biochem Biophys Res Commun, 2012. 417(4): p. 1133-8.

36. Williams, S.A., et al., Enzymatically active prostate-specific antigen promotes growth of human prostate cancers. Prostate, 2011. 71(15): p. 1595-607.

CHAPTER 3

DIETARY EARLY GLYCATION PRODUCTS PROMOTE THE GROWTH OF PROSTATE TUMORS MORE THAN ADVANCED GLYCATION END-PRODUCTS (AGES) THROUGH MODULATION OF MACROPHAGE POLARIZATION

Chen, Y., Guo, T.L. Dietary early glycation products promote the growth of prostate tumors more than advanced glycation end-products (AGEs) through modulation of macrophage polarization. *Molecular Nutrition & Food Research* **2019**, 63(4): 1800885.

3.1 Abstract

Scope: Glycation products are ubiquitous in food at high concentrations in the Western diet. The well-controlled glycation resulting in the production of early glycation products (EGPs) has been proposed as a strategy to improve the physicochemical properties of food proteins. However, the health effects of EGPs are unknown. It has been shown that the Western diet (glycation prone) is associated with a higher mortality in prostate cancer (PCa) patients than the prudent diet; therefore, we have investigated the role of EGPs in prostate tumorigenesis.

Methods and results: C57BL/6 male mice were treated with the vehicle (water), non-reacted samples, EGPs and AGEs by gavage. EGPs (600 mg/kg/day) promoted the growth of subcutaneously transplanted TRAMP-C2 PCa cells the most among these groups. Significantly, increases in the circulation monocytes and tumor-associated M2 macrophages were observed in EGP-treated mice, and the M2/M1 ratio was also increased in the EGP group when compared to that of water and AGEs. In the human PCa cell and macrophage co-cultures, EGPs increased the spheroid size, and importantly, macrophages were also polarized toward M2.

Conclusions: EGPs induced the proliferation of PCa cells either directly or by assisting PCa cells to polarize macrophages toward M2.

3.2 Introduction

Prostate cancer (PCa) is the most frequently diagnosed cancer and the second killer of men in the U.S.[1] A recent study demonstrated that the Western diet increased the death rate in PCa patients compared to the prudent diet.[2] The Western diet is characterized by high contents of red meats, butter, high-fat dairy products and refined grains, while the prudent diet contains high amounts of vegetables, fruits, whole grains and fish.[3] One characteristic of the Western diet is that they are prone to glycation and abundant in glycation products.[4] Advanced glycation end-products (AGEs) have been extensively studied for their toxicity in both healthy people and PCa patients; however, early & intermediate glycation products (EGPs) have been neglected even though they are ubiquitous in food. On the contrary, many advantages of EGPs have been reported, such as improved thermostability[5] and altered allergenicity.[6] Our previous *in vitro* studies using murine and human PCa cell lines suggested that EGPs could promote the growth of PCa cells by modulating macrophages (Mφs), whereas AGEs directly promoted the PCa cell proliferation.[7]

Mφs are abundantly present within the tumor microenvironment (TME) at stages of cancer immunosurveillance and immunoediting,[8] and named as tumor-associated Mφs (TAMs). The dual roles of TAMs are related to their polarized status – pro-inflammatory/anti-tumoral M1 vs. anti-inflammatory/pro-tumoral M2. When Mφs were co-cultured with MKN45 cells (a human gastric adenocarcinoma cell line) and HMEC-1 cells (a human endothelial cell line), M1 reduced the invasive ability of cancer cells and the angiogenesis network, whereas M2 enhanced these processes.[9] Intraperitoneal injection of ID8 cells (a mouse ovarian cancer cell line) induced

accumulation of the M2 subtype of Mφs in the peritoneal cavity, leading to the formation of spheroids, a sign of transcoelomic metastasis.[10] Since M2 plays pivotal roles in assisting cancer cells to escape immunosurveillance and increase growth, most TAMs are referred to the M2 biased pro-tumoral Mφs.

We hypothesized that the EGPs exerted their pro-tumoral effects by polarizing Mφ towards M2. To test the hypothesis, EGPs and three controls (i.e., water, non-reacted samples (NR), AGEs) were fed to mice in two PCa murine models to evaluate their PCa promoting potential, and spheroid co-culture systems were further employed to extrapolate the animal data to human cells. We found that EGPs promoted PCa proliferation more than the notorious AGEs by polarizing Mφs towards M2.

3.3 Materials and Methods

3.3.1 PCa mouse models and treatment regimens

Male C57BL/6 mice were obtained from Jackson Laboratories (Bar Harbor, ME), and maintained in the Coverdell Vivarium at the University of Georgia. All mice were housed in polysulfone cages with access to Diet 5053 (PicoLab® Rodent Diet 20, LabDiet, MO) and filtered tap water *ad libitum*. The facility was maintained on a 12-h light/dark cycle at 21-24 °C with a relative humidity of 20-60%. All animal experiments were conducted under the protocol A2016 06-007-Y3-A2 approved by the University of Georgia Institutional Animal Care and Use Committee (IACUC).

Dietary EGPs were generated from whey protein isolate (WPI, Fonterra (USA) Inc, Rosemont, IL) and glucose (Sigma-Aldrich, St. Louis, MO) as reported before: the freeze-dried powder containing WPI and glucose was incubated at a_W of 0.53 and 55 °C for different durations (0, 8 and 240 h for NR, EGPs and AGEs, respectively).[7] C57BL/6 males (6-10 weeks) were gavaged with NR, EGPs and AGEs at the dose of 600 mg/kg/day, or water at the same volume. Since there were no physiologically relevant EGP data available, the dose was chosen based on the level of AGEs quantitated by measuring carboxymethyllysine (CML, a widely used AGE marker). It was equivalent to the amount that a mouse received from the diet[11] (323 ng CML/g Diet 5053, 100.07 μg CML/g AGE sample). Additional CML quantification in this study further supported the dose of 600 mg/kg/day was physiologically relevant. After 8 weeks of treatment, the mice were s.c. injected with 1×10^6 TRAMP-C2 cells (murine PCa cell line) in the flank area and maintained for another 3 weeks. This experiment was repeated by s.c. injecting 2×10^6 TRAMP-C2 cells after dosing with NR, EGPs or AGEs for 4 weeks.

To test the effect of a xenobiotic on the immune system, a 2-week continuous exposure is sufficient; however, a 4-week exposure results in immunological alterations that are more consistent to human.[12] Longer exposure may be considered depending on the pharmacokinetic of the compounds. In this study, both 4-week and 8-week treatments generated similar effects on PCa growth. Hence, a 4-week continuous dosing regimen was used for TRAMP-C2-Mφ co-injection model. The mice were gavaged with water, NR, EGPs and AGEs as described above, and then s.c injected a mixture of 1×10^6 TRAMP-C2 cells and 3×10^5 peritoneal Mφs. They were euthanized at post-injection day 15. Mouse Mφs were harvested by lavage from the peritoneal

cavity of C57BL/6 females after thioglycolate recruitment.[13] Each mouse was i.p. injected with 1 ml autoclaved thioglycolate solution (0.05 g/ml). After 4 days, mice were euthanized, and the peritoneal cavity was lavaged with 10 ml cold PBS. Cells were collected by centrifugation and cultured in RPMI medium (supplemented with 10% FBS, 10 mM HEPES, and 50 μg/ml gentamycin) at 37 °C with 5% CO_2 for 3-4 h. After washing 3 times with cold PBS, the adherent cells were considered Mφs, which could be dissociated by Cellstripper non-enzymatic cell dissociation solution (Corning, Manassas, VA).

Body weight (BW) was recorded weekly, and the tumor length and width were measured when the tumors were palpable. Prior to TRAMP-C2 cell injection, blood was collected in tubes with K2E (BD Microtainer, Franklin Lakes, NJ) for blood smear. The blood film was fixed with 100% methanol and then stained with Wright-Geimsa Stain (Sigma-Aldrich, St. Louis, MO). Sera were collected at week 8 and before euthanizing, and stored at -80 °C before quantitating the levels of CML and cytokines/chemokines. After euthanizing the mice, tumors were separated and weighted. A section of 0.2-0.4 g tumor was saved in PBS. Spleens were removed and placed in 3 ml PBS for further processing.

3.3.2 Serum CML level quantitation

Serum CML level was quantitated using OxiSelect CML competitive ELISA kit (Cell Biolabs, San Diego, CA) as described before.[7] The plate was coated with CML conjugates overnight (16-18 h), followed by adding 50 μl standards/diluted sera. The standards were prepared using CML-BSA provided by the manufacturer, with the detection range of 0.1-12.5 μg CML-BSA/ml

(equivalent to 4.5-576 ng CML/ml). There were no dilutions for sera from the water, NR and EGP groups, and those from the AGE group were 1:1 diluted. The CML was recognized by the anti-CML monoclonal primary antibody. After adding, the HRP-conjugated secondary antibody, substrate and stop solution were added, and the absorbance was read at 450 nm in a Synergy 4 hybrid multi-mode microplate reader (BioTek Instruments, Inc, Winooski, VT).

3.3.3 Cytokine/chemokine quantitation

The cytokines/chemokines in the sera were detected by the bead-based multiplex ELISA technique using the MILLIPLEX MAP Mouse Cytokine/Chemokine Kit (Millipore, Billerica, MA). In brief, standards/diluted serum samples (1:1 in the dilute buffer) and magnetic antibody-beads were added into each well of a 96-well plate. The plate was sealed, wrapped with foil, and incubated on an orbital shaker at 4 °C overnight. After washing, biotinylated antibodies were added and followed by the addition of streptavidin-phycoerythrin. Finally, all the beads were resuspended in 150 μl PBS, and run on a Bio-Plex (Bio-Rad, Inc., Hercules, California). Bio-Plex Manager 6.1.1 was used for data acquisition and analysis. Thirty-two cytokines/chemokines were included in the kit. The working range for IL-13 was 12.8-40,000 pg/ml, and 3.2-10,000 pg/ml for others. IL-4 was below the lower limit of quantitation of the standard curve and fell in the extrapolated range.

3.3.4 Tumor/tissue processing and flow cytometry

The immune cells were purified from tumors and spleens. Tumors were minced, and digested by DNase and collagenase (Sigma-Aldrich) at 37°C for 30 min. The digested samples were filtered through a 40 μm cell strainer to collect single cell suspensions. The leukocytes were isolated with a double Ficoll gradient (Histopaque 1077 and 1119, Sigma-Aldrich) centrifugation at 500 x g for 35 min at room temperature. Spleens were mashed, and the red blood cells were lysed with ACK lysing buffer (Gibco, Grand Island, NY) at the ratio of 1:100 (v/v) for 5 min. The solutions were removed by centrifuge at 300 x g at 4 °C for 8 min, and splenocytes were washed once using cold PBS and then resuspended in PBS.

Mφ polarization was indicated by the cell surface marker detected by flow cytometry. The immune cells were stained with antibodies (anti-mouse F4/80 (BM8, FITC, eBioscience), CD80 (16-10A1, PE-CD594, BD Horizon), CD209 (LWC06, Alexa Fluor, Novus Biologicals)) in PBS with 20% FBS at 4° C in dark for 30 min and then quantitated on a Becton Dickinson LSRII Flow Cytometer (BD Biosciences). The data were processed and analyzed using FlowJo v10 (FlowJo, LLC, Ashland, OR). M2 and M1 Mφs were characterized as $F4/80^{+}CD209^{+}CD80^{-}$ and $F4/80^{+}CD209^{-}CD80^{+}$, respectively. Fluorescence Minus One (FMO) controls were used for gating setup.

3.3.5 Western blot for iNOS quantitation

U937 cells (a human monocytic cell line, 2×10^{5}/400 μl) were pipetted into each well of flat-bottom 48-well plates, and differentiated with 10 nM phorbol 12-myristate 13-acetate (PMA) for 24 h. Another 400 μl RPMI medium with or without NR or EGPs were added with the final

concentration being 10 mg/ml. After 48 h incubation, Mφs were lysed in Pierce IP lysis buffer (Pierce Biotechnology, Rockford, IL) supplemented with protease inhibitors (Calbiochem, La Jolla, CA) for 5 min on ice. Proteins were separated by 10% SDS-PAGE gel, transferred to a Hybond-P polyvinylidene difluoride (PVDF) membrane, detected by anti-mouse/human iNOS antibody (Abcam, Cambridge, MA), and visualized by SuperSignal West Pico Chemiluminescent Substrate (Pierce Biotechnology) and Kodak Image Station 4000R Pro (Carestream Health, Inc., Rochester, NY). Carestream Molecular Imaging Software 5.0.2 was used to process the images, and the band intensities were reported.

3.3.6 Spheroid co-culture

A 50 µl of agarose (1.5% (w/v)) was added into each well of 96-well plates to create a base platform for the spheroid culture. A mixture of 1,000 LNCaP cells and 300 PMA-differentiated U937 cells (d-U937 cells) was cultured in 130 µl RPMI medium in the presence of 10 mg/ml NR, EGP or AGE samples. The media were changed every other day. The dissociation reagents were trypsin-EDTA solution (Sigma-Aldrich) for LNCaP cells and Cellstripper non-enzymatic cell dissociation solution for d-U937 cells. The spheroids were imaged by AmScope ToupView 3.7 and processed by ImageJ, or subjected to flow cytometric analysis at day 7. For the spheroids imaged by confocal macroscope (Nikon, Tokyo, Japan), LNCaP and d-U937 cells were pre-stained with MitoTracker Probes Deep Red FM and Green FM (Invitrogen Ltd., Eugene, OR) prior to co-culture, respectively. For the flow cytometric analysis, only d-U937 cells were pre-stained with Green FM. At the end of culture, the cells were stained with anti-human CD80

(2D10.4, Alex Fluor, Novus Biologicals) and CD163 (GHI/61, PE-CF594, BD Horizon) antibodies, and the other procedures were the same as described in *3.3.4*.

3.3.7 Statistical analysis

The statistical analysis was performed on JMP Pro 13 (SAS Inc., Cary, NC) using a one-way analysis of variance (ANOVA), and the differences between means were analyzed using Tukey-Kramer *post hoc* test. All tests were two-sided, and significance was accepted at $p < 0.05$.

3.4 Results

3.4.1 EGPs promote PCa growth more than AGEs

To study the potentiating effects of EGPs on PCa, C57BL/6 males were gavaged with EGPs for 8 weeks to maintain a stable serum EGP level, and then s.c. injected with TRAMP-C2 cells to mimic the post-diagnostic tumors. Water, NR and AGEs were used as controls. No significant difference was detected for the BW among the four groups within the dosing period (Fig. 3.1A), suggesting that the glycation products were not overtly toxic to the mice. Between days 9-11 after TRAMP-C2 cell injection, AGE-treated mice developed the largest tumors. After day 12, the tumors in EGP-treated mice showed a sudden increase in size and an aggressive growth in the following days (Fig. 3.1B). At day 21, the order of tumor weight from high to low was EGPs > NR, AGEs > Water (Fig. 3.1C). Similar results were produced in another independent experiment. The Ki-67 staining of the tumors showed that the EGP group had the highest

percentage of proliferating cells, which was followed by the groups of AGEs and NR (Fig. S1). All the results indicated that EGPs promoted s.c. PCa growth the most *in vivo*.

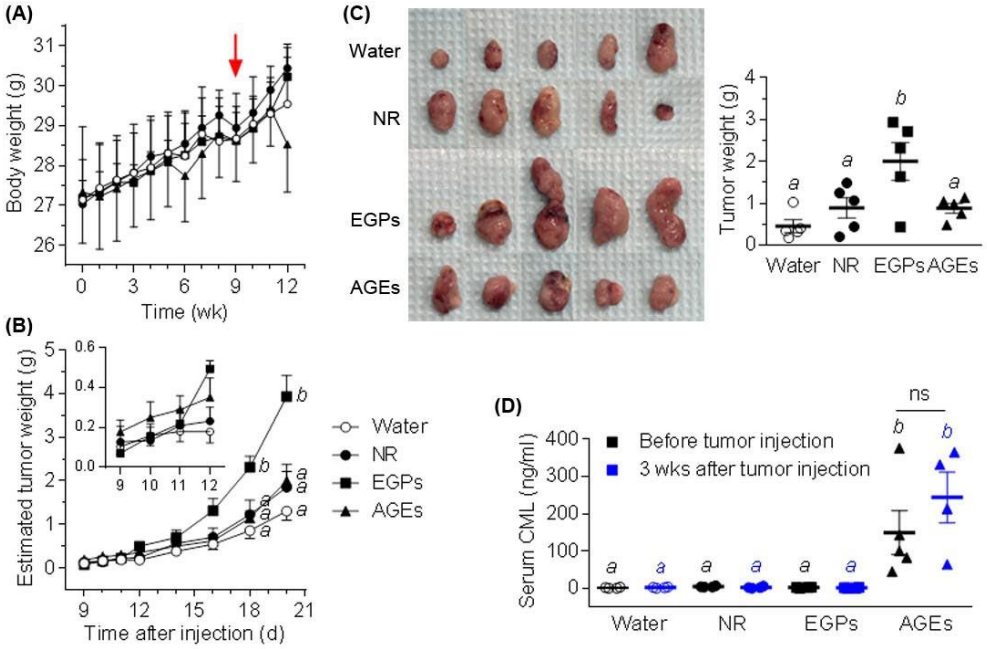

Fig 3.1 EGPs promote PCa more than AGEs *in vivo*. Male C57BL/6 mice were gavaged with water, NR, EGPs or AGEs for 8 weeks and then 1×10^6 TRAMP-C2 cells were s.c. injected in the flank area. (A) BWs were recorded weekly. Red arrow indicated the date for TRAMP-C2 cell injection. (B) The weight of the s.c. tumor was estimated as: length × width^2/2000 (g). (C) The tumors were separated and weighted after the mice were euthanized. (D) Serum CML levels before and after tumor injection (mean ± SE, n = 5). One mouse in the AGE group (serum CML level at 375.63 ng/ml before tumor injection) showed tumor necrosis and moribundity prior to the end of the experiment. *a*, *b*, $p < 0.05$; ns, not significant.

Because EGPs were precursors of AGEs, and AGEs promoted PCa cell proliferation directly,[7] the serum CML levels in the mice before and after tumor injection were measured to determine if the PCa-promoting effect of EGPs *in vivo* was due to the conversion of EGPs to AGEs. Fig. 3.1D showed that mice from the water, NR and EGP groups had their serum CML levels at the baseline. In contrast, mice from the AGE group had significantly elevated serum CML levels

after dosing for 8 weeks, and those were further increased after tumor growing. These findings indicated that EGPs had their distinctive ways to promote PCa proliferation that were independent of AGEs.

3.4.2 Mφs are involved in the PCa promoting effect of EGPs

The cytokines/chemokines were detected, and the fold changes compared to water control were shown in the heatmap (Fig. 3.2A) with original data and detected significance shown in Table S1. NR produced small changes compared to water. EGPs decreased G-CSF, IL-4 and IL-5, and increased IL-7, IL-10, LIF and MIG. Among those significantly increased by EGPs, IL-10 was known to be anti-inflammatory. AGEs increased IL-6, IL-12p70, IL-17 and RANTES, with the pro-inflammatory IL-12p70 up-regulated most. When comparing EGPs to AGEs, several cytokines were oppositely regulated: the pro-inflammatory IL-6 and IL-17 were down-regulated by EGPs but up-regulated by AGEs, and the pro-tumoral IL-7 and LIF were up-regulated by EGPs but down-regulated by AGEs. White blood cell (WBC) counting showed that, after 8 weeks of treatment, EGPs slightly increased %WBCs (Fig. 3.2B upper panel) and significantly increased %monocytes (Fig. 3.2B lower panel). These data suggested that EGPs were anti-inflammatory in C57BL/6 males and could regulate monocytes, which might lead to an M2 biased M2/M1 balance. In addition, increased spleen weights were observed in EGP-dosed tumor-bearing mice (Fig. 3.2C). Although the spleen weight did not correlate with the tumor weight in the EGP group, they were highly correlated in other three groups (Fig. 3.2D), indicating that EGPs had a greater disruption of the immunosurveillance than the other treatments.

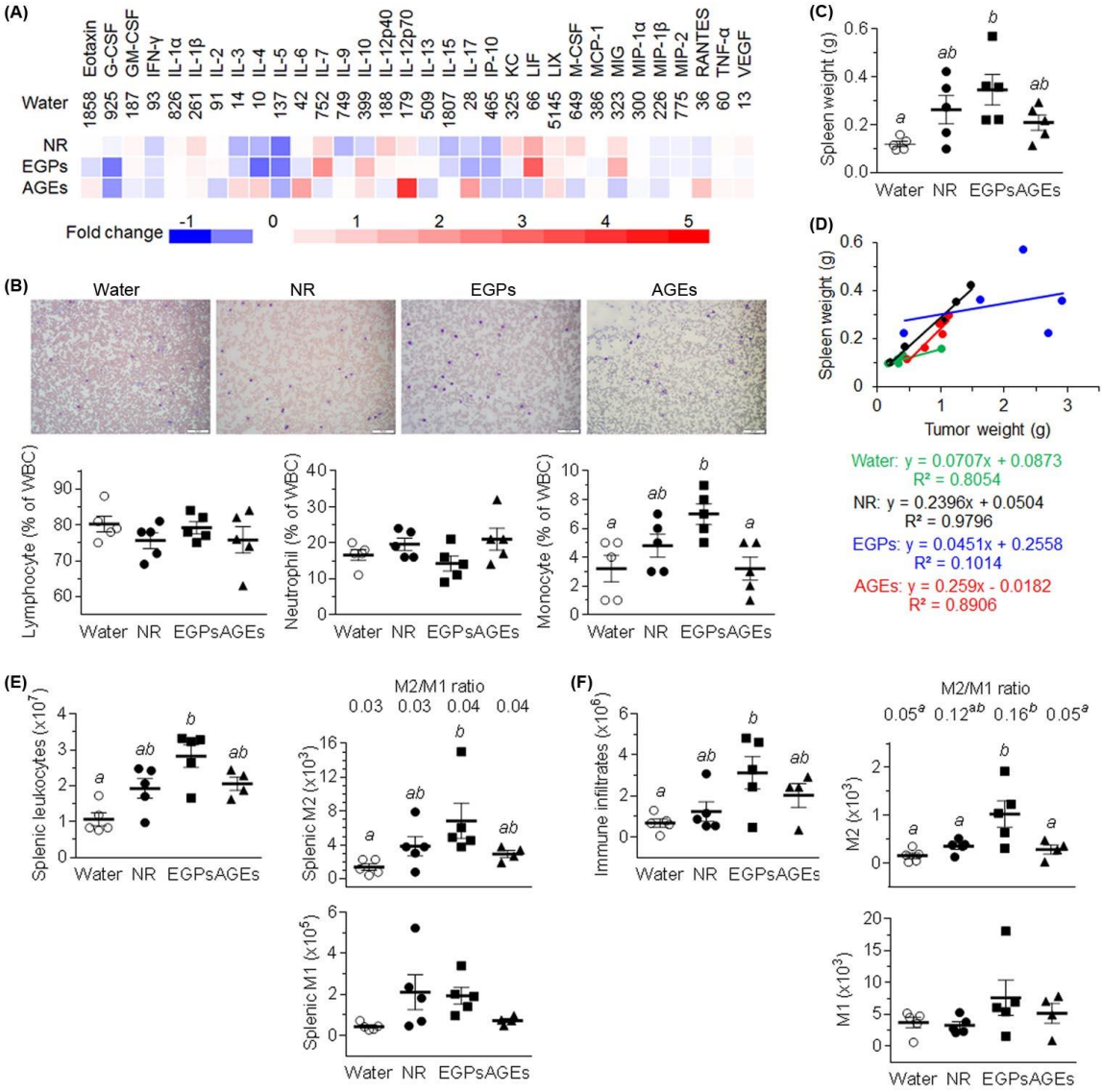

Fig 3.2 EGPs facilitate TAM polarization toward M2. After the C57BL/6 males were dosed for 8 weeks, the systemic immunity was altered: (A) heatmap showing the alteration of serum cytokine/chemokine levels, and (B) counts of WBC differentials showing that EGP treatment specifically increased the %monocytes in the circulation. The color of each slide was calibrated with its own background. Red dots were red blood cells, and purple circles were WBCs, which were further identified according to their morphologies (Fig. S2) (mean ± SE, n = 5). The TRAMP-C2 cells were s.c. injected thereafter and grew for 21 days. After euthanized the mice, (C) spleens were weighted. (D) The correlation between the spleen weights and the tumor weights. (E) The splenic leukocytes and macrophages, and (F) total immune infiltrates in the tumors and TAMs were analyzed (mean ± SE, n = 4-5). *a*, *b*, $p < 0.05$.

All the immunological findings implied that EGPs were likely to exert the pro-tumoral effects through regulating Mφs to become the anti-inflammatory subtype, so the splenic Mφs and TAMs were studied by analyzing the differential expression of CD80 (an M1 marker) and CD209 (an M2 marker).[14] When compared to water, NR and AGEs, EGPs increased total splenic leukocytes (Fig. 3.2E left panel), M2 (Fig. 3.2E right panel) and other cell populations (e.g., NK cells and $CD8^+$ T cells; data not shown). These results indicated a non-specific and systematic immune activation by EGPs. In addition, the M2/M1 ratio was slightly increased by EGPs compared to water and NR (Fig. 3.2E right panels), suggesting a shifted balance towards anti-inflammation in EGP-treated mice. In the tumor immune infiltrates, however, the M2/M1 ratio of the EGP group was significantly increased compared to the water and AGE groups (Fig. 3.2F right panels). Furthermore, the absolute numbers of M2 in tumors were significantly higher than all other groups. These results suggested that EGPs polarized Mφs towards M2 either directly or by assisting PCa cells to do so.

Direct injection of immune cells had been used in regulating PCa initiation[15] and treating PCa.[16] TAMs in solid tumors could proliferate in situ[17], and TAM accumulation was found to positively correlate with chemoattractants involved in monocyte recruitment.[18] Therefore, a mixture of TRAMP-C2 cells and peritoneal Mφs was s.c. injected into the flank area of C57BL/6 males to further illustrate the function of Mφs in EGP-promoted PCa growth. After the tumor grew for 2 weeks, a decrease in BW was observed in the EGP group, indicating a rapid tumor growth (Fig. 3.3A), which was confirmed by the estimated tumor weight (Fig. 3.3B). Tumors grew faster in the presence of pre-injected Mφs than tumor cells alone (Fig. 3.3B vs. Fig. 3.1B): the EGP-dosed mice had tumors being palpable at day 3 after injection, while the other three

groups had tumors being palpable between days 7-9 (Fig. 3.3B). At day 15, tumors in the EGP-dosed mice had an average weight of 2 g, while the others had average tumor weights between 0.6-0.9 g (Fig. 3.3C).

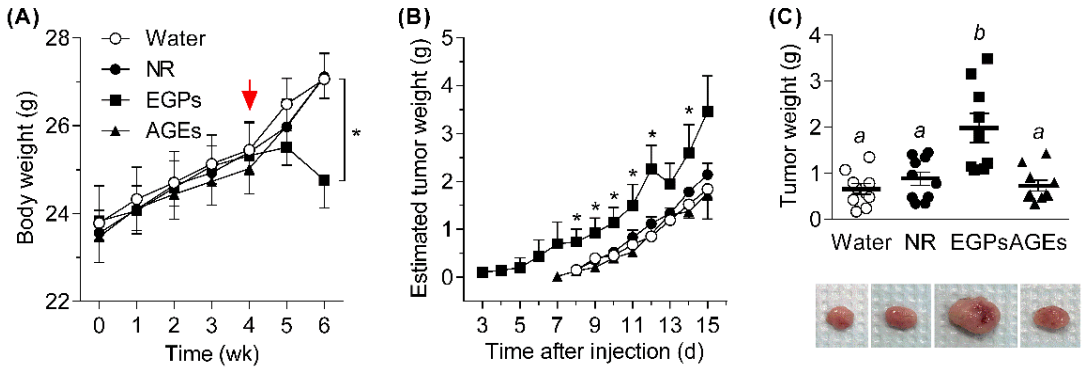

Fig 3.3 TAMs enhance the PCa-proliferating effect of EGPs *in vivo*. Male C57BL/6 mice were gavaged with water, NR, EGPs or AGEs for 4 weeks and then a mixture of TRAMP-C2 cells and peritoneal Mφs was s.c. injected in the flank area. (A) BWs were recorded weekly. Red arrow indicated the date for TRAMP-C2 cell injection. (B) The weight of the s.c. tumor was estimated as: length × width^2/2000 (g), and the non-palpable tumors were recorded as "0 g". The average weight was plotted when it was larger than "0 g". (C) The tumors were separated and weighted after the mice were euthanized. Representative tumor pictures were shown. One case of metastasis occurred in the EGP group (mean ± SE, n = 9-10). *, $p < 0.05$ vs either water, NR or AGEs control; *a, b, c*, $p < 0.05$.

3.4.3. EGPs promote human PCa cell proliferation by polarizing Mφs towards M2

Consistent with *in vivo* observations, EGPs increased the spheroid size of *in vitro* murine cell co-culture when the applied concentrations were below 2.5 mg/ml (Fig. S3). The actual differences in spheroid sizes among the groups were likely larger because the pictures captured the areas of a maximal cross section of the spheroids. To extrapolate the findings from the mouse model to humans, this co-culture system was extended to human PCa cell line LNCaP cells and d-U937 Mφs. Similarly, EGP treatment produced the largest spheroid (Fig. 3.4A&B) with the highest

number of viable Mφs indicated by the intensity of green fluorescence (Fig. 3.4A). The Mφ polarization (CD80 as the M1 marker and CD163 as the M2 marker)[14] within the spheroids was further analyzed using flow cytometry. The results showed that EGP treatment induced the highest M2 polarization (Fig. 3.4C&D). To further confirm the effect of EGPs on Mφ polarization, d-U937 cells were cultured alone with medium, NR and EGPs, and the iNOS (an M1 marker) expression was quantitated by Western blots. EGPs significantly down-regulated the expression of iNOS (Fig. 3.4E). The M2 marker, Arginase 1, was not inducible in this cell line even upon IL-4 and IL-10 stimulation.[19]

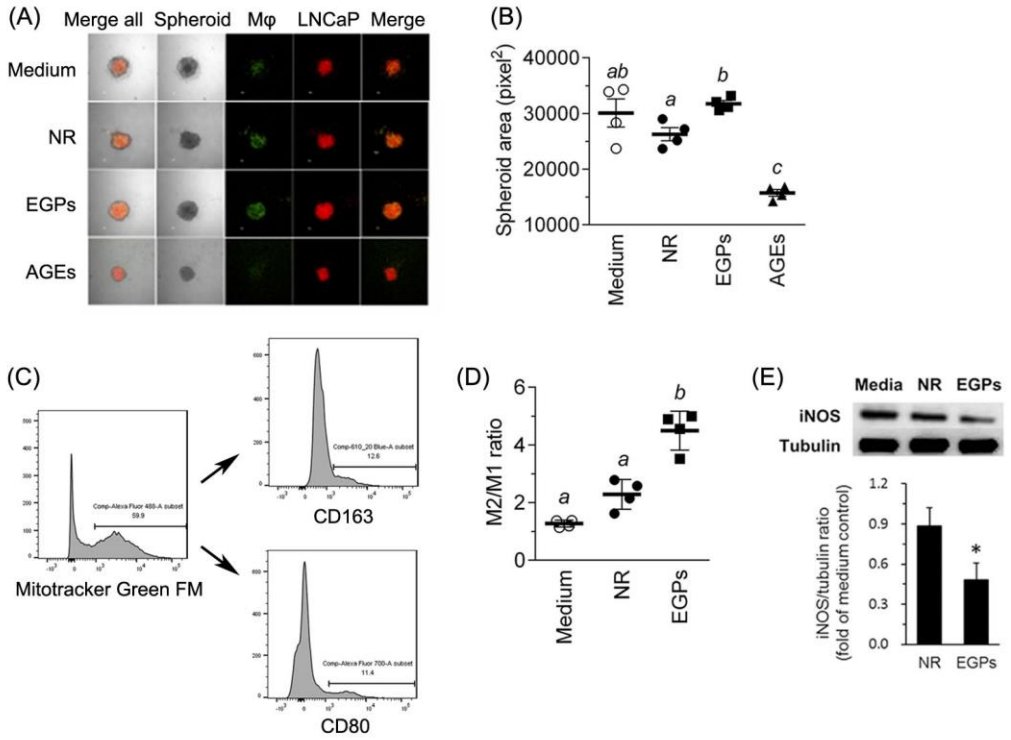

Fig 3.4 EGPs promote the co-cultured spheroid growth by polarizing Mφ towards M2. (A) Representative images of the spheroids, and (B) the areas of the maximal cross section of the spheroids. The Mφ polarization was studied using flow cytometry. The gating strategies were shown in (C), and the M2/M1 ratios in the spheroids shown in (D) were calculated as $\%CD163^{+}/\%CD80^{+}$ (mean ± SE, n = 4). No Mφs (Green FM) were detected after AGE treatment, likely due to cytotoxicity. (E) iNOS expression by d-U937 cells after treated with medium, NR or EGPs for 48 h (mean ± SE, n = 3). *, *a*, *b*, *c*, $p < 0.05$.

3.5 Discussion

Several observations from this study using different *in vivo* and *in vitro* models supported the notion that EGPs promoted PCa via regulating Mφs. In our first animal study, EGP treatment generated the largest tumor of s.c. transplanted PCa with the highest percentage of proliferating cells, despite that two cases of moribundity occurred in the AGE group. When Mφs were mixed into the transplanted PCa cells, EGP-dosed mice had the largest tumors, and required one week less time to reach the same tumor weight when PCa cells were injected alone. Additionally, no moribundity occurred in the AGE group while one case of metastasis occurred in the EGP group. These findings suggested that Mφs were involved in the EGP-promoted PCa development. The mechanistic studies revealed that EGPs biased the Mφ polarization towards M2 in murine models and human Mφs, and this regulatory effect of EGPs was further enhanced in the TME. Since cancer cells were reported to secrete factors to polarize Mφs toward a pro-tumoral M2 phenotype,[20] it was likely that EGPs facilitated these functions of the PCa cells. When a higher M2 polarization existed in the TME of EGP-dosed mice, the M2-polarized TAMs contributed to the immunosuppressive microenvironment,[21] and thus, the promotion of tumor growth and metastasis,[22] as reported for PCa.[23] This study focused on PCa proliferation and tumor size, and the results suggested that other tumor processes (i.e., migration, angiogenesis, necrosis/apoptosis, tumor infiltrating lymphocytes) might also be affected, which require further studies.

AGEs were known as cancer initiators and promoters, and this study further confirmed it. Dietary AGE consumption contributed to the body's AGE pool, evidenced by increased serum

AGE/CML levels in both humans[24] and C57BL/6 mice.[11] PCa growth and increased tumor grades could also elevate AGE levels.[25] In this study, consumption of rodent diet (Diet 5053) did not increase the serum CML level to reach the threshold of detection[24] in mice. Oral administration of additional AGEs increased the CML level in sera, and this amount of AGEs did not generate overt toxicity to healthy mice but promoted the PCa development. Glycative stress from AGEs was concluded as a factor for cancer onset and progression, including PCa, and activation of the receptor for AGEs (RAGE)/sRAGE was considered the major molecular mechanism.[26] Previous studies identified an increased expression of RAGE on both PCa cells[25] and pro-tumoral TAMs (in Glioma).[27] For example, HMGB1, a ligand of RAGE, was reported to activate RAGE-SOCS1/SHIP-1 axis, and thus, polarize Mφ towards M2.[9] However, RAGE-mediated M2 polarization was not the mechanism for this study, because the dietary AGE-promoted effect was attenuated when Mφs were mixed with the PCa cells. It was possible, however, that certain AGEs upregulated pro-inflammatory cytokines/chemokines, which were also observed in human Mφs,[28] and this Th1-like inflammatory response could increase cancer cell death. Therefore, the effect of AGEs on PCa was possibly due to the balance of direct cancer promoting effects and upregulation of pro-inflammatory responses.

In summary, this study showed that dietary EGPs polarized the Mφ towards M2 either directly or by assisting the PCa cells to do so, which in turn helped maintain the immunosuppressive environment for tumor growth. Although a larger tumor is not necessarily synonymous with tumor progression, the novel findings demonstrated the interference of diet/nutrients on the systematic immunity and thus the immunosurveillance for PCa, emphasizing the importance of diet for immunotherapy development in PCa patients.

Author contributions: Y. Chen and T. L. Guo designed the study. Y. Chen and T. L. Guo did the animal experiments, Y. Chen performed the cell experiments, T. L. Guo conducted the flow cytometry. Y. Chen analyzed the data. Y. Chen wrote the manuscript, and T. L. Guo edited it.

Acknowledgement: The authors thank Fonterra (USA) Inc (Rosemont, IL) for supplying WPI samples. LNCaP cell line was a gift from Dr. Lianchun Wang (Department of Biochemistry and Molecular Biology & the Complex Carbohydrate Research Center, UGA). Anti-iNOS antibody was provided by Dr. Shiyou Chen (Department of Physiology and Pharmacology, UGA). The authors would like to thank Dr. Tamas Nagy (Department of Pathology, UGA) for helping with IHC slides, Drs. Thomas M. Krunkosky and Robert M. Gogal (VBDI, UGA) with Western blot analysis, and CVM Cytometry Core Facility (the College of Veterinary Medicine, UGA) for assisting confocal microscopic and flow cytometric analysis. This study was supported in part by NIH R21ES24487 (TL Guo), NIH R41AT009523 (TL Guo) and Interdisciplinary Toxicology Program at UGA.

References

1. R. L. Siegel, K.D. Miller, A. Jemal, Cancer statistics, 2018. CA Cancer J. Clin. 2018, 68, 7.

2. M. Yang, S. A. Kenfiled, E. L. van Blarigan, J. L. Batista, H. D. Sesso, J. Ma, M. J. Stampfer, J. E. Chavarro, Dietary patterns after prostate cancer diagnosis in relation to disease-specific and total mortality. Cancer Prev. Res. (Phila) 2015, 8, 545.

3. F. B. Hu, Dietary pattern analysis: a new direction in nutritional epidemiology. Curr. Opin. Lipidol. 2002, 13, 3.

4. J. Uribarri, S. Woodruff, S. Goodman, W. Cai, X. Chen, R. Pyzik, A. Yong, G. E. Striker, H. Vlassara, Advanced glycation end products in foods and a practical guide to their reduction in the diet. J. Am. Diet Assoc. 2010, 110, 911.

5. Y. Chen, X. Chen, T. L. Guo, P. Zhou, Improving the thermostability of beta-lactoglobulin via glycation: the effect of sugar structures. Food Res. Int. 2015, 69, 106.

6. M. Perusko, M. van Roest, D. Stanic-Vucinic, P. J. Simons, R. H. H. Pieters, T. C. Velickovic, J. J. Smit, Glycation of the major milk allergen beta-lactoglobulin changes its allergenicity by alterations in cellular uptake and degradation. Mol. Nutr. Food Res. 2018, 62, 1800341.

7. Y. Chen, N. M. Filipov, T. L. Guo, Dietary glycation products regulate immune homeostasis: early glycation products promote prostate cancer cell proliferation through modulating macrophages. Mol. Nutr. Food Res. 2018, 62, 1700641.

8. G. P. Dunn, L. J. Old, R. D. Schreiber, The immunobiology of cancer immunosurveillance and immunoediting. Immunity 2004, 21, 137.

9. A. Rojas, F. Delgado-Lopez, R. Perez-Castro, I. Gonzalez, J. Romero, I. Rojas, P. Araya, C. Anazco, E. Morales, J. Llanos, HMGB1 enhances the protumoral activities of M2 macrophages by a RAGE-dependent mechanism. Tumour Biol. 2016, 37, 3321.

10. M. Yin, X. Li, S. Tan, H. J. Zhou, W. Ji, S. Bellone, X. Xu, H. Zhang, A. D. Santin, G. Lou, W. Min, Tumor-associated macrophages drive spheroid formation during early transcoelomic metastasis of ovarian cancer. J. Clin. Invest. 2016, 126, 4157.

11. W. Cai, M. Ramdas, L. Zhu, X. Chen, G. E. Striker, H. Vlassara, Oral advanced glycation endproducts (AGEs) promote insulin resistance and diabetes by depleting the antioxidant defenses AGE receptor-1 and sirtuin 1. Proc. Natl. Acad. Sci. U. S. A. 2012, 109, 15888.

12. T. L. Guo, K. L. White, Methods to access immunotoxicity. in Comprehensive Toxicology, Vol 5 (Eds: C. A. McQueen), Elsevier, Waltham, MA, USA 2010, Ch. 5.30.

13. X. Zhang, R. Goncalves, D. M. Mosser, The isolation and characterization of murine macrophages. Curr. Protoc. Immunol. 2008, Ch. 14, Unit 14 1.

14. Y. Xu, R. Romero, D. Miller, L. Kadam, T. N. Mial, O. Plazyo, V. Garcia-Flores, S. S. Hassan, Z. Xu, A. L. Tarca, S. Drewlo, N. Gomez-Lopez, An M1-like macrophage polarization in decidual tissue during spontaneous preterm labor that is attenuated by rosiglitazone treatment. J. Immunol. 2016, 196, 2476.

15. L. Y. Fang, K. Izumi, K. P. Lai, L. Liang, L. Li, H. Miyamoto, W. J. Lin, C. Chang, Infiltrating macrophages promote prostate tumorigenesis via modulating androgen receptor-mediated CCL4-STAT3 signaling. Cancer Res. 2013, 73, 5633.

16. Q. Zhang, T. L. Jang, X. Yang, I. Park, R. E. Meyer, S. Kundu, M. Pins, B. Javonovic, T. Kuzel, S. J. Kim, L. van Parijs, N. Smith, L. Wong, N. M. Greenberg, Y. Guo, C. Lee, Infiltration of tumor-reactive transforming growth factor beta insensitive CD8+ T cells into the tumor parenchyma is associated with apoptosis and rejection of tumor cells. Prostate 2006, 66, 235.

17. P. Tymoszuk, H. Evens, V. Marzola, K. Wachowicz, M. H. Wasmer, S. Datta, E. Muller-Holzner, H. Fiegl, G. Bock, N. van Rooijen, I. Theurl, W. Doppler, In situ proliferation contributes to accumulation of tumor-associated macrophages in spontaneous mammary tumors. Eur. J. Immunol. 2014, 44, 2247.

18. C. Murdoch, A. Giannoudis, C. E. Lewis, Mechanisms regulating the recruitment of macrophages into hypoxic areas of tumors and other ischemic tissues. Blood 2004, 104, 2224.

19. M. Munder, F. Mollinedo, J. Calafat, J. Canchado, C. Gil-Lamaignere, J. M. Fuentes, C. Luckner, G. Doschko, G. Soler, K. Eichmann, F. M. Muller, A. D. Ho, M. Goerner, M. Modolell, Arginase I is constitutively expressed in human granulocytes and participates in fungicidal activity. Blood 2005, 105, 2549.

20. S. Sousa, R. Brion, M. Lintunen, P. Kronqvist, J. Monkkonen, P. L. Kellokumpu-Lehtinen, S. Lauttia, O. Tynninen, H, Hoensuu, D. Heymann, J. A. Maatta, Human breast cancer cells educate macrophages toward the M2 activation status. Breast Cancer Res. 2015, 17, 101.

21. I. Daurkin, E. Eruslanov, T. Stoffs, G. Q. Perrin, C. Algood, S. M. Gilbert, C. J. Rosser, L. M. Su, J. Vieweg, S. Kusmartsev, Tumor-associated macrophages mediated immunosuppression in the renal cancer microenvironment by activating the 15-lipoxygenase-2 pathway. Cancer Res. 2011, 71, 6400.

22. L. Shen, A. Sundstedt, M. Ciesielski, K. M. Miles, M. Celander, R. Adelaiye, A. Orillion, E. Ciamporcero, S. Ramakrishnan, L. Ellis, R. Fenstermaker, S. I. Abrams, H. Eriksson, T. Leanderson, A. Olsson, R. Pili, Tasquinimod modulates suppressive myeloid cells and enhances cancer immunotherapies in murine models. Cancer Immunol. Res. 2015, 3, 136.

23. Y. Yin, X. Huang, K. D. Lynn, P. E. Thorpe, Phosphatidylserine-targeting antibody induces M1 macrophage polarization and promotes myeloid-derived suppressor cell differentiation. Cancer Immunol. Res. 2013, 1, 256.

24. T. Koschinsky, C. J. He, T. Mitsuhashi, R. Bucala, C. Liu, C. Buenting, K. Heitmann, H. Vlassara. Orally absorbed reactive glycation products (glycotoxins): an environmental risk factor in diabetic nephropathy. Proc. Natl. Acad. Sci. U. S. A. 1997, 94, 6474.

25. D. Foster, L. Spruill, K. R. Walter, L. M. Nogueira, H. Fedarovich, R. Y. Turner, M. Ahmed, J. D. Salley, M. E. Ford, V. J. Findlay, D. P. Turner. AGE metabolites: a biomarker linked to cancer disparity? Cancer Epidemiol. Biomarkers Prev. 2014, 23, 2186.

26. J. A. Lin, C. H. Wu, C. C. Lu, S. M. Hsia, G. C. Yen, Glycative stress from advanced glycation end products (AGEs) and dicarbonyls: an emerging biological factor in cancer onset and progression. Mol. Nutr. Food Res. 2016, 60, 1850.

27. X. Chen, L. Zhang, I. Y. Zhang, J. Liang, H. Wang, M. Ouyang, S. Wu, A. C. C. da Fanseca, L. Weng, Y. Yamamoto, H. Yamamoto, R. Natarajan, B. Badie, RAGE expression in tumor-associated macrophages promotes angiogenesis in glioma. Cancer Res. 2014, 74, 7285.

28. M. Pertynska-Marczewska, S. Kirakidis, R. Wait, J. Beech, M. Feldmann, E. M. Paleolog, Advanced glycation end products upregulate angiogenic and pro-inflammatory cytokine production in human monocyte/macrophages. Cytokine 2004, 28, 35.

CHAPTER 4

GLYCATED WHEY PROTEINS PROTECT NOD MICE AGAINST TYPE 1 DIABETES BY INCREASING ANTI-INFLAMMATORY RESPONSES AND DECREASING AUTOREACTIVITY TO SELF-ANTIGENS

Chen, Y., Nagy, T., Guo. T.L. *Journal of Functional Foods* **2019**, 56, 171-181. Reprinted here with permission of publisher

4.1 Abstract

Our previous studies suggested that early glycation products (EGPs) generated in the first step of Maillard reaction/glycation were anti-inflammatory. The objectives of the present study were to determine the effects of EGPs derived from the whey protein isolate (WPI)-glucose system on type 1 diabetes (T1D), and the underlying immunological mechanisms. In non-obese diabetic (NOD) mice, EGPs at the physiological dose of 600 mg/kg/day increased glucose metabolism, decreased non-fasting blood glucose levels and T1D incidence, decreased insulin resistance, and decreased the pancreatic immune infiltration. The protective effects were accompanied with decreases in $CD4^{-}CD8^{+}$ thymocytes, $CD8^{+}$ T cells and serum insulin autoantibody levels, and increases in splenic $CD4^{+}CD25^{+}$ T cells, macrophage M2/M1 ratio and serum IL-10 level. However, similar treatment with EGPs produced minimal effect on the multiple low-dose streptozotocin-induced hyperglycemia. In conclusion, EGPs protected NOD mice against T1D via increasing anti-inflammatory immune responses and decreasing autoreactivity to self-antigens.

4.2 Introduction

Type 1 diabetes (T1D) is a disease due to autoimmune destruction of insulin-producing pancreatic β-cells. In the non-obese diabetic (NOD) mouse, one of the murine models for human T1D, innate immune cells (e.g., dendritic cells, macrophages, neutrophils) infiltrate the pancreas as early as 3 weeks of age, and then attract $CD4^+$ and $CD8^+$ T cells into the pancreas at 4-6 weeks of age (Pearson, Wong, & Wen, 2016) to abruptly initiate insulitis (intra-islet inflammatory infiltrate). The mechanisms of T cell induced β-cell death include: 1) direct cell-cell contact through recognition of MHC class I molecules by $CD8^+$ T cells; 2) killing β-cells through surface receptor or secreted cytokines/chemokines by recognizing β-cell antigen presented by antigen-presenting cells (APCs; e.g., B cells, macrophages) (Mathis, Vence, & Benoist, 2001). T cells further recruit other immune cells to directly kill β-cells or facilitate the function of T cells. Other important pancreatic infiltrates are B cells and macrophages. B cell plays as APC and costimulator for T cells, and boosts the production of autoantibodies (Pearson et al., 2016). Macrophage is a vital APC and cytokine/chemokine-secreting cell.

Anti-inflammatory agents have the potential for T1D prevention. For example, the anti-inflammatory protein, alpha1-antitypsin (AAT), prevented T1D in NOD mice (Song et al., 2004) and reduced %HbA1c and pancreatic autoantibodies in newly diagnosed T1D children/adolescents (Rachmiel et al., 2016). Anti-inflammatory components from diet, such as polyherbal supplementation that decreased NF-κB activity and chemotaxis chemokines (i.e., CCL2 and CXCL10) in 832/13 rat insulinoma cells, could stabilize blood glucose level (BGL) and prevent T1D in NOD mice with decreased $CD3^+$ infiltrates in the pancreas (Burke et al.,

2015). Early glycation products (EGPs) refers to the Schiff base and Amadori (or Heyns) compounds generated at the first few steps of glycation (Beisswenger, 2012). and continuous reactions will lead to the production of notorious advanced glycation end-products (AGEs). AGEs are ubiquitous in foods (Uribarri et al., 2010), and about 10% of the orally consumed AGEs are absorbed in the gastrointestinal tract (Koschinsky et al., 1997) and contribute to body's AGE pool. When the parental NOD8.3 male and NOD/ShiLt female mice were exposed to a diet containing AGE during the periods of pregnancy and lactation, the AGE exposed female offspring had elevated circulating AGEs and exacerbated insulitis (Borg et al., 2018), suggesting that dietary AGEs could contribute to the initiation and exacerbation of T1D. However, the consumption of infant formula, which had higher Nε-(carboxymethyl)lysine (CML) level (an AGE marker) compared to breast milk, did not change the BGL or plasma insulin level in old infants (Klenovics et al., 2013), suggesting other components in the infant formula might be anti-hyperglycemia. The quantitation of early and advanced glycation markers showed that EGPs considerably outweighed AGEs in infant formulas regardless of the product forms and processing methods (Birlouez-Aragon et al., 2004; Hegele, Buetler, & Delatour, 2008).

Our previous studies reported that dietary EGPs could regulate the inflammatory process when applied to human macrophages (phorbol 12-myristate 13-acetate (PMA)-differentiated-U937 cells) (Y. Chen, Filipov, & Guo, 2018), and polarize tumor-associated macrophages toward the anti-inflammatory phenotype M2 in C57BL/6 male mice (Chen & Guo, 2019), which implied an protective effect of EGPs against autoimmune dysregulation. Furthermore, the oral consumption of whey protein derived EGPs did not increase the serum CML level, excluding the possibility of biotransformation of EGPs into AGEs in physiological conditions (Chen & Guo, 2019).

Therefore, it was hypothesized that EGPs could protect against T1D through the regulation of immune responses. To test this hypothesis, two T1D murine models were employed. EGPs delayed the T1D onset and reduced the T1D incidence in the autoimmune prone NOD mice. However, minimal effects were observed in the multiple low dose (MLD) streptozotocin (STZ)-induced hyperglycemia in C57BL/6 females, in which chemical destruction of pancreatic β-cells was the major mechanism. Because these EGPs are produced from food-grade raw materials involving only well-controlled heating, they are still considered food. Therefore, the beneficial effect observed on T1D prevention would highly qualify EGPs as nutraceuticals or medical food for patients with insulitis and T1D.

4.3 Material and methods

4.3.1 EGP preparation and identification

Dietary EGPs were generated from whey protein isolate (WPI, Fonterra (USA) Inc, Rosemont, IL) and glucose (Sigma-Aldrich, St. Louis, MO). They were prepared as described before (Chen et al., 2018), and summarized in a simplified flow diagram (Fig. 4.1A). In brief, a solution containing WPI and glucose was freeze-dried, and the powders were further incubated in sealed desiccator maintained at a_W 0.53 and 55 °C for different durations. Glycation markers were quantitated and the 8 h samples were determined as EGPs (Chen et al., 2018). The reacted sample were stored at -20 °C prior to use, and thawing in a sealed desiccator containing silica gel at room temperature. The compositions of WPI and glycated products were analyzed by LC-MS (Bruker Daltonics, Billerica, MA) equipped with BioBasic-4 column (Thermo Fisher Scientific,

Waltham, MA). The samples were dissolved in Milli-Q water at 1 mg/ml, and filtered through a 0.45 μm filter membrane. A 2 μl sample was injected at minute 11. Solvent A was aqueous solution containing 0.1% formic acid and solvent B was 100% acetonitrile. The elution was performed at a flow rate of 50 μl/min from 0 to 2%B within 11 min and to 100% in the following 50 min. A positive ionization mode was used, and the cone voltage was 45 V. The m/z range was 400-3000 with scan time of 5 s (0.2 s interval). The data were analyzed on MassLynx V4.1 and MassEnt1 (Waters Co., Milford, MA), and the average degree of substitution per protein (DSP) was calculated as the following formula (Chen, Liu, Labuza, & Zhou, 2013):

$$\text{Average DSP} = \sum_{i=0}^{n} i \times I_i \,/\, \sum_{i=0}^{n} I_I$$

Where i is the number of glucose attached; I is the peak intensity of proteins attached with i glucose.

4.3.2 Mice and treatment

C57BL/6 mice and NOD mice obtained from the Charles River Laboratories (Wilmington, MA) and Taconic Biosciences (Rensselaer, NY), respectively, were housed in the Coverdell Vivarium at the University of Georgia (UGA). All mice were maintained on a 12-h dark/light cycle at 21-24 °C with 20-60% relative humidity, with access to food and filtered tap water ad libitum. Mice aged 0-4 week were kept on breeder chow (5058, PicoLab® Rodent Diet 20, LabDiet, MO), and switched to normal chow (5053) afterwards. All mice were euthanized by CO_2 inhalation

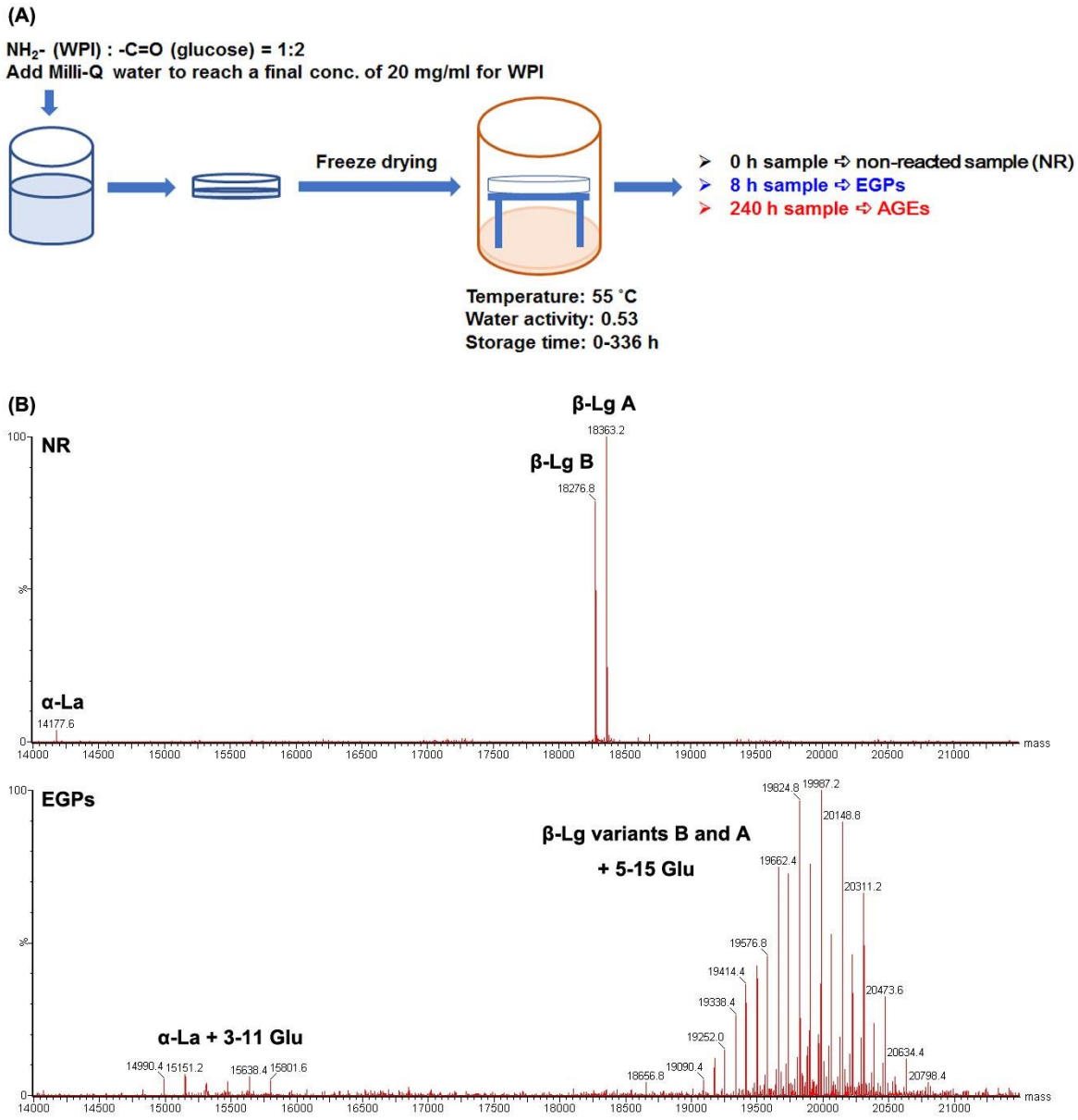

Fig 4.1 EGPs contain mainly the glycated whey proteins. (A) Scheme for EGP preparation. Whey protein isolate (WPI) and glucose were dissolved in Milli-Q water and the solution was freeze-dried. The resulted powders were incubated in a sealed desiccator maintained at a_W 0.53 and 55 °C. Samples were removed at different time points to quantitate the glycation markers for different glycation stages as described before. The 8 h samples were determined as EGPs, with 0 and 240 h samples as non-reacted (NR) and advanced glycation end-products (AGEs) controls, respectively. (B) Deconvoluted mass spectra (mass displayed: 14,000-21,500 Da) for NR and EGPs. NR samples were basically the same as WPI (Supplementary Fig. 3). In the EGP samples, all proteins were glycated: α-La had 3-11 glucoses attached; β-Lg had 5-15 glucoses attached.

followed by cervical dislocation. The use of the animals was approved by UGA Institutional Animal Care and Use Committee (IACUC).

Since there was no *in vivo* reference dose available for EGPs, the dose (600 mg/kg body weight (BW)/day) was determined following previous reports of *in vivo* dietary advanced glycation end-products (AGE)-treatment (Cai et al., 2012), which would give the mouse an equivalent amount of AGEs to that they obtained from the diet (Supplementary Fig. 1). Toxicity (3 months duration) of both EGPs and AGEs was tested in female and male C57BL/6 mice prior to following experiments. No difference on BW was detected (data not shown), suggesting that these glycation products at this dose did not generate overt toxicity.

4.3.2.1 MLD STZ-induced hyperglycemia in C57BL/6 females

C57BL/6 female mice (6-8 weeks old) were randomly separated into 5 groups (5-6 per group), and gavaged with non-reacted samples (NR), EGP, AGEs, autoclaved purified water and glucose solution (14.1 mg/ml) in the same volume. After 8 weeks, the mice were rendered diabetic with STZ injection (50 mg/kg BW/day intraperitoneally (i.p.) in citrate buffer for 4 consecutive days). Dosing with glycation products were continued for another 4 weeks.

4.3.2.2 NOD mice

NOD mouse is a spontaneous T1D murine model in which the penetrance of diabetic genotype in NOD mouse can be strongly modified by dietary factors (Leiter, 1993). Age-matched NOD

females (6-8 weeks old) were randomly separated into 3 groups (4 in each group with one repeat), and gavaged with NR, EGP and autoclaved purified water in the same volume for 4 weeks. In the secondary experiment, two groups of age-matched NOD females (6-8 weeks old, 10-11 in each group) were treated in the same way for 8 weeks. Although a 2-week continuous exposure was sufficient to test the effect of a xenobiotic on the immune system; however, a longer than 4-week exposure resulted in immunological alterations that were more consistent to humans (Guo & White, 2010). In our colonies, NOD females developed T1D starting at week 8-9. Therefore, the 4-week exposure was for the detection of the immunological changes prior to massive T1D initiation, while the 8-week exposure allowed a good comparison of T1D incidence upon different treatments. In the third experiment, age-matched non-diabetic NOD males were randomly separated into 2 groups (approximately 24 weeks old, 15-13 in each group) and gavaged with NR and EGPs for up to 6 months.

4.3.3 T1D relevant endpoints: BW, BGL, glucose tolerance test (GTT), insulin tolerance test (ITT), food and water consumptions

BW, food and water consumptions were measured weekly. BGL was measured weekly or bi-weekly in small sample of venous blood (tail nick) with Bayer's CONTOUR blood glucose meter (Bayer Health Care LLC, Mishawaka, IN). Diabetes was defined as BGL > 200 mg/dL in two consecutive weeks. For GTT, mice were fasted for 16 h, and i.p. injected with glucose water solution at the dose of 2 g/kg BW. For ITT, mice were fasted for 4 h, and i.p. injected with bovine insulin (Sigma-Aldrich) PBS solution at the dose of 6.4×10^{-3} mg/kg BW. To determine if the glucose in the glycation samples could elevate the non-fasting BGL, two groups of

C57BL/6 females were used for orally challenged GTT: non-fasted mice were gavaged with water or 14.1 mg/ml glucose solution at 0.01 ml/g BW. The BGL was measured at 0, 15, 30, 60 and 120 min, and all mice were prevented from reaching food during the tests.

4.3.4 Histopathological scoring for the pancreatic β-islets

A section of tissue from the pancreas head were dissected and fixed in 10% buffered formalin. The hematoxylin and eosin (H&E) staining was performed by Clinical Pathology Laboratory (College of Veterinary Medicine, UGA), and the slides were analyzed blindly on an Olympus BX41 light microscope (Olympus Corporation, Tokyo, Japan) by a board-certified pathologist using the criteria described in Table 1. For STZ-destructed pancreases, β-islet inflammation and vacuolation were scored. For NOD females, β-islet inflammation was graded.

4.3.5 Tissue processing and flow cytometry

Pancreatic immune infiltrates were purified following the protocol by Epshtein et al. (Epshtein, Sakhneny, & Landsman, 2017) with small modifications. A section of 0.1-0.15 g tissue from the pancreas head was dissected, cut into small pieces, and placed into 2 ml cold PBS. A 1 ml of digestive buffer was added to reach the final concentrations of collagenase (Sigma-Aldrich) at 0.05 mg/ml and DNase (Sigma-Aldrich) at 5 U/ml. The tube was incubated at 37 °C for 30-45 min with the rotator speed at 20 rpm in a Robbins Scientific Model 1000 Hybridization Incubator. The digestion was stopped by adding 10 ml cold PBS, and the solution was centrifuged at 300 x g at 4 °C for 8 min. The supernatant was removed, and the pellet was resuspended in 6 ml PBS

and passed through a 40 μm-cell strainer placed on a 50 ml conical polypropylene tube. The original tube was washed using 7 ml PBS twice by passing through the cell strainer into the collection tube. The PBS was removed by centrifugation, and the cells were resuspended in PBS to reach a proper concentration (10^6/ml) for flow cytometric analysis.

Spleen was separated and placed into 3 ml cold PBS. Cell suspensions were prepared by mashing the spleen using the frosted ends of two microscope slides. Red blood cells were lysed using the ACK lysing buffer (Gibco by Life Technologies, Orand Island, NY) and the buffer was removed by centrifugation at 300 x g at 4 °C for 8 min. The cell pellet was washed once using cold PBS and then resuspended in PBS. Thymus was separated and placed into 2 ml cold PBS. The single-cell suspensions were prepared the same way as spleen but without lysis.

Splenic and pancreatic cells were stained for the following surface markers conjugated with fluorophores: CD3 (145-2C11, PerCP-Cy5.5, BD Pharmingen), CD4 (RM4-5, V450, BD Horizon), CD8 (53-6.7, APC-H7, BD Pharmingen), CD25 (PC61, APC, BD Pharmingen), F4/80 (BM8, FITC, eBioscience), CD209 (LWC06, Alexa Fluor, Novus Biologicals), CD80 (16-10A1, PE-CD594, BD Horizon); B220 (RA3-6B2, FITC, eBioscience), CD40L (MR1, PE, eBioscience). Thymocytes were stained using CD4 (L3T4, PE, eBioscience) and CD8a (Ly-2, FITC, BD Pharmingen); CD44 (IM7, PE, BD Pharmingen) and CD25 (7D4, FITC, BD Pharmingen). Fluorescence Minus One (FMO) controls were performed for gating setup (Maecker & Trotter, 2006). After adding the antibodies, cells were incubated at 4 °C in the dark for 30 min. The cells were washed, and acquired on a Becton Dickinson LSRII Flow Cytometer (BD Biosciences). The flow cytometric data were analyzed using FlowJo v10 (FlowJo, LLC,

Ashland OR). Leukocytes were characterized as $CD4^+$ T cells ($CD3^+CD4^+CD8^-$), $CD4^+CD25^+$ T cells ($CD3^+CD4^+CD8^-CD25^+$), $CD8^+$ T cells ($CD3^+CD4^-CD8^+$), macrophages ($F4/80^+$), M1 ($F4/80^+CD80^+CD209^-$), M2 ($F4/80^+CD80^-CD209^+$), B ($B220^+$), CD40 ligand positive B cells ($B220^+CD40L^+$), and thymocytes (CD8/CD4 or CD24/CD44).

4.3.6 Cytokine/chemokine quantitation

Blood was obtained from the orbital sinus after mouse being deeply anesthetized. The serum was collected and stored at -80 °C prior to use. Thirty-two cytokines/chemokines in the sera were detected by the bead-based multiplex ELISA technique using the MILLIPLEX MAP Mouse Cytokine/Chemokine Kit (Millipore, Billerica, MA) following the manufacturer's instructions. The beads were run on a Bio-Plex (Bio-Rad, Inc., Hercules, California), and the data was collected and analyzed using Bio-Plex Manager 6.1.1. The working range was 12.8-40,000 pg/ml for IL-13, and 3.2-10,000 pg/ml for the rest. IL-3 and IL-5 were not detected in the samples; IL-4 was below the lower limit of quantitation of the standard curve with some samples fell in the extrapolated range.

4.3.7 Measurement of immunoglobulin (Ig) isotypes and insulin autoantibodies (IAAs)

The serum levels of Ig isotypes (i.e., IgM, IgG_1, IgG_{2b}, IgG_{2c}) were detected using ELISA Quantitation Kits (Bethyl Laboratories Inc., Montgomery, TX). IgG2c was a substitute for IgG2a in NOD mice because IgG2a was not expressed in inbred strains with Igh1-b allele (Martin, Brady, & Lew, 1998). The sera from NOD females were measured using two commercially

available IgG2a antibodies (i.e., Bethyl, SouthernBiotech), and the O.D. was consistently found to be 0.2 at the dilution from 1/10 to 1/1000 (data not shown), which agreed with the previous study (Martin et al., 1998). Therefore, an O.D. < 0.2 was considered the background for all sera to eliminate the false positive caused by hemolysis. The 96 well flat-bottom high binding microplate was coated with 100 μl/well primary antibody (5 μg/ml) at 4 °C for overnight (16-18 h), and then blocked with 5% skim milk powder in 0.05% PBST at room temperature for 1 h. After washing with 0.05% PBST, a 100 μl standard or sample was added. The standard curve was prepared by diluting Mouse Reference Serum provided by the Manufacturer with the diluent (2% skim milk powder in 0.02% PBST). A series of dilutions was conducted for sera samples, and only the dilution with optimal detection was reported: IgM (1/5,000), IgG1 (1/500,000), IgG2b (1/20,000), IgG2c (1/50,000). After 2 h incubation at room temperature, the plate was washed and a 100 μl HRP-conjugated secondary antibody was applied. The plate was incubated at room temperature at dark for 1 h, and then washed. A 100 μl Ultra TMB-ELISA Substrate Solution (Thermo Scientific, Rockford, IL) was added, and the reaction was stopped by an addition of 100 μl 1 M H_2SO_4 solution after 5-10 min. The absorbance was read at 450 nm in a Synergy 4 hybrid multi-mode microplate reader (BioTek Instrument, Inc., Winooski, VT).

For the IAA titers (Quintana & Cohen, 2001; Wan, Thomas, & Unanue, 2016), the plates were coated overnight with bovine insulin (10 μg/ml in carbonate solution (pH=9.6), 100 μl) at 4 °C. To check the specificity of the assay, diluted sera were divided into two aliquots and incubated in the presence or absence of 10 μg/ml insulin on ice for 1 h. HRP-conjugated goat anti-mouse IgM or anti-mouse IgG were used as the secondary antibodies (Bethyl). The O.D. threshold was 0.06,

which was determined by a serial dilution from 1/5 to 1/2500. The other steps were the same as described above.

4.3.8 Statistics

Data were presented as mean ± SE. Comparisons of means were tested by one-way ANOVA using JMP Pro 13 (SAS Inc., Cary, NC). Tukey-Kramer *post hoc* test was conducted when the omnibus test was significant for the comparison of three or more groups. The comparisons of means between EGPs and water/NR were tested using Student's t test, and the survival curves were compared using Gehan-Breslow-Wilcoxon test performed on GraphPad Prism 6 (GraphPad Software, San Diego, CA).

4.4 Results

4.4.1 The composition of EGPs

The composition of WPI powders was firstly verified by LC-MS. As shown in Supplementary Fig. 2, the powders were highly purified and contained mainly α-lactalbumin (α-La, 14,178 Da) and two variants of β-lactoglobulin (β-Lg, variant B: 18,277 Da; A: 18,363 Da). The two peaks with an increase in molecular weight of 324 Da of β-Lg variants were probably resulted from 1 lactose attachment during powder manufacture, such as spray drying. When NR and EGPs were analyzed, the components in NR samples were highly consistent with WPI, suggesting that the freeze-drying steps did not generate glycation products (Fig. 4.1B upper panel). After 8 h

reaction, no original forms of α-La or β-Lg remained (Fig. 4.1B lower panel). All the α-La reacted with 3-11 glucoses, with the 6-glucose attached α-La being the most abundant and the average DSP of 7.2. Both variants of β-Lg were attached by 5-15 glucoses. The 10-glucose attached form was the most abundant and the average DSP was 9.7 for both variants, which agreed with a previous study that the two variants showed similar reactivity during glycation (Chen, Liang, Liu, Labuza, & Zhou, 2012).

4.4.2 EGPs have minimal effect on MLD-STZ-induced hyperglycemia

C57BL/6 females were pretreated with EGPs for 8 weeks to stabilize the levels of circulating EGPs, and the effects of EGPs on BGL in these healthy animals were monitored at the same time. In addition to water control, two additional controls including glucose solutions and NR were included because NR and glycation product samples contained glucose, which might affect the BGL. Therefore, GTT was conducted with oral challenge of the glucose solution that was equivalent to the amount of glucose in NR sample. The results showed that orally intake of this amount glucose did not elevate the BGL immediately after dosing in healthy mice (Supplementary Fig. 3A). AGEs were used as a positive control since they were widely reported to be detrimental for both healthy and diabetic individuals (Cai et al., 2012). Supplementary Fig. 3B showed that no significant difference was detected for BW during treatment, suggesting none of the treatments generated overt toxicity. For the non-fasting BGL, it stayed between 110-125 mg/dL in EGP group, while it fluctuated between 110-160 mg/dL in the 4 control groups (Supplementary Fig. 3C). GTT was conducted after dosing for 8 weeks. The BGLs of EGP-treated group were significantly lower at 15 min after challenge when compared to those of NR

and AGE-treated groups, although there were no differences compared to those of water- and glucose-treated groups (Supplementary Fig. 3D). During ITT, no significant difference was detected at any time points among the groups. These results suggested that EGPs could stabilize BGL. Therefore, the effect on T1D was further studied in two T1D models.

The first T1D model was the MLD-STZ-induced hyperglycemia in C57BL/6 females. After 8 weeks dosing, STZ was i.p. injected to specifically destroy pancreatic β-cells and thus induce hyperglycemia in these mice. After STZ injection, mice treated with glucose solution showed the least changes in BW, and water, NR and EGP-treated mice had moderate decreases in the BW while AGE-treated mice had the most decreases in BW (Fig. 4.2A). In addition, mice from the EGP group ate and drank the least (Fig. 4.2B-C). The glucose solution-treated mice maintained the non-fasting BGL around 150 mg/dL after STZ injection; the non-fasting BGLs in the water and EGP groups slightly increased; however, NR and AGE-treated mice showed a continuous increase in their non-fasting BGL (Fig. 4.2D). During GTT, NR and AGE-treated mice had increased BGL more than the mice from the other three groups within the first 30 min, and AGE group had a significantly increased BGL at 120 min compared to water, glucose and EGP group (Fig. 4.2E left panel). During ITT, NR treated mice showed the highest fasting BGL, followed by AGEs, NR, EGPs, water and glucose solution. At 30 min after insulin injection, AGE group had the highest BGL, followed by NR/EGPs and water/glucose solution (Fig. 4.2E right panel). An overall evaluation of the diabetes severity suggested that AGEs > NR > EGPs, water ≥ glucose, based on the above various endpoints of T1D: BW, food and water consumption, non-fasting BGL, and BGL change during GTT and ITT. Histopathological assessment of β-islets was conducted from the aspects of inflammation and vacuolation, and the level of vacuolation but not

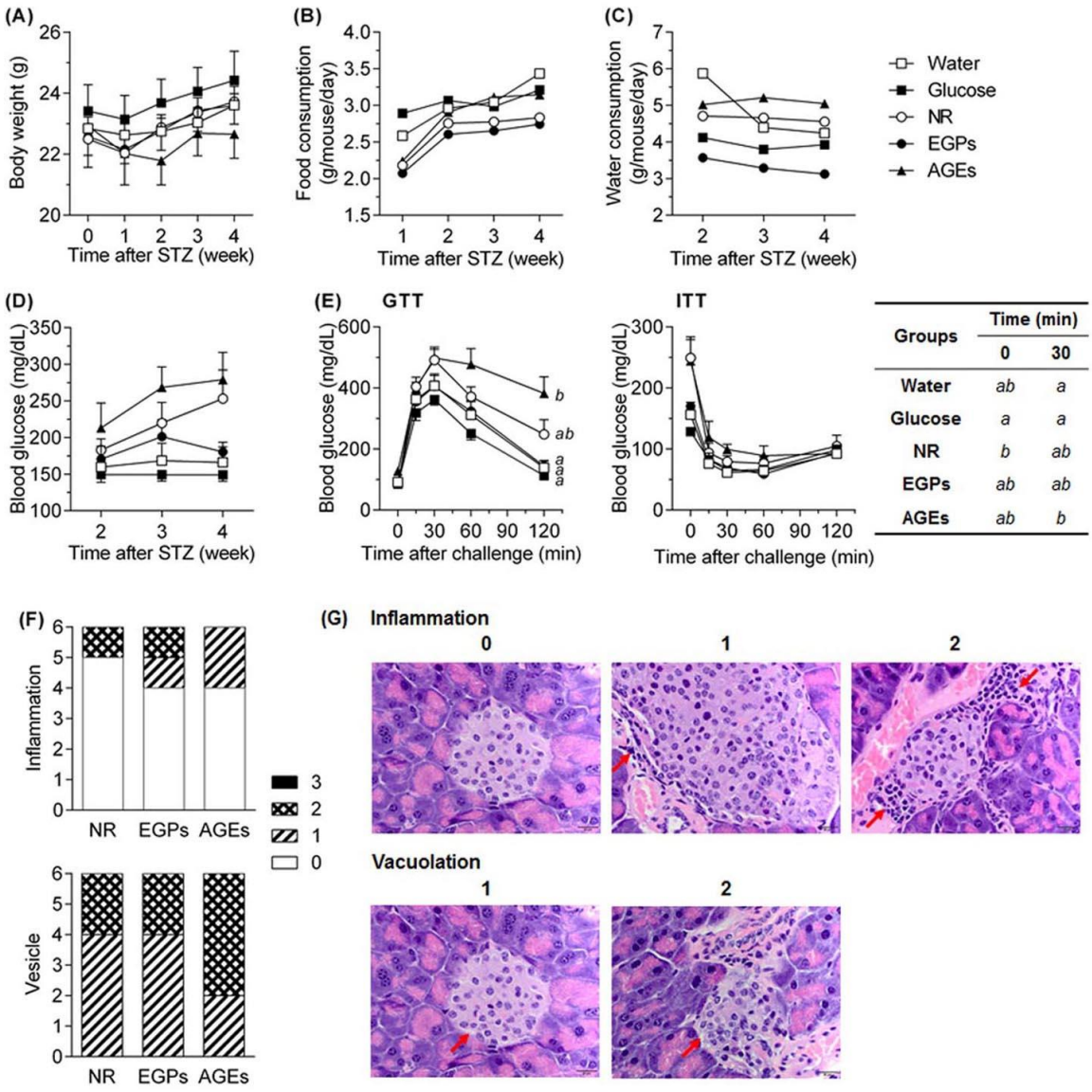

Groups	Time (min)	
	0	30
Water	*ab*	*a*
Glucose	*a*	*a*
NR	*b*	*ab*
EGPs	*ab*	*ab*
AGEs	*ab*	*b*

Fig 4.2 EGPs have minimal effects on multiple low dose (MLD)-streptozotocin (STZ)-induced hyperglycemia. The hyperglycemia in C57BL/6 females were induced by STZ injection (50 mg/kg body weight (BW)/day, i.p., 4 doses). (A) BW, (B) food consumption, (C) water consumption and (D) non-fasting BGL were measured weekly or biweekly. (E) Glucose tolerance test (GTT) and insulin tolerance test (ITT) were measured at week 5 post STZ injection. Significance detected during ITT was shown in the table (food and water consumption were measured by cage; the other results were presented as mean ± SE, n = 5-6). (F) The histopathological changes of β-islets from each animal were evaluated from aspects of inflammation and vacuolation by scoring from 0 to 3. Representative images of β-islets of detected scores are shown in (G). Red arrows in the upper panels indicate inflammatory cells, and those in the lower panels indicate vacuoles. *a, b*, $p < 0.05$.

inflammation correlated with the ranking of diabetes severity (Fig. 4.2F-G). Cytoplasmic vacuolation was due to the remarkable destruction of islets induced by STZ (Amniattalab, Malekinejad, Rezabakhsh, Rokhsartalab-Azar, & Alizade-Fanalou, 2016), and the results suggested that AGEs facilitated the destructive function of STZ while EGPs and NR control had similar effects.

4.4.3 Alleviation of T1D by EGPs in NOD mice is associated with reduced pancreatic immune infiltrates

4.4.3.1 EGPs delay TID onset in NOD females

The other T1D murine model used was NOD mouse. NOD females were dosed with water, NR or EGPs for 4 weeks. There was no significant difference in BW between controls and EGPs (Fig. 4.3A) and organ weights including spleen, thymus, liver, kidney and heart (Supplementary Table 1) that were commonly used as toxicity indications of test compounds. These observations suggested that NR or EGPs at this dose did not generate overt toxicity to NOD females. Comparing to NR and water controls, EGPs significantly decreased non-fasting BGL of the non-diabetic mice after dosing for 2 weeks (Fig. 4.3B), but did not alter the BGLs during GTT or ITT, which were conducted after dosing for 4 weeks (Fig. 4.3C). Another set of NOD females were continuously dosed with NR and EGPs for up to 8 weeks to monitor the non-fasting BGL and the response to glucose and insulin challenges (Fig. 4.3D-E). EGPs significantly lowered the non-fasting BGL since week 1, increased the glucose tolerance during GTT, and decreased the insulin resistance during ITT, when compared to NR control. Additionally, the T1D incidence was

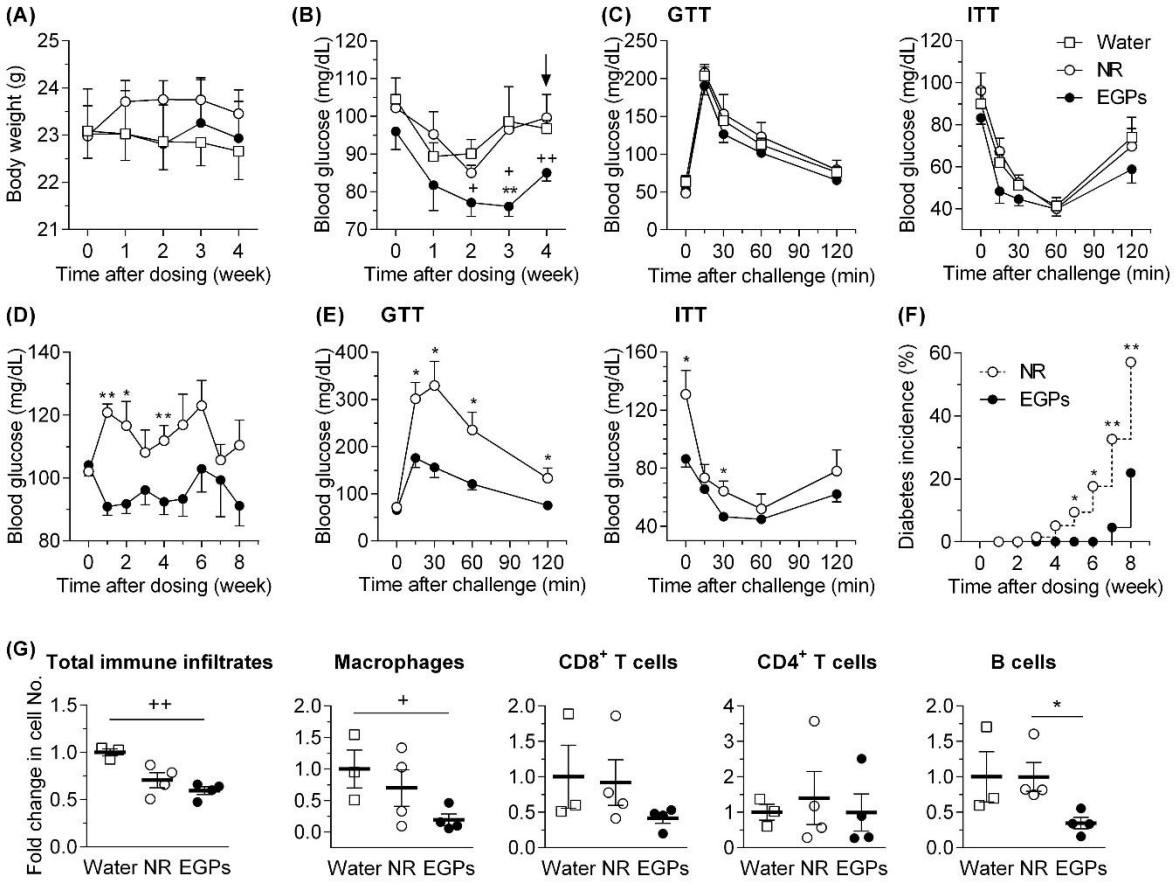

Fig 4.3 EGPs delay type 1 diabetes (T1D) onset in NOD females. NOD females (6-8 weeks old) were orally gavaged with water, NR or EGPs for 4 weeks. (A) BW and (B) non-fasting BGL were monitored weekly. The BGL change in the non-diabetic mice is summarized and graphed, the arrow indicates T1D incidence in water and NR groups. (C) GTT and ITT were conducted at the end of week 4 (mean ± SE, n = 7-8, the data was combined of two independent repeats). Another set of age-matched NOD females were dosed with NR or EGPs. The non-fasting BGL change of the non-diabetic mice is shown in (D). (E) GTT and ITT were conducted after dosing for 8 weeks (mean ± SE, n = 7-11). (F) The diabetes incidence was recorded (diabetic: BGL > 200 mg/dL, n_{NR} = 11, n_{EGPs} = 10). (G) The pancreases of non-diabetic NOD females (being treated for 4 weeks) were harvested, and the number of immune cells (i.e., total immune infiltrates, macrophages, $CD8^+$ T cells, $CD4^+$ T cells, B cells) within pancreas were dissociated and analyzed by flow cytometry (mean ± SE, n = 3-4). +, $p < 0.05$, ++, $p < 0.01$ EGPs vs water; *, $p < 0.05$, **, $p < 0.01$ EGPs vs NR.

recorded: NR treated mice started to show T1D incidence at week 3 (9-11 weeks old) and had a total incidence close to 60% at week 8 (14-16 weeks old); in comparison, EGPs treated mice did

not show T1D incidence until week 7 (13-15 weeks old) and had an overall incidence at approximately 20% (Fig. 4.3F).

Since the mechanism of T1D in NOD is manifested as immune dysregulation and immune cells infiltrating into pancreas (Delovitch & Singh, 1997), the inflammation in β-islets was firstly evaluated by histopathology, but no significant differences were detected (Supplementary Fig. 4). The negative finding was probably because the treatment started between week 6-8 while insulitis in NOD mouse started at week 4-6, and EGPs might have minimal effect on the already infiltrated immune cells. The subtle difference would be beyond the sensitivity of the semi-quantitative histopathology. Therefore, the pancreatic immune infiltrates of the non-diabetic NOD females after dosing for 4 weeks were dissociated and evaluated by flow cytometry. EGPs decreased the total immune infiltrates in the pancreas, and decreased the number of macrophages, $CD8^+$ T cells and B cells by 50% when comparing to water and NR controls with significant changes observed in B cells between NR and EGPs. However, there were no differences among the groups in the $CD4^+$ T infiltrate number (Fig. 4.3G).

4.4.3.2 EGPs produce protective effects in NOD males

Non-diabetic NOD males were randomized into two groups (age matched) and dosed with NR or EGPs. NOD males have later T1D onset and lower incidence compared to females, so they were kept longer than 16 weeks. EGP-treated mice maintained the BW, whereas NR-treated mice

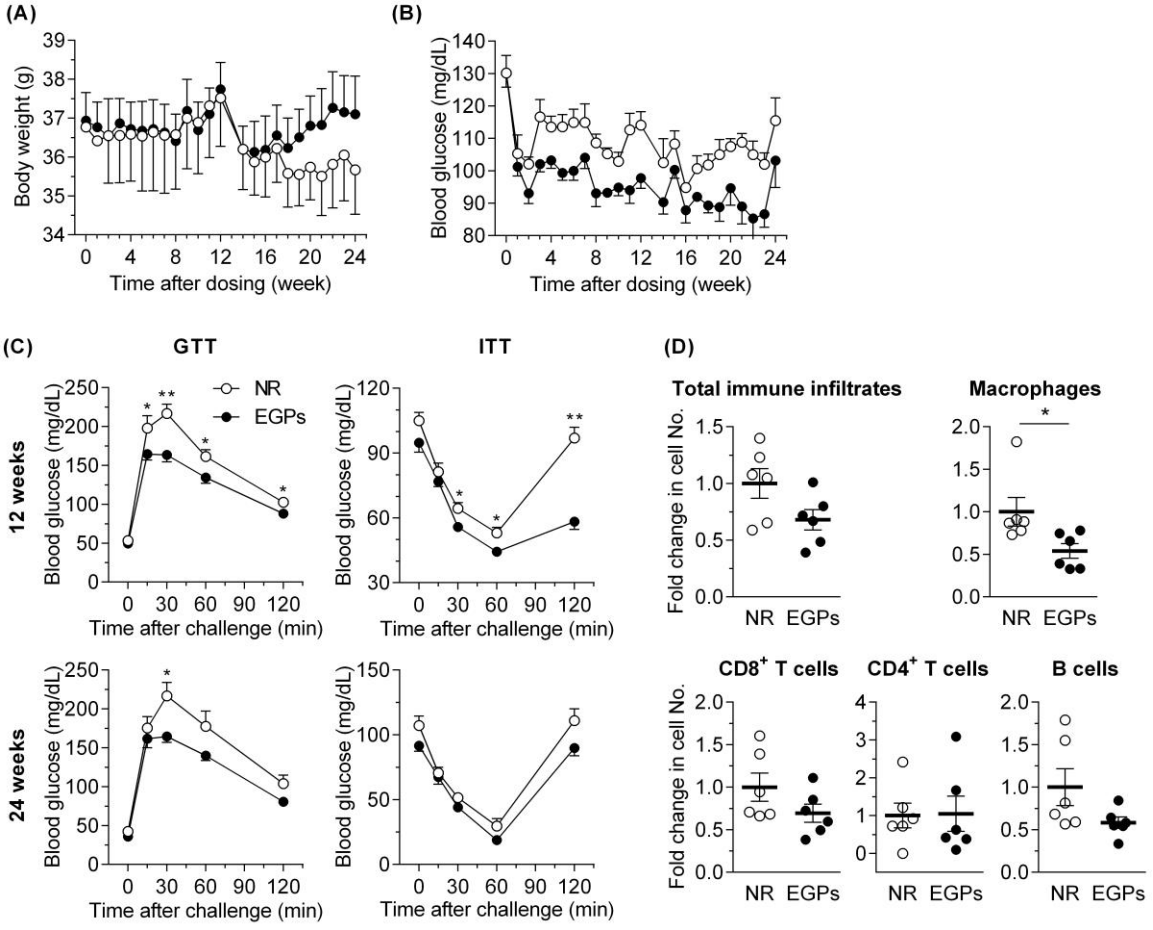

Fig 4.4 EGPs have protective effects on NOD males. Age matched diabetic free NOD males (> 16 weeks old) were dosed with NR or EGPs for 24 weeks. (A) BW and (B) non-fasting BGL were recorded. (D) GTT and ITT were performed at week 12 and 24 (mean ± SE, n = 11-15 for week 12, n = 6 for week 24). (E) After 24 weeks of treatment, the immune cells (i.e., total immune infiltrates, macrophages, $CD8^+$ T cells, $CD4^+$ T cells, B cells) within pancreas were dissociated and studied using flow cytometry (mean ± SE, n = 6). *, $p < 0.05$, **, $p < 0.01$.

started to show a decrease in BW starting at week 18 post treatment (Fig. 4.4A), suggesting that chronic oral intake of EGPs might have generated protective effects in the autoimmune male NOD mice. EGPs decreased and maintained the non-fasting BGL at normal level (vs. NR), and significantly increased the glucose metabolism and decreased insulin resistance during GTT and

ITT, respectively (Fig. 4.4C-D). Furthermore, fewer immune cells infiltrated into the pancreas, and fewer macrophages, $CD8^+$ T and B infiltrates within pancreas were detected when compared to NR (Fig. 4.4E), and this was highly consistent with NOD females.

4.4.4 EGPs alter the immunity in NOD mice

By studying the effects of EGPs on T1D using two models (i.e., MLD-STZ-induced, NOD mouse), it was reasonable to hypothesize that EGPs exerted the protective effect against T1D through regulating the immunity. Therefore, the following section was to understand how the immunity, especially the aspects relevant to T1D progression, was affected by EGPs. After being treated for 4 weeks, non-diabetic NOD females were euthanized and the immune cell populations in primary and secondary lymphoid organs were studied. In the thymus, CD4CD8 and CD25CD44 thymocytes were studied (Fig. 4.5A). EGPs decreased the CD8 single positive cells but not the others. In the spleen, the percentage of M2 (anti-inflammatory) was slightly increased while %M1 (pro-inflammatory) was decreased by EGPs, leading to a significant increase of M2/M1 ratio (Fig. 4.5B upper panel). These results revealed the anti-inflammatory feature of EGPs. In addition, the percent $CD4^+CD25^+$ T cells was increased even though the total $CD4^+$ T cells were unaffected, and $\%CD8^+$ T cells was decreased by EGPs (Fig. 4.5B lower panel). For the splenic B cells, EGPs decreased the CD40 ligand positive populations ($B220^+CD40L^+$, the $p \approx 0.05$, Fig. 4.5B lower panel).

The profiles of serum cytokines/chemokines were examined. Comparing to background (water), NR and EGPs consumptions had an enhancing effect on most cytokines/chemokines including

G-CSF, GM-CSF, IL-1β, IL-2, IL-6, IL-7, IL-10, IL-12p40, IL-12p70, IL-13, IL-15, IL-17, INF-γ, LIF, M-CSF, MCP-1, MIG, MIP-2, RANTES and VEGF (Supplementary Table 2). Key T1D regulators were separately graphed in Fig. 4.6. EGPs had little effects on the most important Th1 (INF-γ) and Th2 (IL-4) markers for pancreatic β-islets destruction and protection in NOD mice,

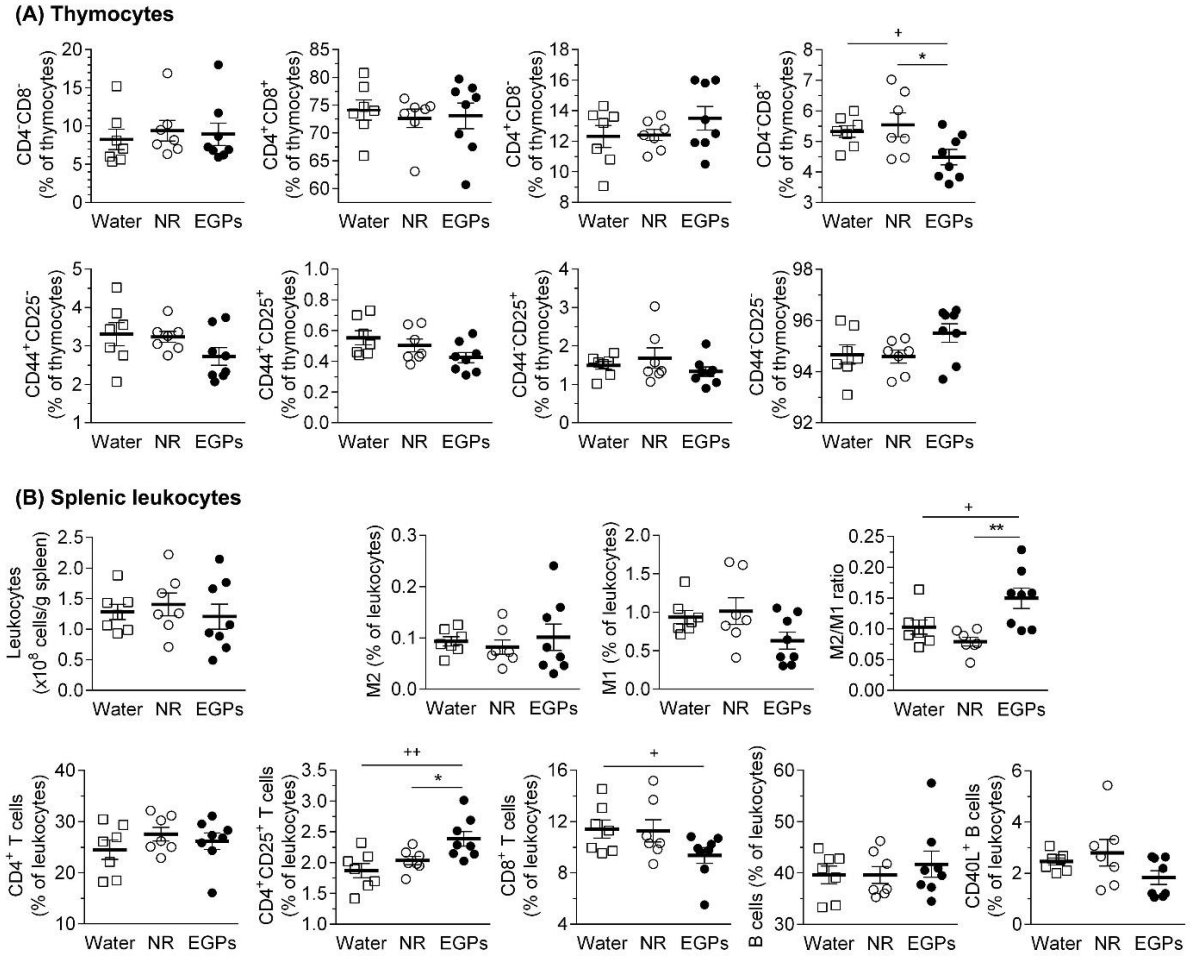

Fig 4.5 EGPs decrease CD8⁺ T cells, and increase splenic M2/M1 ratio and CD4⁺CD25⁺ T cells. NOD females (6-8 weeks old) were orally gavaged with water, NR or EGPs for 4 weeks. (A) CD4/CD8 and CD44CD25 thymocytes were studied. (B) Splenic leukocytes, macrophages (M2 ($F4/80^+CD209^+CD80^-$), M1 ($F4/80^+CD209^-CD80^+$) and M2/M1 ratio), $CD4^+$ T cells ($CD3^+CD4^+CD8^-$), $CD4^+CD25^+$ T cells ($CD3^+CD4^+CD8^-CD25^+$), $CD8^+$ T cells ($CD3^+CD4^-CD8^+$), B cells ($B220^+$) and $CD40L^+$ B cells ($B220^+CD40L^+$) were studied by flow cytometry (mean ± SE, n = 7-8). +, $p < 0.05$, ++, $p < 0.01$ EGPs vs water; *, $p < 0.05$, **, $p < 0.01$ EGPs vs NR.

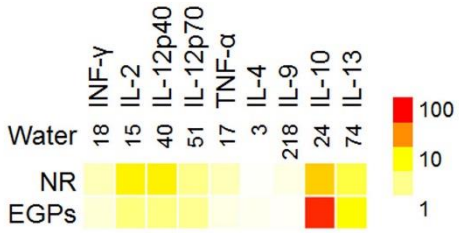

Fig 4.6 EGPs increase serum IL-10. The serum cytokines/chemokines from NOD females were quantitated, and the key regulators for T1D were graphed (mean ± SE, n = 7-8). The scale indicates the fold change. IL-10 was increased 86- and 3-folds by EGPs when compared to water and NR, respectively.

respectively. For the other pro-inflammatory cytokines (i.e., IL-2, IL-12p40, IL-12p70, TNF-α), EGPs significantly increased IL-2 and IL-12p70, numerically increased IL-12p40, and had no effects on TNF-α when compared to water. EGPs significantly decreased IL-2 and IL-12p40, and had no effect on either IL-12p70 or TNF-α when compared to NR. All the other T1D relevant anti-inflammatory cytokines (i.e., IL-9, IL-10, IL-13) were either significantly or numerically increased by EGPs when compared to water and NR. Strikingly, IL-10, another vital Th2 marker other than IL-4, was increased 86- and 3-folds by EGPs compared to water and NR, respectively. Taken together, EGPs shifted the cytokine/chemokine profile toward anti-inflammation despite the omnibus activation effect, which was highly in accordance with the M2 biased polarization in the spleen.

The serum levels of IgM, IgG_1, IgG_{2b} and IgG_{2c} were measured. The baseline levels of the 4 Ig isotypes in the water group was IgG_1 > IgG_{2c} > IgG_{2b} > IgM (Fig. 4.7A). EGPs significantly decreased IgM and IgG_1 when compared to water; and significantly decreased IgG_1 when compared to NR (Fig. 7A). In the autoimmune prone NOD mice, autoantibodies were IgG predominant, and both IgG and IgM classes could recognize self-antigens known to induce diabetes, such as insulin (Quintana & Cohen, 2001). When IAA titers were measured, EGPs significantly decreased anti-insulin IgM and IgG when compared to water and NR (Fig. 4.7B).

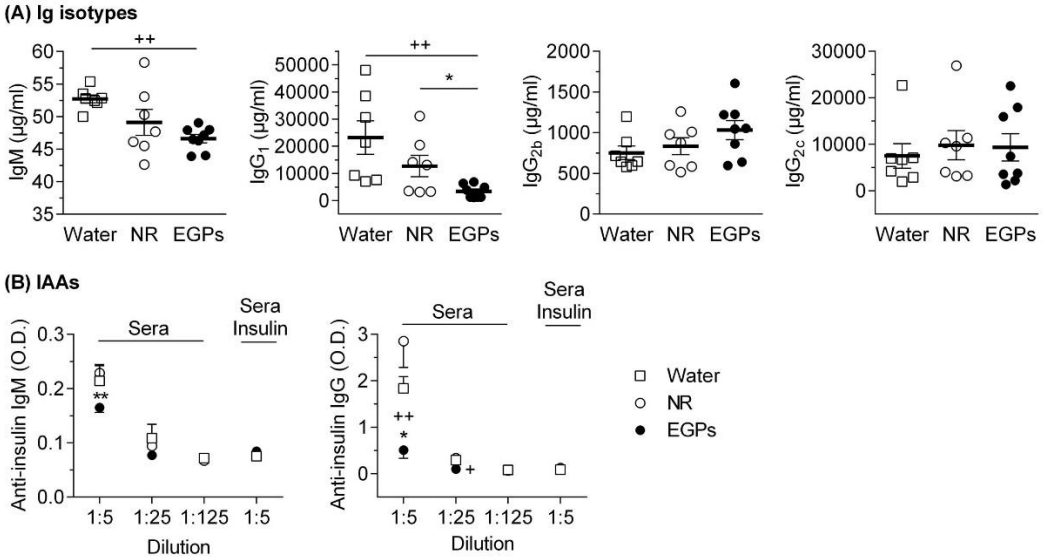

Fig 4.7 EGPs decrease IgG1 and insulin autoantibodies (IAAs). (A) The Ig isotypes (i.e., IgM, IgG_1, IgG_{2b}, IgG_{2c}) in the sera from NOD females were detected by ELISA (mean ± SE, n = 7-8). (B) Anti-insulin IgM and IgG were measured. To determine the specificity of IAAs, sera at the dilution of 1:5 were incubated with 10-fold excess of insulin (right column of both panels, mean ± SE, n = 4). +, $p < 0.05$, ++, $p < 0.01$ EGPs vs water; *, $p < 0.05$, **, $p < 0.01$ EGPs vs NR.

4.5 Discussion

Overall, this study provides support for possible nutraceutical application of WPI-derived EGPs for patients with insulitis and T1D. As data from the NOD females suggested, oral consumption of EGPs delayed the T1D onset and decreased the T1D incidence over 50%. Studies in both NOD males and females showed decreased and stabilized non-fasting BGLs, increased glucose metabolism during GTT and increased insulin sensitivity during ITT, which were accompanied with reduced pancreatic immune infiltrates. However, in another T1D model, the STZ-induced β-cell destruction in C57BL/6 females that was much less immune-dependent, the protective effect of EGPs against T1D diminished. The seemingly contradictory results from two T1D models suggested that EGPs were likely to exert their effect through modulating the immunity.

When the immune changes in the non-diabetic NOD mice were evaluated to reveal the underlying mechanisms, EGPs were found to affect the immune system in the following three aspects. First, EGPs decreased the $CD8^+$ T cells in NOD mice. Since $CD8^+$ T cells were believed to be the main effector cells to attack β-islets (Mathis et al., 2001), a decrease of CD8 single positive cells in the thymus and $CD8^+$ T cells in the periphery could be one reason how EGPs protected NOD mice from T1D. In the thymus, EGPs decreased the CD8 single positive thymocytes without affecting the other CD4CD8 and CD44CD25 subpopulations, which suggested that EGPs might affect the positive or negative thymic selection and required further studies.

Secondly, EGPs were anti-inflammatory for NOD mice. On the one hand, splenic M2/M1 ratio was increased by EGPs, suggesting a regulation of macrophage polarization towards anti-inflammatory M2. It was reported that injection of M2 macrophages to the prediabetic NOD recipients protected >80% of treated mice against T1D for at least 3 months (Parsa et al., 2012). On the other hand, serum IL-10 was up-regulated 86- and 3-folds by EGPs compared to water and NR, respectively. Importantly, IL-10-deficient mice experienced severe T1D (Tian et al., 2001). In our previous studies, IL-10 was also identified as one of the most up-regulated cytokines/chemokines when EGPs was applied to human macrophages (PMA-differentiated-U937 cells), and peritoneal macrophages from C57BL/6 females (Chen et al., 2018) and C57BL/6 males (Chen & Guo, 2019).

The third aspect addressed the autoreactivity. It was reported that CD40 ligand expression on B cells could initiate insulitis and antigen-specific T cell responses (Balasa et al., 1997). When B cells were activated by a combination of CD40 ligand and IL-4 *ex vivo*, an enhanced insulin-processing and presentation of B:12-20 epitope to 8F10 $CD4^+$ T cells was observed. These T cells helped anti-insulin B cells to produce IAAs (Wan et al., 2016). Therefore, our observation that EGPs decreased the $CD40L^+$ B cells might lead to a decreased autoreactivity. Indeed, when IAAs were quantitated, the level of anti-insulin IgG, the predominant anti-insulin Ig class in NOD mice, was dramatically decreased by EGPs.

The mode of action (MOA) of EGPs, however, had not been investigated in this work. EGPs had been found naturally existing in dairy products and synthesized in experimental conditions, but data regarding absorption, distribution, metabolism and excretion (ADME) was rare. It was reported that sugar moiety attachment through glycation protected the cleavage site from trypsin hydrolysis (Chen et al., 2013). A chromatographic profiling of *in vitro* gastric and intestinal digested sodium caseinate showed that galactose glycation resulted in the reduction of peptide amount (Corzo-Martinez, Avila, Moreno, Requena, & Villamiel, 2012), which would possibly lead to reduced intestinal absorption of the glycated proteins. Furthermore, a comprehensive review suggested that the absorption rate of protein-bound Amadori products was 3-10% (Pischetsrieder & Henle, 2012). In the small intestine, dietary protein antigens were important to induce periphery regulatory T cells (pTregs), which expressed high level of IL-10 and suppressed effector T cells (Kim et al., 2016). The consistently increased circulating IL-10 levels in both C57BL/6 males (Chen & Guo, 2019) and NOD females probably suggested the periphery regulatory T cells induction in the intestine, even though the other cells, such as M2

macrophages, $CD4^+CD25^+Foxp3^-$ T cells (Fujio et al., 2010), $CD19^{hi}CD1d^{hi}CD5^+$ (mouse) (Yanaba et al., 2008) and $CD24^{hi}CD27^+$ (human) (Iwata et al., 2011) regulatory B cells, could secrete IL-10 as well. Also, the probably reduced intestinal absorption increased the chances of gut fermentation. *In vitro* culture of *Intestinimonas AF211* converted Amadori compounds into butyrate (Bui et al., 2015), and daily butyrate gavage attenuated 2,4,6-trinitrobenzene sulfonic acid (TNBS) induced colitis lesions in rats through affecting the Th17/pTreg lineage (Zhang et al., 2016). Further studies showed that protein bounded Amadori compounds derived from wheat gluten-glucose system could not inhibit the growth of *Escherichia coli* and *Staphlococcus aureus*, but their homologous advanced products could (del Castillo et al., 2007), suggesting that EGPs might not be as toxic as AGEs to gut microbes.

4.6 Conclusions

In summary, oral intake of WPI-derived EGPs delayed the T1D onset in NOD females through modulating the immunity. EGP consumption reduced $CD8^+$ T cells and IAAs, and increased IL-10, $CD4^+CD25^+$ T cells and the anti-inflammatory responses by shifting M2/M1 balance toward M2. These data strongly suggested the applicable potential of EGPs as a nutraceutical for individuals with insulitis and T1D. The active components had been narrowed down to mostly β-lg attached by 5-15 glucoses and small amount of α-la modified by 3-11 glucose by using LC-MS. Further studies are required if the active molecules need to be identified individually. Besides WPI-derived EGPs, those produced from other proteins remains unclear regarding effects on immunoregulation as well as immune diseases such as T1D. Future studies would also focus on the molecular mechanisms how the EGP component(s) generate the anti-inflammatory

effects. Besides T1D, EGPs might be beneficial for other autoimmune diseases as indicated by the data of NOD males. Expanded studies with focuses on other autoimmune diseases might enlarge the application of EGPs as a nutraceutical.

Author contributions: Y. C. and T. L. G. designed the studies; Y. C. performed the animal studies, T. L. G conducted the flow cytometry experiments, and T. N. performed the histopathological assessment; Y. C. analyzed the data and performed the statistical analysis; Y. C. graphed the data and wrote the manuscript, and T. L. G. edited it.

Acknowledgments: The authors would thank Fonterra (USA) Inc (Rosemont, IL) for supplying WPI samples. The authors greatly appreciate Drs. Robert M. Gogal (VBDI, UGA) and Nikolay M. Filipov (Department of Physiology and Pharmacology, UGA) for their critical comments, the training and assistance provided by the CVM Cytometry Core Facility (UGA) regarding the flow cytometric analysis, Dr. Dennis Phillips for helping with the LC-MS analysis, and Julie Nelson (Cytometry Shared Resource Laboratory, UGA) for the assistance with Luminex. This work was supported by in part by NIH R21ES24487, NIH R41AT009523, the USDA National Institute of Food and Agriculture (grant no. 2016-67021-24994/project accession no. 1009090) and Interdisciplinary Toxicology Program at UGA.

Reference

Amniattalab, A., Malekinejad, H., Rezabakhsh, A., Rokhsartalab-Azar, S., & Alizade-Fanalou, S. (2016). Silymarin: A Novel Natural Agent to Restore Defective Pancreatic beta Cells in Streptozotocin (STZ)-induced Diabetic Rats. Iran J Pharm Res, 15(3), 493-500.

Balasa, B., Krahl, T., Patstone, G., Lee, J., Tisch, R., McDevitt, H. O., & Sarvetnick, N. (1997). CD40 ligand-CD40 interactions are necessary for the initiation of insulitis and diabetes in nonobese diabetic mice. Journal of Immunology, 159(9), 4620-4627.

Beisswenger, P. J. (2012). Glycation and biomarkers of vascular complications of diabetes. Amino Acids, 42(4), 1171-1183.

Birlouez-Aragon, I., Pischetsrieder, M., Leclere, J., Morales, F. J., Hasenkopf, K., Kientsch-Engel, R., Ducauze, C. J., Rutledge, D. (2004). Assessment of protein glycation markers in infant formulas. Food Chemistry, 87(2), 253-259.

Borg, D. J., Yap, F. Y. T., Keshvari, S., Simmons, D. G., Gallo, L. A., Fotheringham, A. K., Zhuang, A., Slattery, R. M., Hasnain, S. Z., Coughlan, M. T., Kantharidis, P., Forbes, J. M. (2018). Perinatal exposure to high dietary advanced glycation end products in transgenic NOD8.3 mice leads to pancreatic beta cell dysfunction. Islets, 10(1), 10-24.

Bui, T. P., Ritari, J., Boeren, S., de Waard, P., Plugge, C. M., & de Vos, W. M. (2015). Production of butyrate from lysine and the Amadori product fructoselysine by a human gut commensal. Nat Commun, 6, 10062.

Burke, S. J., Karlstad, M. D., Conley, C. P., Reel, D., Whelan, J., & Collier, J. J. (2015). Dietary polyherbal supplementation decreases CD3+ cell infiltration into pancreatic islets and prevents hyperglycemia in nonobese diabetic mice. Nutr Res, 35(4), 328-336.

Cai, W., Ramdas, M., Zhu, L., Chen, X., Striker, G. E., & Vlassara, H. (2012). Oral advanced glycation endproducts (AGEs) promote insulin resistance and diabetes by depleting the antioxidant defenses AGE receptor-1 and sirtuin 1. Proc Natl Acad Sci U S A, 109(39), 15888-15893.

Chen, Y., Filipov, N. M., & Guo, T. L. (2018). Dietary Glycation Products Regulate Immune Homeostasis: Early Glycation Products Promote Prostate Cancer Cell Proliferation through Modulating Macrophages. Mol Nutr Food Res, 62(3).

Chen, Y., & Guo, T. L. (2019). Dietary Early Glycation Products Promote the Growth of Prostate Tumors More than Advanced Glycation End-Products through Modulation of Macrophage Polarization. Mol Nutr Food Res, 63(4), e1800885.

Chen, Y., Liang, L., Liu, X. M., Labuza, T. P., & Zhou, P. (2012). Effect of Fructose and Glucose on Glycation of beta-Lactoglobulin in an Intermediate-Moisture Food Model System: Analysis by Liquid Chromatography-Mass Spectrometry (LC-MS) and Data-Independent Acquisition LC-MS (LC-MSE). Journal of Agricultural and Food Chemistry, 60(42), 10674-10682.

Chen, Y., Liu, X. M., Labuza, T. P., & Zhou, P. (2013). Effect of molecular size and charge state of reducing sugars on nonenzymatic glycation of beta-lactoglobulin. Food Research International, 54(2), 1560-1568.

Corzo-Martinez, M., Avila, M., Moreno, F. J., Requena, T., & Villamiel, M. (2012). Effect of milk protein glycation and gastrointestinal digestion on the growth of bifidobacteria and lactic acid bacteria. Int J Food Microbiol, 153(3), 420-427.

del Castillo, M. D., Ferrigno, A., Acampa, I., Borrelli, R. C., Olano, A., Martinez-Rodriguez, A., & Fogliano, V. (2007). In vitro release of angiotensin-converting enzyme inhibitors, peroxyl-radical scavengers and antibacterial compounds by enzymatic hydrolysis of glycated gluten. Journal of Cereal Science, 45(3), 327-334.

Delovitch, T. L., & Singh, B. (1997). The nonobese diabetic mouse as a model of autoimmune diabetes: immune dysregulation gets the NOD. Immunity, 7(6), 727-738.

Epshtein, A., Sakhneny, L., & Landsman, L. (2017). Isolating and Analyzing Cells of the Pancreas Mesenchyme by Flow Cytometry. J Vis Exp(119). doi:10.3791/55344.

Guo, T. L., & White, K. L. (2010). Comprehensive Toxicology (Ed: C. A. McQueen). Elsevier, Waltham, MA. Ch. 5.30.

Hegele, J., Buetler, T., & Delatour, T. (2008). Comparative LC-MS/MS profiling of free and protein-bound early and advanced glycation-induced lysine modifications in dairy products. Analytica Chimica Acta, 617(1-2), 85-96.

Iwata, Y., Matsushita, T., Horikawa, M., Dilillo, D. J., Yanaba, K., Venturi, G. M., . . . Tedder, T. F. (2011). Characterization of a rare IL-10-competent B-cell subset in humans that parallels mouse regulatory B10 cells. Blood, 117(2), 530-541.

Kim, K. S., Hong, S. W., Han, D., Yi, J., Jung, J., Yang, B. G., Lee, J. Y., Lee, M., Surh, C. D. (2016). Dietary antigens limit mucosal immunity by inducing regulatory T cells in the small intestine. Science, 351(6275), 858-863.

Klenovics, K. S., Boor, P., Somoza, V., Celec, P., Fogliano, V., & Sebekova, K. (2013). Advanced Glycation End Products in Infant Formulas Do Not Contribute to Insulin Resistance Associated with Their Consumption. Plos One, 8(1).

Koschinsky, T., He, C. J., Mitsuhashi, T., Bucala, R., Liu, C., Buenting, C., Heitmann, K., Vlassara, H. (1997). Orally absorbed reactive glycation products (glycotoxins): an environmental risk factor in diabetic nephropathy. Proc Natl Acad Sci U S A, 94(12), 6474-6479.

Leiter, E. H. (1993). The NOD mouse: a model for analyzing the interplay between heredity and environment in development of autoimmune disease. ILAR Journal, 35(1), 11.

Maecker, H. T., & Trotter, J. (2006). Flow cytometry controls, instrument setup, and the determination of positivity. Cytometry A, 69(9), 1037-1042. doi:10.1002/cyto.a.20333

Martin, R. M., Brady, J. L., & Lew, A. M. (1998). The need for IgG2c specific antiserum when isotyping antibodies from C57BL/6 and NOD mice. J Immunol Methods, 212(2), 187-192.

Mathis, D., Vence, L., & Benoist, C. (2001). beta-Cell death during progression to diabetes. Nature, 414(6865), 792-798. doi:10.1038/414792a

Parsa, R., Andresen, P., Gillett, A., Mia, S., Zhang, X. M., Mayans, S., Holmberg, D., Harris, R. A. (2012). Adoptive transfer of immunomodulatory M2 macrophages prevents type 1 diabetes in NOD mice. Diabetes, 61(11), 2881-2892.

Pearson, J. A., Wong, F. S., & Wen, L. (2016). The importance of the Non Obese Diabetic (NOD) mouse model in autoimmune diabetes. J Autoimmun, 66, 76-88.

Pischetsrieder, M., & Henle, T. (2012). Glycation products in infant formulas: chemical, analytical and physiological aspects. Amino Acids, 42(4), 1111-1118.

Quintana, F. J., & Cohen, I. R. (2001). Autoantibody patterns in diabetes-prone NOD mice and in standard C57BL/6 mice. J Autoimmun, 17(3), 191-197. doi:10.1006/jaut.2001.0544

Rachmiel, M., Strauss, P., Dror, N., Benzaquen, H., Horesh, O., Tov, N., . . . Lebenthal, Y. (2016). Alpha-1 antitrypsin therapy is safe and well tolerated in children and adolescents with recent onset type 1 diabetes mellitus. Pediatr Diabetes, 17(5), 351-359. doi:10.1111/pedi.12283

Song, S., Goudy, K., Campbell-Thompson, M., Wasserfall, C., Scott-Jorgensen, M., Wang, J., . . . Flotte, T. R. (2004). Recombinant adeno-associated virus-mediated alpha-1 antitrypsin gene therapy prevents type I diabetes in NOD mice. Gene Ther, 11(2), 181-186. doi:10.1038/sj.gt.3302156

Tian, J., Zekzer, D., Hanssen, L., Lu, Y., Olcott, A., & Kaufman, D. L. (2001). Lipopolysaccharide-activated B cells down-regulate Th1 immunity and prevent autoimmune diabetes in nonobese diabetic mice. Journal of Immunology, 167(2), 1081-1089.

Uribarri, J., Woodruff, S., Goodman, S., Cai, W., Chen, X., Pyzik, R., Yong, A., Striker, G. E., Vlassara, H. (2010). Advanced glycation end products in foods and a practical guide to their reduction in the diet. J Am Diet Assoc, 110(6), 911-916.

Wan, X., Thomas, J. W., & Unanue, E. R. (2016). Class-switched anti-insulin antibodies originate from unconventional antigen presentation in multiple lymphoid sites. J Exp Med, 213(6), 967-978.

Yanaba, K., Bouaziz, J. D., Haas, K. M., Poe, J. C., Fujimoto, M., & Tedder, T. F. (2008). A regulatory B cell subset with a unique CD1dhiCD5+ phenotype controls T cell-dependent inflammatory responses. Immunity, 28(5), 639-650. doi:10.1016/j.immuni.2008.03.017

Zhang, M., Zhou, Q., Dorfman, R. G., Huang, X., Fan, T., Zhang, H., Yu, C. (2016). Butyrate inhibits interleukin-17 and generates Tregs to ameliorate colorectal colitis in rats. BMC Gastroenterol, 16(1), 84. doi:10.1186/s12876-016-0500-x

CHAPTER 5

CONCLUSIONS AND FUTURE DIRECTIONS

In conclusion, this dissertation has demonstrated that EGPs could affect disease progressions through immunoregulation. The results consistently supported the notion that EGPs were anti-inflammatory, even though their effects on PCa and T1D were opposite (Fig 5.1). In PCa, EGPs polarized macrophages toward anti-inflammatory/pro-tumoral M2, and increased the PCa cell proliferation. In the T1D model, EGPs decreased the $CD8^+$ T cells and insulin auto-antibodies, and increased circulating IL-10 and splenic M2/M1 ratio. Importantly, the M2/M1 ratio and serum IL-10 were up-regulated in both disease models.

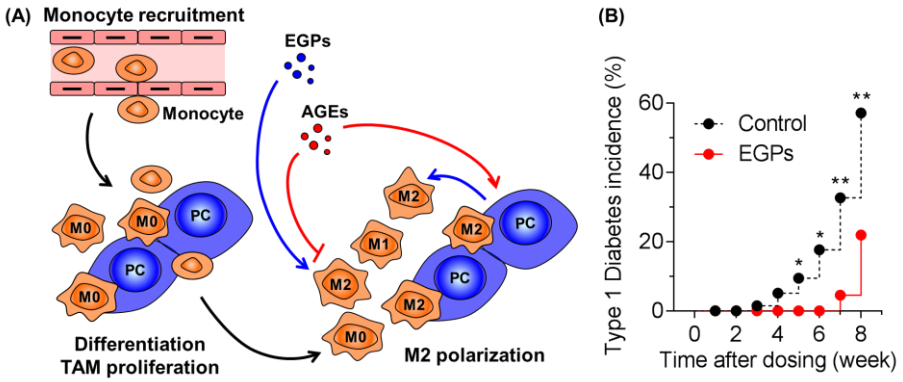

Figure 5.1. Graphic summary. (A) Early glycation products (EGPs) either directly or by assisting PCa cells polarize macrophages toward M2, leading to the proliferation of PCa cells. The effects of AGEs on PCa growth are possibly dependent on the difference between directly promoting PCa cell proliferation and activating macrophages to kill PCa cells. (B) Oral gavage of dietary EGPs decreased the T1D incidence by half in NOD female mice.

Even though orally administrated EGPs elicited anti-inflammatory function in both PCa and T1D models, it is premature to promote the nutraceutical application in humans at this stage. especially without understanding the mechanisms how of EGPs exert their immunoregulatory functions. After ingestion, dietary EGPs are digested in the intestine. Since the binding positions of the reducing sugars are lysine and arginine, some of the enzymatic cleavage sites of proteins are blocked by glycation modification. A chromatographic profiling of *in vitro* gastric and intestinal digested sodium caseinate showed that galactose glycation resulted in the reduction of peptide amount (Corzo-Martinez, Avila, Moreno, Requena, & Villamiel, 2012), and a comprehensive review suggested that the absorption rate of protein-bound Amadori products was 3-10% (Pischetsrieder & Henle, 2012). More than 90% of orally administered EGPs stay in the GI tract. Considering the low fecal FL contents, it is highly possible that gut microbiota destroys most of the EGPs in the colon. It has been shown that *in vitro* culture of *Intestinimonas* AF211 converted Amadori compounds into the short chain fatty acid butyrate (Bui et al., 2015), and daily butyrate gavage attenuated 2,4,6-trinitrobenzene sulfonic acid (TNBS) induced colitis lesions in rats by affecting the Th17/pTreg lineage (Zhang et al., 2016). Importantly, a 'Medicinal food' diet yielding high amounts of short chain fatty acid acetate and butyrate provided a beneficial effect on the immune system and protected against T1D (Marino et al., 2017). The distribution and metabolism of the absorbed EGPs are unclear except that absorbed FL in rats would not be used as lysine source, and 10% of the ingested FL was secreted in the urine (Finot, Magnenat, Mottu, & Bujard, 1978). It is also unclear if the absorbed EGPs would promote the production of endogenous EGPs. Apparently, large sets of data were missing regarding the ADME of EGPs, which would be essential for understanding how EGPs and their metabolites exert the anti-inflammatory function.

With the phenotypic observations made in the selected animal models in this dissertation, another priority for next step is to understand the mechanisms in which EGPs directly affect the immune cells. For example, our *in vitro* data showed that EGP treatment could decrease the expression of iNOS, which was an M1 marker, and upregulate the M2/M1 ratio based on cell surface markers in the presence of PCa cells. Unfortunately, we were unable to identify any specific target receptors or signaling pathways link to this current work. It had been reported that HMGB1 binding to RAGE could induce M2 polarization and RAGE was an important receptor for AGEs (Rojas et al., 2016). However, EGPs at the concentration of up to 10 mg/ml were unable to induce the RAGE expression in human Mφs when analyzed by Western blots, suggesting that EGPs did not exert the anti-inflammatory effect by binding to RAGE. Other receptors and pathways involved in M2 polarization of Mφ (Biswas & Mantovani, 2010) could be the candidates. There are 4 subtypes of M2 Mφs based on the applied stimuli and the resultant transcriptional changes: the M2a activation is a response to IL-4 and IL-13; M2b to immune complexes and bacterial lipopolysaccharide (LPS), M2c to glucocorticoids and TGF-β; M2d to IL-6 and adenosines (Wang, Zhang, Wu, Rong, & Guo, 2018). Among these 4 subtypes, the M2b is most likely the subtype activated by EGPs.

The EGPs used is this dissertation were mainly derived from WPI and glucose. Even though the glycine-glucose derived EGPs exerted similar effects on the cytokine/chemokine profiling of Mφs, more research is needed to investigate the immunoregulatory effect of dietary EGPs originated from other food materials. This dissertation clearly demonstrated that dietary EGPs were pro-tumoral for PCa patients, but protective against T1D after oral consumption. With the

compelling evidences presented that dietary EGPs produce different disease-specific effects on disease progression through immunoregulation, they may have future applications for nutraceutical or even pharmaceutical use.

References

Biswas, S. K., & Mantovani, A. (2010). Macrophage plasticity and interaction with lymphocyte subsets: cancer as a paradigm. Nat Immunol, 11(10), 889-896.

Bui, T. P., Ritari, J., Boeren, S., de Waard, P., Plugge, C. M., & de Vos, W. M. (2015). Production of butyrate from lysine and the Amadori product fructoselysine by a human gut commensal. Nat Commun, 6, 10062.

Corzo-Martinez, M., Avila, M., Moreno, F. J., Requena, T., & Villamiel, M. (2012). Effect of milk protein glycation and gastrointestinal digestion on the growth of bifidobacteria and lactic acid bacteria. Int J Food Microbiol, 153(3), 420-427.

Finot, P. A., Magnenat, E., Mottu, F., & Bujard, E. (1978). Biologic availability and metabolic transit of amino acids modified by technological processing. Ann Nutr Aliment, 32(2-3), 326-338.

Marino, E., Richards, J. L., McLeod, K. H., Stanley, D., Yap, Y. A., Knight, J., McKenzie, C., Kranich, J., Oliveira, A. C., Rossello, F. J., Krishnamurthy, B., Nefzger, C. M., Macia, L., Thorburn, A., Baxter, A. G., Morahan, G., Wong, L. H., Polo, J. M., Moore, R. J., Lockett, T. J., Clarke, J. M., Topping, D. L., Harrison, L. C., Mackay, C. R. (2017). Gut microbial metabolites limit the frequency of autoimmune T cells and protect against type 1 diabetes. Nat Immunol, 18(5), 552-562.

Pischetsrieder, M., & Henle, T. (2012). Glycation products in infant formulas: chemical, analytical and physiological aspects. Amino Acids, 42(4), 1111-1118.

Rojas, A., Delgado-Lopez, F., Perez-Castro, R., Gonzalez, I., Romero, J., Rojas, I., Araya, P., Anazco, C., Morales, E., Llanos, J. (2016). HMGB1 enhances the protumoral activities of M2 macrophages by a RAGE-dependent mechanism. Tumour Biol, 37(3), 3321-3329.

Wang, L. X., Zhang, S. X., Wu, H. J., Rong, X. L., & Guo, J. (2018). M2b macrophage polarization and its roles in diseases. J Leukoc Biol. doi:10.1002/JLB.3RU1018-378RR

Zhang, M., Zhou, Q., Dorfman, R. G., Huang, X., Fan, T., Zhang, H., Zhang, J., Yu, C. (2016). Butyrate inhibits interleukin-17 and generates Tregs to ameliorate colorectal colitis in rats. BMC Gastroenterol, 16(1), 84.

APPENDICES

Appendix A. Supplementary Data in Chapter 2

Cell line	Source	Androgen receptor	Androgen sensitivity	PSA
LNCaP	Lymph node metastasis	+ mutated	+	+
PC-3	Lumbar metastasis	-	-	-

Supplement 1 Characteristics of LNCaP and PC-3. PSA, prostate-specific antigen.

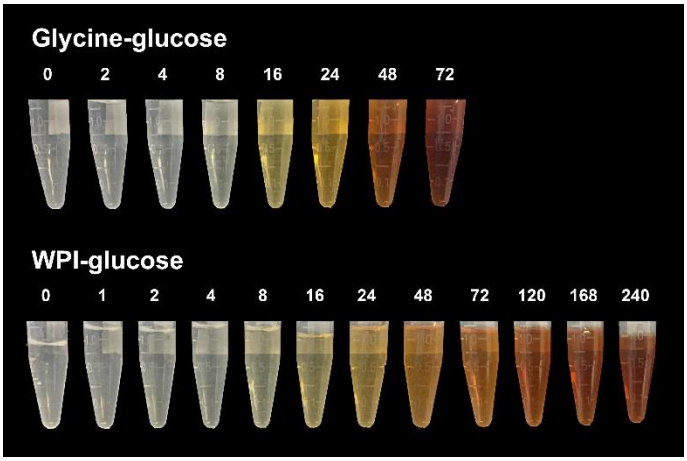

Supplement 2. Sample pictures after being dissolved in phenol red free RPMI medium. The browning color indicated the high reaction extent. Numbers indicated the reaction time (h).

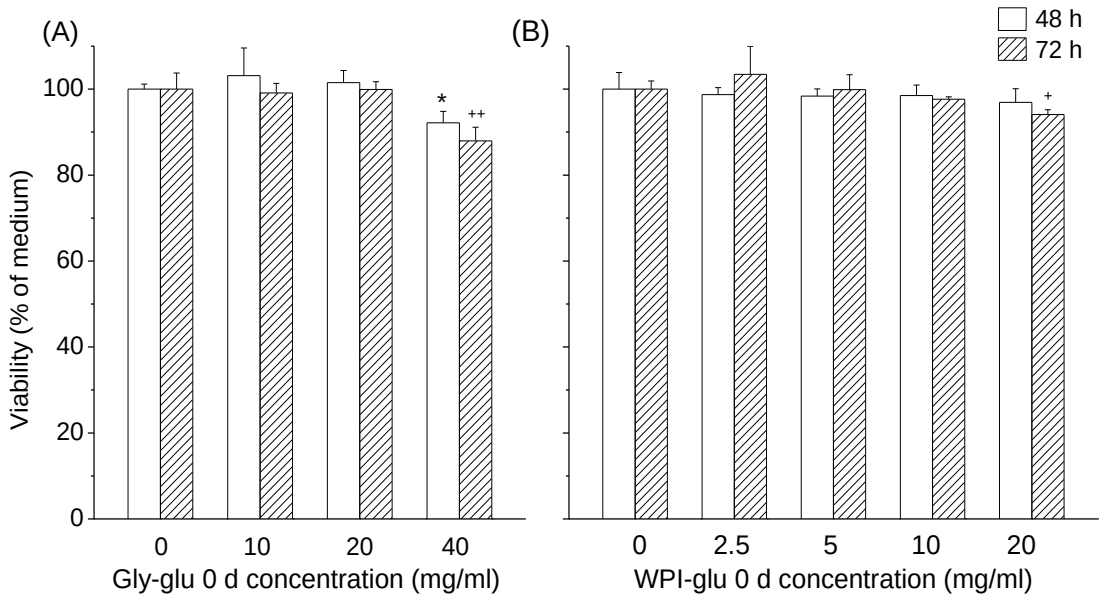

Supplement 3. The toxicity of non-reacted glycine-glucose (A) and WPI-glucose samples (B) (mean ± SD, n = 6). Different bars indicate different treatment time. *, p <0.05 vs. medium control for 48 h; +, $p < 0.05$, ++, $p < 0.01$) vs. medium control for 72 h.

Cytokine/chemokine	G 0 (pg/ml)	W 0 (pg/ml)
EGF	13.22 ± 1.79	16.84 ± 1.95
VEGF	3322.67 ± 407.70	6184.75 ± 988.77
G-CSF	73.33 ± 12.60	177.28 ± 27.68
GM-CSF	36.30 ± 5.73	54.05 ± 9.63
IL-3	3.81 ± 1.03	2.04 ± 0.09
IL-7	27.38 ± 2.26	24.26 ± 5.03
IL-1ra	8017.33 ± 1316.12	7291.00 ± 1120.27
IL-4	39.61 ± 7.33	40.96 ± 2.48
IL-10	277.78 ± 34.13	1904.5 ± 67.34
IL-13	11.84 ± 1.66	10.15 ± 1.06
IL-1α	8.72 ± 0.77	8.21 ± 1.29
IL-1β	7.92 ± 1.00	10.19 ± 1.29
IL-2	6.18 ± 1.82	5.46 ± 0.49
IL-5	6.00 ± 1.16	4.6275 ± 0.99
IL-6	7.86 ± 0.85	7.20 ± 1.16
IL-12p40	38.95 ± 8.37	72.38 ± 1.71
IL-12p70	22.70 ± 3.46	25.79 ± 3.18
IL-15	10.05 ± 1.05	9.93 ± 0.94
IL-17	11.50 ± 1.54	15.88 ± 3.03
IFN-γ	21.07 ± 4.20	30.25 ± 4.54
TNF-α	2103.83 ± 383.14	745.24 ± 100.80
TNF-β	9.28 ± 1.46	12.43 ± 1.88
IL-8	14914.83 ± 1946.51	9654.75 ± 838.19
Eotaxin	32.04 ± 2.85	50.20 ± 4.04
CXCL10	3631.00 ± 325.34	1965.00 ± 118.73
CCL2	20496.3 ± 610.20	11746.3 ± 215.27
RANTES	11746.6 ± 645.64	36576.00 ± 1756.35
CCL3	7204.33 ± 858.29	19051.00 ± 360.51
CCL4	3835.67 ± 750.35	3826.5 ± 771.60
INF-α2	81.58 ± 11.01	120.54 ± 18.12

Supplement 4. The cytokine/chemokine levels from the 0-h sample treatment

GOID	GO term	% Associated genes	Associated genes
Functions identified for cytokines/chemokines instead of EGPs			
GO:0001774	negative regulation of microglial cell activation	6.67	IL4
GO:0002740	negative regulation of cytokine secretion involved in immune response	14.29	IL10
GO:0002904	positive regulation of B cell apoptotic process	25.00	IL10
GO:0030886	negative regulation of myeloid dendritic cell activation	25.00	IL10
GO:0030889	negative regulation of B cell proliferation	5.88	IL10
GO:0043031	negative regulation of macrophage activation	14.29	IL4
GO:0032682	negative regulation of chemokine production	6.25	IL10
GO:0032695	negative regulation of interleukin-12 production	5.88	IL10
GO:0032717	negative regulation of interleukin-8 production	6.67	IL10
GO:0042536	negative regulation of tumor necrosis factor biosynthetic process	16.67	IL10
GO:0050868	negative regulation of T cell activation	2.20	IL10, IL4
GO:0071650	negative regulation of chemokine (C-C motif) ligand 5 production	33.33	IL10
Non directionally altered functions			
GO:0000018	regulation of DNA recombination	3.13	IL10, IL4
GO:0002204	somatic recombination of immunoglobulin genes involved in immune response	5.00	IL10, IL4
GO:0002208	somatic diversification of immunoglobulins involved in immune response	5.00	IL10, IL4
GO:0005133	Pertussis	2.67	IL8, IL10
GO:0005140	Leishmaniasis	2.74	IL10, IL4
GO:0005144	Malaria	4.08	IL8, IL10
GO:0005310	Asthma	6.45	IL10, IL4
GO:0005320	Autoimmune thyroid disease	3.77	IL10, IL4
GO:0005321	Inflammatory bowel disease (IBD)	3.08	IL10, IL4
GO:0005330	Allograft rejection	5.26	IL10, IL4
GO:0005132	Salmonella infection	2.33	CCL4, IL8
GO:0010155	regulation of proton transport	6.25	IL4
GO:0032601	connective tissue growth factor production	50.00	IL4
GO:0034465	response to carbon monoxide	20.00	IL10
GO:0036499	PERK-mediated unfolded protein response	5.26	IL8
GO:0039694	viral RNA genome replication	7.14	IL8
GO:0044126	regulation of growth of symbiont in host	5.00	IL10
GO:0045091	regulation of single stranded viral RNA replication via double stranded DNA intermediate	12.50	IL8
GO:0051045	negative regulation of membrane protein ectodomain proteolysis	16.67	IL10
GO:0060670	branching involved in labyrinthine layer	7.14	IL10

	morphogenesis		
GO:0071288	cellular response to mercury ion	25.00	IL4
GO:1901741	positive regulation of myoblast fusion	5.56	IL4

Supplement 5. The EGPs functions identified but not included for the graphing.

Appendix B. Supplementary Data in Chapter 3

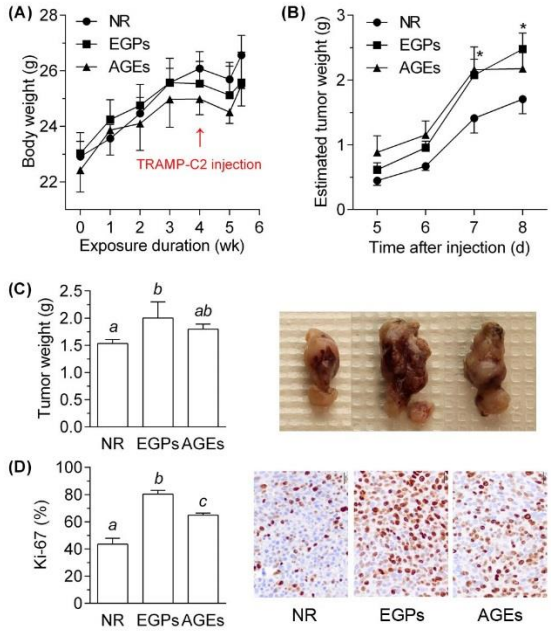

Fig. S1. A repeat of the experiment in Fig. 1. EGPs promoted PCa *in vivo* more than AGEs. Male C57BL/6 mice were gavaged with NR, EGPs or AGEs for 4 weeks, and then 2×10^6 TRAMP-C2 cells were subcutaneously (s.c.) injected in the flank area. (A) Body weights were recorded weekly. (B) The weight of the s.c. tumor was estimated as: length × width^2/2000 (g). (C) The tumors were separated and weighted after the mice were euthanized. (D) The tumor was fixed in 10% buffered formalin, and a section in the middle was cut for Ki-67 immunohistochemistry, which was performed by Clinical Pathology Laboratory (College of Veterinary Medicine, UGA). Proliferation index of the tumor was calculated as the percentage of the Ki-67 positive staining cells (mean ± SE, n = 5). A moribund event occurred in the AGE-group. *, $p < 0.05$ vs NR in EGP group; *a*, *b*, *c*, $p < 0.05$.

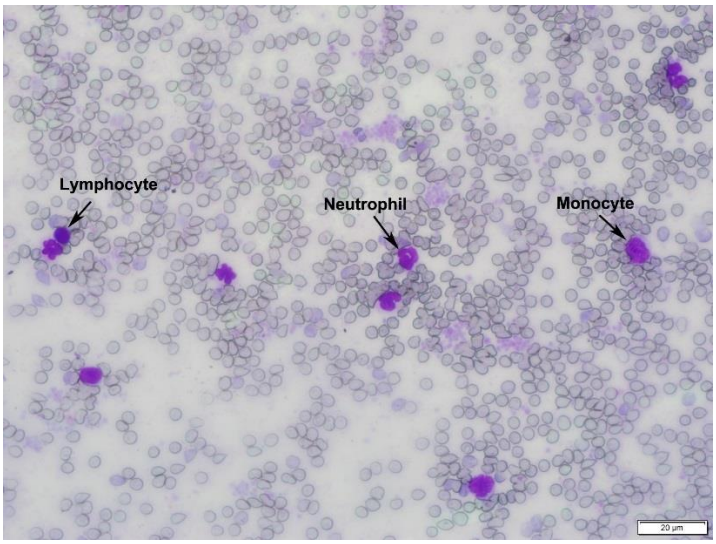

Fig. S2. Morphology of different types of leucocytes identified in the blood smear.

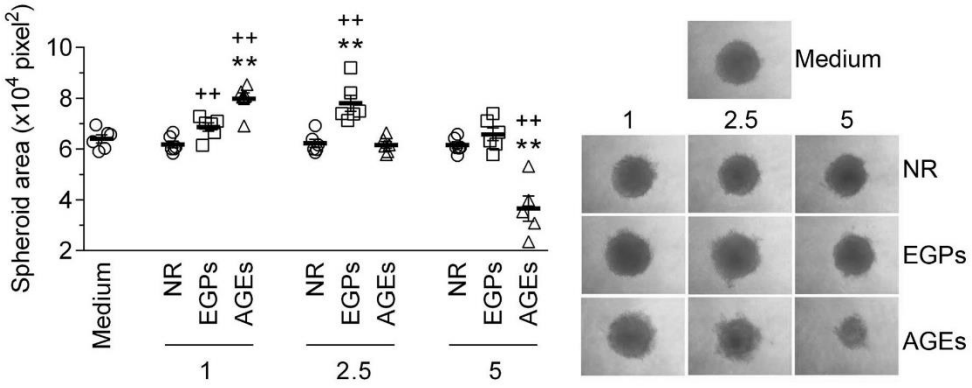

Fig. S3. Spheroids of TRAMP-C2 and peritoneal Mφ co-culture. A mixture of 500 TRAMP-C2 cells and 150 peritoneal Mφs was added into each well covered with 50 µl of agarose (1.5% (w/v)) and cultured in 130 µl DMEM medium (high glucose, supplemented with 10% FBS and 50 µg/ml gentamycin). The media were changed every other day, and the spheroids were imaged at day 7. Number indicated the concentrations of glycation sample applied (mg/ml; mean ± SE, n = 6). **, $p < 0.01$ vs medium; ++, $p < 0.01$ vs NR.

Table S1. Serum cytokine/chemokine levels.

Cytokine (pg/ml)	Treatment			
	Water	NR	EGPs	AGEs
Eotaxin	1858.33 ± 234.84	1918 ± 181.19	1603.67 ± 42.38	2559.28 ± 936.41
G-CSF	3045.34 ± 532.96	887.24 ± 402.22	435.41 ± 89.30	539.29 ± 77.47
GM-CSF	186.97 ± 15.01	221.74 ± 44.89	213.60 ± 28.53	174.55 ± 14.84
IFN-γ	93.44 ± 10.76	76.74 ± 10.93	82.36 ± 8.72	80. 86 ± 7.8
IL-1α	825.62 ± 64.98	942.74 ± 186.39	863.93 ± 62.27	871.37 ± 165.55
IL-1β	261.44 ± 13.18	433.83 ± 204.60	329.80 ± 56.94	311.89 ± 98.70
IL-2	91.02 ± 16.66	96.26 ± 53.45	102.88 ± 23.16	74.65 ± 9.59
IL-3	13.75 ± 3.50 *ab*	9.83 ± 2.40 *a*	11.37 ± 1.68 *ab*	23.94 ± 7.76 *b*
IL-4	10.18 ± 5.10 *ab*	7.26 ± 2.87 *ab*	4.19 ± 0.47 *a*	19.74 ± 7.07 *b*
IL-5	137.48 ± 48.78	61.86 ± 19.13	63.96 ± 5.76	94.03 ± 24.30
IL-6	41.66 ± 10.95	44.63 ± 16.02	37.39 ± 3.68	117.10 ± 54.05
IL-7	752.33 ± 84.35	1392.88 ± 925.08	2394.93 ± 1286.04	680.55 ± 117.32
IL-9	748.71 ± 66.02	536.86 ± 57.45	713.69 ± 203.39	796.94 ± 104.14
IL-10	398.94 ± 57.01 *a*	334.48 ± 15.35 *a*	914.92 ± 239.25 *b*	649.06 ± 125.99 *a*
IL-12p40	187.58 ± 21.90	384.95 ± 250.80	231.44 ± 52.12	175.73 ± 24.58
IL-12p70	179.25 ± 18.26 *a*	270.20 ± 108.29 *ab*	195.02 ± 32.24 *a*	899.13 ± 425.80 *b*
IL-13	509.18 ± 49.35	455.64 ± 97.86	543.36 ± 76.19	423.42 ± 32.65
IL-15	1807.22 ± 276.06	1322.68 ± 108.74	1514.72 ± 96.56	1901.83 ± 615.30
IL-17	27.70 ± 2.96 *ab*	22.99 ± 2.33 *a*	18.95 ± 2.38 *a*	80.56 ± 36.46 *b*
LIF	65.56 ± 6.52	174.76 ± 118.82	272.77 ± 146.11	53.99 ± 9.18
LIX	5145.09 ± 1054.08 *a*	7380.50 ± 925.80 *ab*	7327.09 ± 328.21 *ab*	8786.41 ± 1704.82 *b*
IP-10	465.04 ± 95.72	327.69 ± 48.03	320.31 ± 36.08	366.82 ± 60.91
KC	325.15 ± 119.01	573.51 ± 338.19	305.24 ± 24.59	259.08 ± 53.48
M-CSF	648.83 ± 103.39	1147.41 ± 713.48	701.82 ± 144.30	544.56 ± 80.11
MCP-1	385.66 ± 19.10	387.62 ± 28.67	373.35 ± 20.05	417.96 ± 68.25
MIG	323.28 ± 34.73	531.81 ±336.51	812.49 ±349.18	259.82 ± 40.05
MIP-1α	300.54 ± 11.51	310.28 ± 47.38	317.72 ± 20.05	293.41 ± 18.07
MIP-1β	226.34 ± 14.92	212.53 ± 10.54	210.37 ± 8.86	202.89 ± 10.56
MIP-2	775.44 ± 31.39	736.45 ± 38.82	734.07 ± 31.96	774.02 ± 40.21
RANTES	36.53 ± 3.31 *ab*	33.19 ± 8.63 *a*	33.50 ± 2.28 *a*	78.57 ± 27.41 *b*
TNF-α	59.73 ± 2.94	65.12 ± 8.63	62.44 ± 4.85	71.21 ± 15.49
VEGF	12.70 ± 1.89	15.56 ± 7.00	12.38 ± 2.10	15.19 ± 1.39

a, *b*, $p < 0.05$

Appendix C. Supplementary Data in Chapter 4

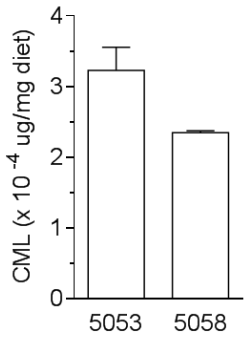

Supplementary Fig. 1. CML quantitation in rodent chow. CML amount was quantitated using OxiSelect CML competitive ELISA kit (Cell Biolabs, San Diego, CA, USA) following the manufacturer's instructions: The levels of 323 ng CML/g in diet 5053 and 235 ng CML/g in diet 5058 were identified.

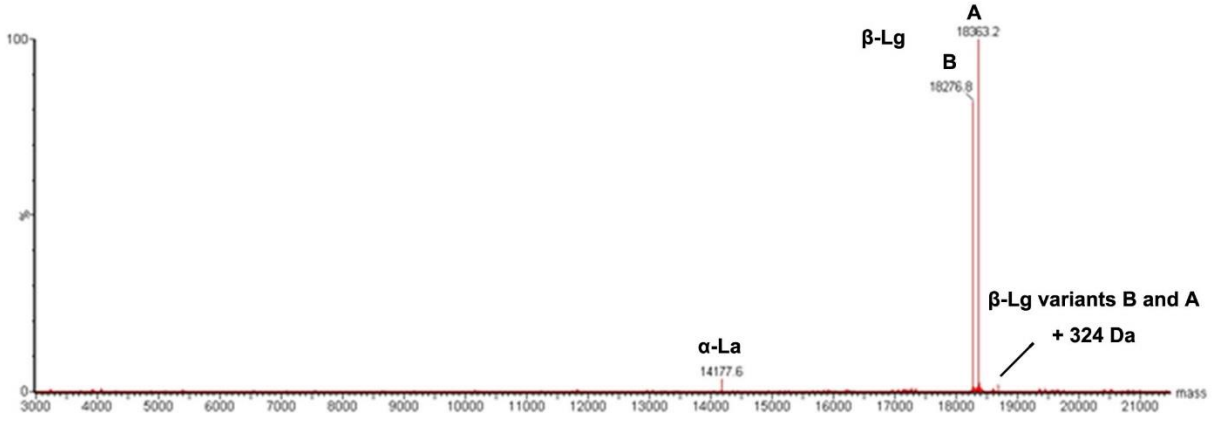

Supplementary Fig. 2. Deconvoluted mass spectrum for WPI powders. The mass displayed is from 3,000 to 21,500 Da. The powders are highly purified and contain mainly α-lactalbumin (α-La, 14,178 Da) and β-lactoglobulin (β-Lg, variant B: 18,277 Da; A: 18,363 Da). The two peaks with an increase in molecular weight of 324 Da of β-Lg variants were probably resulted from one lactose attachment during powder manufacture.

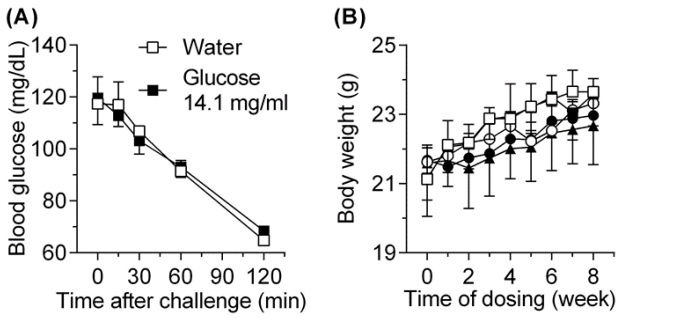

Groups	Week			
	2	6	7	8
Water	*a*	*a*	*ab*	*a*
Glucose	*ab*	*ab*	*a*	*ab*
NR	*b*	*b*	*ab*	*bc*
EGPs	*ab*	*ab*	*b*	*c*
AGEs	*ab*	*ab*	*b*	*abc*

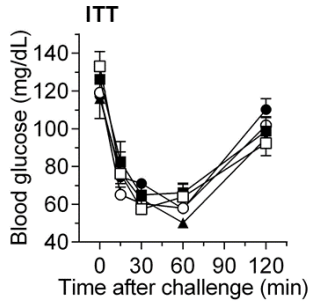

Supplementary Fig. 3. Effect of EGPs on blood glucose levels in healthy mice. C57BL/6 females (6-8 weeks old) were gavaged with water, glucose solution (14.1 mg/ml), NR, EGPs or AGEs. (A) BGL change after orally challenged with glucose solution. (B) BW. (C) Resting BGL; significance was detected at week 2, 6, 7 and 8, and shown in the table. (D) GTT and ITT after dosing for 8 weeks (mean ± SE, n = 5-6). *a*, *b*, *c*, $p < 0.05$.

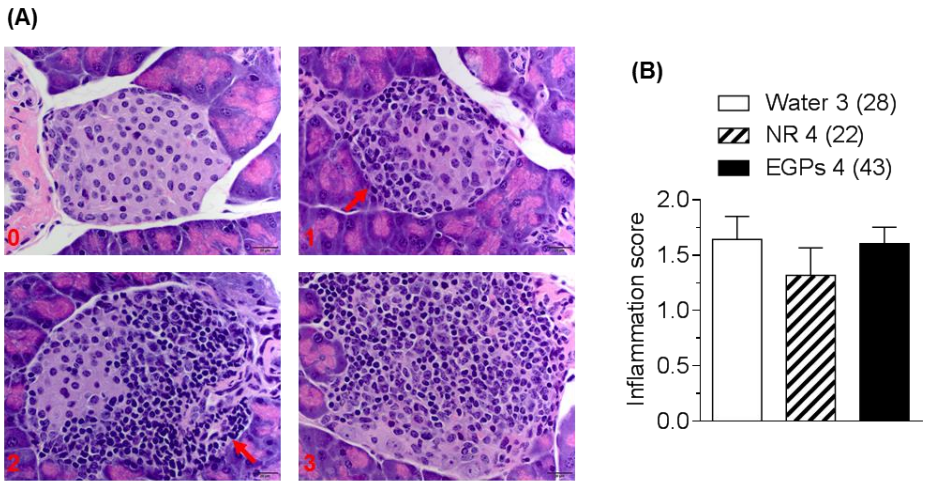

Supplementary Fig. 4. Histopathological assessment of the pancreatic immune infiltrates. After being treated for 4 weeks, pancreases from non-diabetic NOD females were used for histopathological evaluation of the inflammation in β-islets. (A) Representative β-islet for each score with the red numbers in the left corner indicating the inflammation score. Red arrows indicate the infiltrated immune cells. (B) Statistical analysis of the histopathological scores. Numbers indicate the total animals used and the numbers in parenthesis indicate the total islets evaluated.

Supplementary Table 1. Organ/Tissue weight of the non-diabetic NOD females after dosing for 4 weeks.

Group	Organ/Tissue weight (g)					
	Spleen	Thymus	Liver	Kidney	Lung	Heart
Water	0.067 ± 0.002	0.063 ± 0.003	0.996 ± 0.031	0.248 ± 0.009	0.238 ± 0.022	0.125 ± 0.006
NR	0.070 ± 0.002	0.056 ±0. 003	1.116 ± 0.087	0.285 ± 0.028	0.300 ± 0.028	0.129 ± 0.007
EGPs	0.074 ± 0.005	0.057 ± 0.002	0.971 ± 0.060	0.256 ± 0.011	0.239 ± 0.018	0.124 ± 0.005

All data are present in mean ± SE; n = 7 for water and NR groups, and n = 8 for EGP group. No significance was detected.

Supplementary Table 2. Serum cytokine/chemokine levels.

Cytokine (pg/ml)	Treatment		
	Water (EGPs/Water)	NR (EGPs/NR)	EGPs
Eotaxin	1031.36 ± 116.07 (1.20)	890.17 ± 125.03 (1.39*)	1242.36 ± 142.98
G-CSF	185.68 ± 18.87 (1.64^{+})	202.89 ± 27.04 (1.50)	304.22 ± 60.45
GM-CSF	$53.06 \pm 14.63^{+}$ (3.55^{+})	170.51 ± 37.28 (1.10)	188.29 ± 47.43
IL-1α	$461.87 \pm 29.63^{+}$ (1.56)	1060.25 ± 272.30 (0.68)	718.27 ± 152.98
IL-1β	93.70 ± 0.00 (5.22)	766.28 ± 233.47 (0.64)	488.67 ± 157.05
IL-2	$15.25 \pm 1.00^{++}$ (5.58^{+})	213.43 ± 49.67 (0.40*)	85.14 ± 35.92
IL-4	2.72 ± 0.40 (1.58)	3.27 ± 0.56 (1.32)	4.31 ± 0.78
IL-6	5.13 ± 1.05 (6.88^{+})	10.69 ± 3.34 (3.30*)	35.32 ± 11.56
IL-7	$32.80 \pm 16.58^{+}$ (272.02^{+})	6950.60 ± 3632.89 (1.28)	8922.69 ± 3927.65
IL-9	$218.36 \pm 26.77^{+}$ (1.37)	417.34 ± 99.08 (0.72)	299.23 ± 57.33
IL-10	$24.24 \pm 9.44^{+}$ (85.85^{+})	667.98 ± 193.46 (3.12)	2080.98 ± 862.60
IL-12p40	$40.50 \pm 6.67^{+}$ (5.46)	593.84 ± 177.29 (0.37*)	221.20 ± 95.81
IL-12p70	$51.24 \pm 14.29^{+}$ (4.90^{+})	261.75 ± 71.51 (0.96)	251.03 ± 97.92
IL-13	$73.52 \pm 18.04^{++}$ (11.29^{++})	566.84 ± 149.80 (1.46)	829.85 ± 228.90
IL-15	$442.90 \pm 122.85^{++}$ (3.35^{++})	1825.50 ± 174.25 (0.81)	1481.81 ± 265.67
IL-17	2.93 ± 0.01 (9.69)	9.24 ± 3.13 (3.08)	28.43 ± 13.70
INF-γ	$17.91 \pm 2.63^{+}$ (2.49)	61.57 ± 16.89 (0.73)	44.67 ± 15.14
IP-10	202.45 ± 26.55 (1.21)	211.05 ± 10.68 (1.16)	244.89 ± 36.26
KC	$132.43 \pm 12.81^{+}$ (1.04)	205.85 ± 32.06 (0.67*)	137.79 ± 14.54
LIF	$16.93 \pm 5.95^{+}$ (34.12^{+})	430.92 ± 186.80 (1.34)	577.57 ± 245.94
LIX	11721.38 ± 528.42 (1.01)	10832.46 ± 479.05 (1.09)	11858.24 ± 483.36
M-CSF	$70.14 \pm 10.21^{+}$ (12.43^{+})	1069.15 ± 376.20 (0.82)	872.07 ± 410.91
MCP-1	$85.07 \pm 8.30^{+}$ (1.81^{+})	279.34 ± 60.01 (0.55)	154.27 ± 31.49
MIG	$106.64 \pm 13.91^{+}$ (12.38^{+})	1468.21 ± 502.88 (0.90)	1319.66 ± 504.49
MIP-1α	$102.08 \pm 23.40^{++}$ (1.74)	295.99 ± 52.42 (0.60)	177.85 ± 47.54
MIP-1β	$77.32 \pm 2.37^{++}$ (1.55)	172.34 ± 17.83 (0.70)	119.85 ± 29.85
MIP-2	$225.04 \pm 32.50^{++}$ (1.86^{+})	514.01 ± 83.69 (0.82)	419.20 ± 85.07
RANTES	$12.64 \pm 2.52^{++}$ (2.84^{+})	39.54 ± 7.28 (0.91)	35.91 ± 9.56
TNF-α	$17.22 \pm 0.88^{++}$ (2.00)	59.68 ± 11.18 (0.58)	34.43 ± 9.00
VEGF	$2.57 \pm 0.45^{++}$ (2.28^{+})	15.27 ± 3.94 (0.38*)	5.86 ± 1.46

Numbers in brackets indicate the fold changes either EGPs over water or EGPs over NR. +, $p < 0.05$, ++, $p < 0.01$ NR vs water (out of parenthesis), EGPs vs water (in parenthesis); *, $p < 0.05$ EGPs vs NR.